

University of Nebraska - Lincoln

DigitalCommons@University of Nebraska - Lincoln

---

Construction Systems -- Dissertations & Theses

Construction Systems

---

12-2012

## In-Plane Shear Resistance of Sustainable Structural Walls With Large Openings

Matija Radovic

University of Nebraska-Lincoln, mradovic@unomaha.edu

Follow this and additional works at: <https://digitalcommons.unl.edu/constructiondiss>



Part of the [Construction Engineering and Management Commons](#)

---

Radovic, Matija, "In-Plane Shear Resistance of Sustainable Structural Walls With Large Openings" (2012). *Construction Systems -- Dissertations & Theses*. 11. <https://digitalcommons.unl.edu/constructiondiss/11>

This Article is brought to you for free and open access by the Construction Systems at DigitalCommons@University of Nebraska - Lincoln. It has been accepted for inclusion in Construction Systems -- Dissertations & Theses by an authorized administrator of DigitalCommons@University of Nebraska - Lincoln.

**IN-PLANE SHEAR RESISTANCE OF  
SUSTAINABLE STRUCTURAL WALLS WITH  
LARGE OPENINGS**

By:

Matija Radovic

A THESIS

Presented to the Faculty of

The Graduate College at the University of Nebraska

In Partial Fulfillment of Requirements

For the Degree of Master of Science

Major: Construction

Under the Supervision of Terri R. Norton,

Lincoln, Nebraska

December, 2012

## **ACKNOWLEDGMENTS**

First, I would like to thank my advisor, Dr. Terri Norton, for giving me the opportunity to work with her and helping me to become what I am today. I would also like to thank my family for all love and care they provided. Additionally, I will never forget my American family, Dan and Sharon Halm , who made their home always open for me, and helped me and supported along the way. Special thanks also go to Agnite Herman Agbodjan for his invaluable help with construction of the walls. At the end, I would like to thank graduate students and Structural Dynamics Lab colleagues, Mohammad Lashgari and Mehdi Mohseni, for their priceless contribution to my graduate studies.

# **IN-PLANE SHEAR RESISTANCE OF SUSTAINABLE STRUCTURAL WALLS WITH LARGE OPENINGS**

Matija Radovic, M.S.

University of Nebraska, 2012

Adviser: Terri Norton

Shear walls are primary structural systems that support building against lateral loads (tornados and hurricanes). Even though concrete shear walls are the most efficient lateral resisting system, they are rarely used in a residential construction. The reasons for why contractors do not use concrete walls in residential construction were due to higher construction cost and slower construction paces. This study proposes building and testing residential concrete structural wall system that is energy efficient, cost competitive and structurally safe.

In order to decrease environmental impact of the residential construction process, this study proposed implementing sustainability concept while building residential structures. The recycled material was used in the wall's concrete mix, while salvaged material was used for the wall's formwork. To test how experimental concrete mix behaves under high lateral loads, two reinforced concrete shear walls with typical residential profiles were built and evaluated. Shear wall with experimental mix (SW2) showed significantly lower shear capacity (27.7 kips) compared to the shear capacity (40.5 kips) of the wall with control mix (SW1). However obtained shear capacity for both walls was greater than shear demand (21.1kips). The results showed that implementing sustainability concept in residential construction process did not affect its cost competitiveness. The proposed system was shown to be environmentally friendly

and structurally safe, despite excessive compressive strength retardation of experimental concrete mix caused by mineral or chemical contamination.

# Contents

CHAPTER 1. INTRODUCTION .....	1
1.1. Motivation .....	1
1.2. Literature Review .....	6
1.2.1. Insulated Concrete Form Walls .....	6
1.2.2. Sustainable Concrete .....	8
1.2.3. Self-Consolidating Concrete .....	14
1.2.4. Insulated Concrete Form Wall (ICF) as Shear Wall .....	16
1.3. Study Objectives .....	21
1.3.1. First Objective – Concrete Mixes .....	21
1.3.2. Second Objective –Determining Representative Residential Shear Wall Model ...	21
1.3.3. Third Objective- Sustainability and Cost Comparison .....	22
1.4. Hypothesis .....	22
CHAPTER 2. METHODOLOGY OF EXPERIMENTAL ASSESMENT .....	24
2.1. Materials and Material Properties .....	24
2.1.1. Concrete mix materials .....	24
2.1.2. Concrete Mix Design .....	24
2.1.3. Control Concrete Mix .....	25
2.1.4. Experimental Concrete (SCRC) Mix .....	25
2.1.5. Natural aggregate .....	26
2.1.6. Recycled concrete aggregate .....	28
2.1.7. IPF Cement .....	30
2.1.8. Nebraska Fly Ash Class C .....	31
2.1.9. Reinforcement materials .....	32
2.1.10. Formwork materials .....	32
2.2. Concrete Sample Testing and Instrumentation .....	32
2.2.1. Compressive strength test .....	32
2.2.2. Flexural strength test .....	33
2.3. Developing Numerical Models for Finite Element Analysis (FEA) .....	33
2.3.1. Wind Load Structure Profile .....	34

2.3.2.	Wind Load Calculations .....	35
2.3.3.	Computer Models for Finite Element Analysis .....	38
2.3.3.1.	Preliminary calculations for sizing the shear wall.....	38
2.3.3.2.	Determining the Opening Size and Additional Wall Thickness of Models for Finite Element Analysis (F.E.A).....	39
2.3.3.3.	Modeling and Analyzing F.E. Wall Models in SAP2000 .....	40
2.4.	Shear Wall Testing.....	41
2.4.1.	Shear Wall Dimensions.....	42
2.4.2.	Footing –Wall Connection.....	43
2.4.3.	Shear Wall Reinforcement Detailing.....	44
2.4.4.	Shear Wall Testing Procedure .....	45
2.4.4.1.	Footing hold-down connection design .....	47
2.4.4.2.	Shear Strong Wall.....	48
2.4.4.3.	Hydraulic Actuator and Hydraulic Actuator Supporting Frame .....	48
2.4.4.4.	Strain Gauges.....	49
2.4.4.5.	Deflection Gauges -Linear Variable Differential Transducers (LVDT) .....	50
2.5.	Sustainable Construction Methodology in Building Insulated Concrete Wall .....	52
2.5.1.	Sustainable Principles in Building Process.....	52
2.5.2.	Construction Methods in Building ICF Walls .....	54
2.5.2.1.	Formwork Design and Construction.....	54
2.5.2.2.	Concrete Placement .....	56
2.6.	Construction Cost Comparison .....	56
CHAPTER 3. RESULTS .....		57
3.1.	Material Testing Results.....	57
3.1.1.	Compression Strength for Control Concrete Mix (Natural Aggregate).....	57
3.1.2.	Compression Strength for Experimental Concrete Mix (Recycled Aggregate) .....	57
3.1.3.	Flexural Strength of Experimental Concrete Mix (Recycled Aggregate) .....	59
3.2.	Shear Wall Testing Results .....	60
3.2.1.	Shear Wall Testing Result for Control Concrete Mix (SW1).....	60
3.2.2.	Load Displacement Analysis for SW1.....	60
3.2.3.	Shear Stiffness (G) of SW1.....	68

3.2.4.	Strain Analysis for SW1 .....	68
3.2.5.	Concrete Crack Analysis for SW1 .....	69
3.2.6.	Shear Wall Testing for Experimental Concrete Mix (SW2).....	72
3.2.7.	Load Displacement Analysis for SW2.....	72
3.2.8.	Shear Stiffness ( $G'$ ) for SW2.....	80
3.2.9.	Strain Analysis for SW2 .....	80
3.2.10.	Concrete Crack Analysis for SW2.....	81
3.3.	Cost Analysis.....	84
3.3.1.	Cost Analysis of Precast (Industry Standard) ICF .....	84
3.3.2.	Cost Analysis of Site-Build ICF Wall System.....	85
3.3.3.	Cost Analysis of Site-Build Sustainable ICF Wall System .....	86
CHAPTER 4. DISSCUSION AND CONCLUSION .....		88
4.1.	Material Testing Discussion.....	88
4.2.	Shear Wall Testing Discussion .....	89
4.3.	Cost Analysis Discussion.....	90
4.4.	Conclusion.....	92
4.5.	Recommendations for Future Work.....	93
References:.....		95
APPENDIX A.....		100
A-1.	Wind Load Calculations .....	101
A-2.	Sizing the Shear Wall Calculations .....	106
A-3.	F.E. Models of Shear Walls With Openings.....	107
A-4.	Dowel Design Calculations .....	116
A-5.	Formwork Design Calculations .....	117
A-6.	Shear Stiffness Calculations .....	120

## List of Figures

Figure 1. 1. Tornado Occurrence Map FEMA 342 Report (1999) .....	2
Figure 2.1. Gradation Curve for Limestone C67 Class 5S.....	28
Figure 2.2. Gradation Curve for Recycled Concrete Aggregate .....	30
Figure 2.3. Wind Load Profile Structure .....	34
Figure 2.4. Graphical Representation of Procedure for Calculating Wind Loads on the Structure (ASCE 07-10, Figure 27.4-1).....	35
Figure 2.5. Wind Wall Pressure ( $p_w$ ) and Roof Pressure ( $p_r$ ).....	37
Figure 2.6. Schematic Computation of Lateral Wind Force ( $P_w$ ).....	38
Figure 2.7. F.E. Model of 6" Thick Shear Wall with Double Door Opening.....	41
Figure 2.8. Shear Wall Dimensions.....	42
Figure 2.9. Insulated Concrete Form Walls .....	43
Figure 2.10. Reinforcement Mesh Design .....	45
Figure 2.11. Testing Constraint Connections– Overturning and Sliding Constraint Connections .....	48
Figure 2.12. Hydraulic Actuator and Hydraulic Actuator Supporting Frame .....	49
Figure 2.13. Strain Gauge Placement Position .....	50
Figure 2.14. Deflection Transducers Placement and Directional Orientation .....	51
Figure 2.15. Formwork Design .....	55
Figure 3.1. Experimental Mix Compression Test .....	58
Figure 3.2. Flexural Strength Testing for Experimental Concrete Mix.....	59
Figure 3.3. Control Wall Structural Failure .....	60
Figure 3.4. Load-Shear Displacement Curve SW1.....	61
Figure 3.5. Shear Deflections SW1.....	62
Figure 3.6. Crack Propagation at SW1 .....	63
Figure 3.7. Load–Lateral Displacement Curve SW1.....	64

<i>Figure 3.8. LDVT Deflection History SW1</i> .....	65
<i>Figure 3.9. Uplift Deflections SW1</i> .....	66
<i>Figure 3.10. Rotational Deflections (“toe” crushing) SW1</i> .....	67
<i>Figure 3.11. Load-Strain Curve SW1</i> .....	69
<i>Figure 3.12. Concrete Cracks Development</i> .....	70
<i>Figure 3.13. Cracks Generation at Load of 25,000lb (Front and Back Side)</i> .....	71
<i>Figure 3.14. Cracks Generation at Load of 30,000lb (Front and Back Side)</i> .....	71
<i>Figure 3.15. Cracks Generation at Failure Load (Front and Back Side)</i> .....	71
<i>Figure 3.16. Experimental Wall Bearing Failure SW2</i> .....	72
<i>Figure 3.17. Load Shear Displacement Curve SW2</i> .....	73
<i>Figure 3.18. Shear Deflections SW2</i> .....	74
<i>Figure 3.19. Load-Lateral Displacement Curve SW2</i> .....	75
<i>Figure 3.20. LVDTs Deflection History SW2</i> .....	76
<i>Figure 3.21. Uplift Deflections SW2</i> .....	77
<i>Figure 3.22. Uplift Deflection at SW2</i> .....	77
<i>Figure 3.23. Slipping Deflections SW2</i> .....	78
<i>Figure 3.24. Rotational Deflections SW2</i> .....	79
<i>Figure 3.25. Load-Strain Curve SW2</i> .....	80
<i>Figure 3.26. Concrete Crack Development and Propagation SW2</i> .....	81
<i>Figure 3.27. Cracks Generation at Load of 10,000lb (Front Side)</i> .....	82
<i>Figure 3.28. Crack Generation at Load of 21,000lb (Front Side)</i> .....	82
<i>Figure 3.29. Cracks Development at Load of 21,000 lb ( Lower Front Side)</i> .....	83
<i>Figure 3.30. Crack Generation at Failure Load (Front Side)</i> .....	83
<i>Figure 3.31. Precast ICF Wall</i> .....	84
<i>Figure 3.32 Formwork Job Build ICF Wall</i> .....	86
<i>Figure 3.33. Formwork Job Build Sustainable ICF Wall</i> .....	86
<i>Figure 4.1. Cost Comparison ICF Wall Systems</i> .....	86

<i>Appendix A-1 Figure 1. Wind Load Wall (<math>p_w</math>) and Roof Pressures (<math>p_r</math>) .....</i>	<i>104</i>
<i>Appendix A-3. Figure 1. Group 1. Model Dimensions .....</i>	<i>108</i>
<i>Appendix A-3. Figure 2. Wall With Double Door Opening Dimensions .....</i>	<i>110</i>
<i>Appendix A-3. Figure 3. Walls with Large Double Window Opening Dimensions .....</i>	<i>114</i>

*List of Tables*

<i>Table 2. 1. Summary of External Pressure Coefficients .....</i>	<i>36</i>
<i>Table 2. 2. Maximum Shear Stress and Deflection for F.E. Shear Wall Models .....</i>	<i>40</i>
<i>Table 2. 9. Concrete Control Mix Specifications.....</i>	<i>25</i>
<i>Table 2.10. Experimental Mix Specifications .....</i>	<i>26</i>
<i>Table 2. 3.Physical Properties for Gravel Sand 47B Aggregate .....</i>	<i>27</i>
<i>Table 2. 4. Physical Properties for Fine Sand 4110 Aggregate .....</i>	<i>27</i>
<i>Table 2. 5. Recycled Concrete Aggregate Physical Properties .....</i>	<i>29</i>
<i>Table 2. 6. Chemical Composition Nebraska Fly Ash Class C.....</i>	<i>31</i>
<i>Table 2.7. Physical Properties Nebraska Fly Ash Class C.....</i>	<i>31</i>
<i>Table 2.8. Foamular-250 Properties .....</i>	<i>32</i>
<i>Table 2.11. Formwork Spacing Limits.....</i>	<i>54</i>
<i>Table 3.1. Load –Deflection Analysis Summary SW1.....</i>	<i>68</i>
<i>Table 3.2. Load Deflection Analysis Summary SW2.....</i>	<i>79</i>
<i>Table 3. 3. Compression Test Results for Control Concrete Mix .....</i>	<i>57</i>
<i>Table 3.4. Compression test results for experimental mix (wet cured).....</i>	<i>58</i>
<i>Table 3.5. Compression tests (lab cured) .....</i>	<i>59</i>
<i>Table 3. 6. Cost Estimate of Precast ICF Walls .....</i>	<i>84</i>
<i>Table 3.7. Materials Used in Construction of Site Build ICF Wall System .....</i>	<i>85</i>

<i>Table 3.8. Cost Estimate of Job Build ICF Wall.....</i>	<i>86</i>
<i>Table 3.9. Cost Estimate of Job Build Sustainable ICF Wall.....</i>	<i>86</i>
<i>Table 3.9. Cost Estimate of Job Build Sustainable ICF Wall.....</i>	<i>86</i>

## **CHAPTER 1. INTRODUCTION**

### **1.1. Motivation**

*“Sustainable development is development that meets the needs of the present without compromising the ability of future generations to meet their own needs”*- from the World Commission on Environment and Development’s (The Brundtland Commission) report Our Common Future 1987.

Shear walls are primary structural systems that support building against lateral loads. Frame walls (frames) are the other type of structural systems that support buildings against lateral loads. General consensus is that in residential construction shear walls are made of concrete or masonry while frames are made of metal (steel or aluminum) or wood. Lateral loads on structure primary come from winds, earthquakes or blasts. The most critical wind load on residential structures comes from tornados and hurricanes. According to National Oceanic and Atmospheric Administration during 2011 total of 1,691 tornadoes and 176 casualties were reported across the country. These numbers are greater than any other on the record except for 2004, in which it was recorded total of 1,817 tornadoes. FEMA 342 Report (1999) stated that a single tornado in Oklahoma in 1999. “destroyed over 2,750 homes and apartments, damaged approximately 8,000 homes, and was responsible for 41 fatalities and approximately 800 injuries”. Estimated damages were over \$750 million.

The hurricanes are not frequent as tornados (Figure 1.) but they are more extensive and very destructive. The DIIO (2001) report estimated more than \$15 billion in insured property damage was caused by hurricane in 1992 in Florida. Majority of the assessed damaged was made

to residential wooden structures. Russell (2002) reported structural failures in single-family residential masonry structures due to hurricane Andrew in Florida 1992.

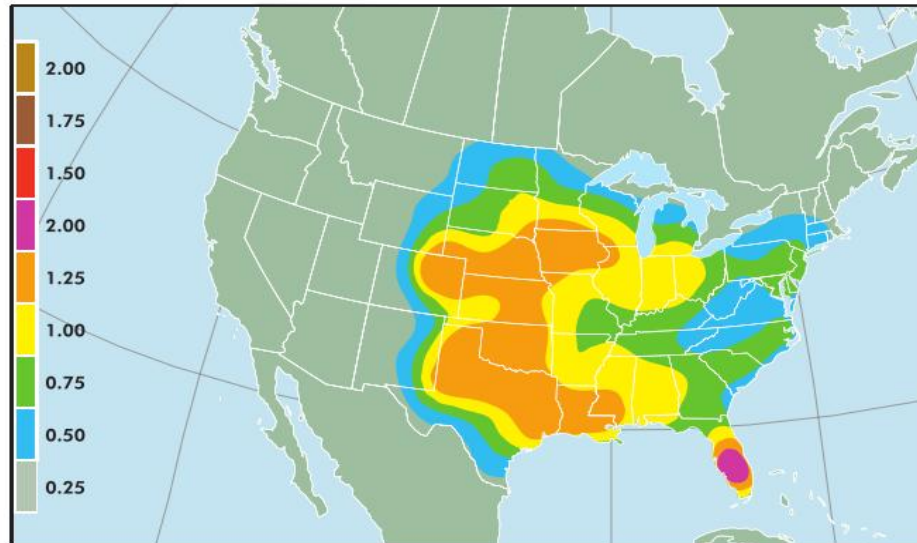


**FIGURE 2-1: Annual probability of tornado occurrence in the continental United States. The numbers in the scale on the left side of the map indicate the number of days per year with at least one tornado within the 2,500 square mile area around specific geographic points.**

**Figure 1. 1. Tornado Occurrence Map FEMA 342 Report (1999)<sup>1</sup>**

It is well documented that concrete shear walls are the most efficient lateral load resisting system. However, they are relatively rarely used in residential construction. The reasons for why contractors do not use concrete walls in residential construction were mostly cited as higher construction cost and slower construction paces (Mehta, 2002). However, a typical wood frame structure needs very costly upgrades for compliance with the codes in areas with high wind load demands. On the other hand concrete residential home would require little upgrading to abide by same high wind code requirements. It is assumed that in disaster prone areas, wood frame structures would have higher home insurance premiums compared to concrete shear wall system.

<sup>1</sup> Figure is taken from FEMA 342 Report (1999)

Additional savings for homeowner could come from energy efficient structural system. In order to address energy efficiency of the construction systems, it is suggested to combine materials with high thermal resistance properties with concrete to build energy efficient structural system (Tovey, 2007).

Currently there are multiple construction systems that use insulation layers to cover concrete core. These construction systems are known as Insulated Concrete Form (ICF) walls and have been patented almost 50 years ago. These walls have been use effectively as both gravity and shear resistant wall systems.

The studies have been conducted to address the shear resistance of the different types of ICF walls with and without openings (NAHB Research Center Report. 2001; 2002). The results suggest that residential shear walls have greater capacity to resist lateral loads than other types of residential walls such as wooden or steel frame walls. In order to better understand the behavior of ICF wall panels to in-plane shear loading, Mehrabi (1999) suggested developing finite element or simple analytical models and to further investigating effects of openings on ICF walls.

There are a few other challenges that residential construction industry faces in promoting sustainable design-build process. Incorporating sustainable concrete mixes in residential construction building process is one of them.

Presently, concrete is the most important and the most widely used building material in the construction industry. It was, conservatively, approximated that around 10 billion tons of concrete is produced each year (Nagaraj, 1993). Concrete prevalence as building material was based on concrete's superior advantages over the other building materials. The mix of concrete's

availability, affordability, applicability and mechanical properties, totals above other construction materials. However, to consider concrete structure to be sustainable, we should analyze impact that concrete's components enact on environment during extraction, utilization and maintenance.

Typical structural concrete contains about 10-15% of cement, 5-8 % of water and 70-80% of aggregate by mass. It is approximated that annual world consumption of cements is 1.6 billion tons, while annual world consumption of sand and rock totals up to 10 billion tons (Mehta, 2002).

While concrete itself is considered environmentally friendly material, environmental costs of the concrete components are not. In 2008, the United States (U.S.) produced approximately 66 million tons of Portland cement (European Cement Association Report 2008). It has been estimated that production of one ton of Portland cement generates one ton of CO<sub>2</sub> (Malhotra, 2000). Additionally, U.S. produces 2 billion tons of aggregate each year and that production is expected to increase to more than 2.5 billion tons per year by the year 2020 (Harrington, 2005). Mining, manufacturing and transporting of huge amounts of aggregate consume substantial amount of energy and initiates enormous environmental cost (Mehta, 2002).

To achieve positive sustainable ranking, concrete industry has to adopt strategies that will reduce environmental impact of cement production and aggregate mining. These strategies include decreasing amount of cement in concrete mixes by replacing it with cementitious material, replacing the natural aggregate with recycled concrete aggregate and to improving mechanical properties and durability of concrete mixes.

An additional environmental issue that concrete industry faces is the disposing construction and demolition waste at landfills. It is reported that over 1 billion tons of construction and demolition waste are generated in the world each year (Mehta, 2002). The most of that construction and demolition waste can be recycled cost-effectively and reused as replacement for the concrete aggregate (Mehta, 2000).

There are a number of studies that used fly ash, furnace slag, and silica fumes as substitute for Portland cement (Olorunsogo, 2002; Tavakoli, 1996; Sago, 2002; Acker, 1997; Wen-Chen, 2004). These studies suggested that is possible to replacing Portland cement with cemenitous substitutes and coarse aggregate with recycled concrete aggregate and still get high strength and good performing concrete.

Additionally, new construction structures could become more sustainable by increasing its energy efficiency. Structure's energy efficiency can be achieved by implementing utilization of the materials that have high thermal resistivity (R value). However, concrete is not known as a high thermally resistive material. An average R value of 4" thick structural concrete is only 0.8 which is about 25 times smaller than average R value of 4" thick extruded polystyrene form used in ICF walls. Energy savings achieved by utilizing ICF walls is an important component of sustainable development concept that has been promoted in the construction industry in last couple of years.

In order to address the need for tornado and hurricane resistant houses this study proposes, testing in-plane shear behavior of sustainable reinforced concrete wall build with sustainable construction methods.

Additionally, the study proposes new concrete mix to be implemented in building concrete residential structures. The new mix would be more environmentally friendly. This is achieved by replacing natural coarse aggregate with recycled concrete aggregate and replacing Portland cement with “greener” IPF cement.

Finally, the study proposes developing, a new, cost-effective, site-build lateral load resisting structural system that will be energy efficient, sustainable and easy to build.

## **1.2. Literature Review**

This section reviews research and information available on insulated concrete form walls, recycled aggregate used in concrete mixes, properties of self-consolidating concrete and shear wall design procedures.

### **1.2.1. Insulated Concrete Form Walls**

Insulated concrete form (ICF) is a precast construction system that is made of concrete core that is sandwiched between two layers of insulation material. Insulating materials are made of polystyrene foam, polyurethane foam or plywood sheets. Insulated forms are prefabricated and assembled at construction site. After the insulating form is cast in place concrete is poured between layers and reinforced with steel bars. Architectural surfaces are applied to interior and exterior wall sides, in order to protect insulating forms from environmental and human exposure.

As reported in the study for the U.S. Department of Housing and Urban Development (2001) construction cost of insulated concrete form (ICF) is 3-5 % higher compared to wood frame residential buildings. However, high thermal resistivity of ICF walls gives far higher return in energy cost-savings over lifetime of the structure compared to the regular wooden

frame structures. Some local residential building codes (Oregon Residential Energy Code, 2012) require that all new residential building walls have to have minimum thermal resistivity value of 15 (R=15), making ICF walls very economical and price competitive compared to other buildings systems. Furthermore, ICF wall homes are more durable and require less maintenance.

According to U.S. Department of Housing and Urban Development report (2001) typical advantages for using ICF in constructions are:

1. Structural Safety -ability to resist damage and protect occupants from fire, wind, earthquakes, and flooding.
2. Comfort- ability to evenly distribute the air temperature in the home and to reduce outside noise.
3. Energy Efficiency-ability to maintain low monthly energy cost.
4. Durability -ability to resist material degradation that may occur over time.
5. Sustainable Construction – ability to reuse construction materials and ability minimize amount of waste generated on site.

Another study (NAHB Research Center, 1998) reports similar advantages for using ICF in residential construction. The study lists better sound insulation, higher fire resistance rating and lower maintenance cost as additional ICF wall advantages.

There are few reported disadvantages (NAHB Research Center, 1998; 2001) when ICF are used in construction of ICW:

1. Cost of manufacturing of prefabricated ICF systems.

2. Need for trained labor.
3. Shipping and storage cost of ICF systems.
4. Constrains in height and rate of concrete placement.

According to the study (NAHB Research Center, 1998),“Site labor, either in the form of competent subcontractors or trained hourly employees, will impact a builder's decision to consider ICFs as a framing method. Regardless of how cost competitive an alternative is to wood framing, if the builder has limited choices for field installation, the risk of committing to ICFs as his or her framing method may be too great”. Thus, there is a need for the development of the ICF construction systems that will not need trained labor to install it.

At present, ICF accounts for only 3.0% of the total housing construction market in the US in 2005 (NAHB Research Center, 2005). However, due to recent spikes in energy prices and home energy efficient tax initiatives, future market for ICF could grow exponentially. American Recovery and Reinvestment Act, mandates significant funding for energy savings in federal buildings. It is approximated that the \$400 billion will be spent on major “green” projects in the commercial building sector (Energy Efficiency Retrofits for Commercial and Public Buildings - Pike Research 2011). Additionally, it is forecasted that energy efficiency savings projects will more than triple in annual revenue to \$6.6 billion by 2013.

### **1.2.2. Sustainable Concrete**

Sustainable concrete refers to concrete that “balances the desire to specify concrete with low environmental impact” (Concrete Center, 2011). The guideline published by Concrete center

in 2011 suggests that sustainable concrete should incorporate use of recycled aggregates, cementitious replacement additives (fly ash, slag silica fume) and admixture additives.

The admixture additives are used to modify physical properties of concrete mainly by making concrete more workable and more durable. The Cement Admixtures Association (CAA) estimates the use of the admixtures in concrete eliminates production of 600,000 tons of CO<sub>2</sub> per year. This number could be significantly higher if taken into account lower maintenance costs and more durable and better performance of concrete structures made with admixtures.

Additionally, the guideline recommends that designer should consider specifying concrete strength at 56<sup>th</sup> day rather than at conventional 28<sup>th</sup> day. The early strength of concrete is mostly dependable on type of Portland cement used and water cement ratio in concrete mix. The guideline argues that concrete mix made of recycled materials shows lower early strength compared to conventional concrete, but no significant difference in compressive strength in later stages. Since majority of residential units will not be occupied and fully in service before concrete reaches desired strength, making this specification will nullify the advantage that conventional concrete has over sustainable concrete.

The “Specifying Sustainable Concrete“ guideline suggests that recycled concrete aggregate should be used only when is locally available. The guideline argues that environmental impact of hauling recycled aggregates to job site will exceed the benefit of using it.

Local availability of recycled material should not be stumbling block in using sustainable concrete for the construction projects. Every year, the United States produces about 157 million metric tons of construction and demolition waste (Chini, 2007). Residential construction, renovation and demolition waste totals 67.5 million tons or 43%, while no-residential waste

(bridges, roads, high rise buildings) accounts for 90.2 million tons or 57 % (Franklin Associates, 1998).

According to EPA report (2003) only 20 to 30 percent of the produced waste is reused or recycled, meaning that more than 115 million tons of construction and demolition waste was landfilled. Franklin Associates report (1997) analyzed the composition of nonresidential construction demolition waste produced in the U.S. It was reported that approximately 66% of nonresidential construction demolition waste was concrete, 16% wood and 9% landfilled debris. It is estimated that about 45 million tons of concrete is landfilled each year in the United States.

Despite high availability of disposed concrete at land-fields, its potential has not been utilized. In current building practice, contractors and designers still give advantages to natural aggregates over recycled concrete aggregates.

After years of independent testing American Society for Testing and Materials (ASTM) and American Association of State Highway and Transportation Officials (AASHTO) have accepted recycled concrete as a source of aggregate into new concrete and have set the quality standards for its use (FHWA report, 2004). Currently, in many construction projects, use of recycled concrete aggregate (RCA) is to supplement the natural aggregates such as crushed stone, sand and gravel.

Michigan Department of Transportation allows the use of RCA as coarse aggregate in Portland cement concrete for curb and gutter, valley gutter, sidewalk, concrete barriers, driveways, temporary pavement, interchange ramps and shoulders (Standard Specifications of Construction, 2003). RCA is also allowed to be used as coarse aggregate in hot mix asphalt and as dense-graded aggregate for base course, surface course, shoulders, approaches and patching.

The use of RCA in a new concrete was initially associated with concrete's workability (flow) problems. It was previously documented that RCA is less dense and has higher water absorption rate than natural aggregate. Buck (1977) reported that shape and surface structure of RCA have more angles when compared to natural concrete aggregate (NCA). The density of RCA ranges from 2380 to 2410 kg/m<sup>3</sup> and SSD specific weight of recycled aggregate ranges from 2.34 to 2.49 (the specific weight of natural aggregate is from 2.50 to 2.61). Additionally the study found that the surface of RCA is more porous and rougher, thus making recycled concrete less dense than conventional concrete.

According to Hansen (1983) the absorption rate of RCA is 8.7% for diameter from 4 to 8 mm, 3.7% for diameter from 16 to 32mm (absorption rate of natural aggregate is only from 0.8% to 3.7%). Since RCA has higher absorption rate, study concluded that concrete mix with RCA needs 10 % more water in order to maintain its workability. The study did not report use any of admixture super-plasticizers in the mix that could address concrete workability problem. Nor did the study report the use of any water retarding admixture. The other solution to this problem could be pre-conditioning of the RCA. In later study, Topcu (1997) suggested that in order to mimic characteristics and performance of natural aggregate, RCA has to be cleaned, washed and its water absorption rate known. Sagoe (2002) also reported that the problem of RCA high water absorbency and the difficulty in maintaining a consistent and uniform saturated surface dry condition. Topcu (2004) also reported decreased workability of recycled concrete made of 50% RCA in concrete mixture.

FHWA Researchers have identified increase in creep and shrinkage when RCA is incorporated into new concrete. They suggested that this finding can be a major issue when RCA is used in structural concrete. Similarly, Limbachiya (2004) reported that shrinkage and creep are

increasing with increasing the RCA content in the mix. It is speculated that lower water/cement ratio in RCA concrete mix together with residual mortar on RCA contributes to increased shrinkage and creep in RCA concrete mixes. However, total RCA replacement of NCA in the concrete mix did not affect abrasion resistance for RCA concrete or did not deteriorated its freeze/thaw capacity.

Since studies have proven that RCA can affect concrete ductility, Xiao (2006) investigated how concrete frames made of RCA will behave under earthquake like loadings. Results showed that RCA frames have lower lateral loading capacity compared to NA frames. However, displacement and energy dissipations were similar between RCA and NA concrete frames, prompting authors to conclude that RCA structures are satisfying Chinese earthquake design standards and can be used in projects.

The concrete designers regularly question whether totally replacing the natural aggregates with RCA will affect concrete strength and other mechanical properties. A number of studies were conducted investigating the strength of the concrete achieved using RCA. The studies (Wen-Chen, 2004; Acker, 1997; Yaprak, 2011) speculated that original concrete quality, environmental exposure and concrete mix proportions effects compressive strength and durability of RCA concrete mixes.

Totally replacing natural aggregate with recycled concrete aggregate and mixing it with fly ash showed that RCA mix will yield lower compression strength but higher tensile strength compared to natural aggregate concrete mix (Wen-Chen, 2004). Another study showed that replacing natural coarse aggregate with 5%, 10% and 12.5 % of RCA will not significantly change expected compressive strength of the concrete (Acker, 1997).

It was reported that replacing only fine natural aggregate with fine RCA also reduces compressive strength of the produced concrete (Yaprak, 2011). But same study concluded that concrete with 50 % of fine RCA can still yield significant compressive strength of 25 MPa (3.5 ksi) at 28days. Additionally, concrete made of 100% of coarse RCA will yield lower early compressive strength, but it will still achieve targeted compressive strength (>70 MPa -10.1 ksi) after 60 days (Limbachiya, 2000).

Since RCA yields higher water absorption rate, it was questioned could RCA replace natural aggregate in high strength concrete (concrete used in structural beams and columns), and still maintain satisfactory engineering properties. Studies showed that if concrete with 100 % RCA has a water/cement ratio lower than concrete with natural aggregate it can produce higher compressive strength (Tavakoli, 1996; Sago, 2002; Olorunsogo, 2002). However, if the water/cement ratio in recycled concrete is kept the same as it is in conventional concrete than recycled concrete shows lower compressive strength (Richardson, 2010).

Because recycled concrete has higher water absorption rate, it was questioned whether it had the same durability properties as natural concrete. Results showed that concrete made of 30% of coarse RCA will have comparable engineering and durability characteristics as concrete made of natural aggregates (Limbachiya, 2004).

Some researchers suggest that if using RCA in structural concrete extra 5-10 % of cement should be added to account for lower compressive strength (Frondistoun-Yannas S, 1977).

Recent study (Tu, 2006) investigated applicability of replacing NA with RCA in high performance concrete (HPC). Results showed that slump, concrete resistivity, ultra pulse velocity and chloride penetration are similar between mixes of RCA and NA in high performance

concretes. However, compressive strength and long term durability values are lower at RCA when compared to NA concrete mixes. The study recommended that RCA should not be used in projects where HPC is required.

Recent research showed that compressive strength reduction and durability issues associated with RCA concrete could be avoided if using blast furnace slag in adequate proportions (Berndt, 2008). Slag has been shown to improve bonding between concrete and natural aggregate (Gao, 2003). Additionally, Otzuki (2003) reported that compressive strength of RCA concrete is dependent on microstructure of the interfacial transition zone between RCA and new cement paste.

Existing research has also shown that incorporating blast furnace slag in concrete mix can improve tensile strength of the RCA concrete. Replacing of 50% cement with slag led to improved tensile strength of a RCA concrete for 15 % when compared to NA concrete (Berndt, 2008). Similarly, Olorunsogo (2002) found that RCA concrete with 35 % of blast furnace slag-65 % Portland cement mix, had increased compressive and tensile strengths when compared to regular NA concrete mix.

### **1.2.3. Self-Consolidating Concrete**

Self-Consolidating Concrete (SCC) is highly flow-able concrete that fills the formwork without help of mechanical consolidation. Another characteristic of SCC is its ability to flow through heavily reinforced or oddly shaped structures effectively filling all voids without excessive aggregate segregation or excessive air migration.

The slump test for self-consolidated concrete ranges from 18-32 inches. The high flow characteristic of the SCC is obtained by using high range water reducing admixtures. The

resistance to segregation of aggregates when placing the concrete is obtained by using admixtures that can modify viscosity of the concrete mixture. In order to achieve high flow-ability and low aggregate segregation it is suggested that the maximal size aggregate for SCC to be 1 ½ inch.

According to National Ready Mix Association advantages of using SCC over regular concrete are:

1. Faster placement rate with no use of mechanical vibration devices.
2. SCC is less permeable, develops high early strength, and provides higher durability than regular concrete.
3. Uniform architectural surface.
4. Improved consolidation around reinforcement and better bond with reinforcement.
5. Improved pumpability and cast on site uniformity.
6. Shorter construction periods and less labor intensive inducing increasing labor savings and reducing labor costs.
7. Greater construction efficiency and increased job safety by eliminating the need for consolidation.

There are more than few reasons to use SCC mix in sustainable concrete. In general, fine material accounts for most the volume in the mix for SCC, making concrete more flow-able and cohesive. Some studies (Corinaldesi, 2004; Dyer, 2000) suggest that building rubble powder and

ash from municipal solid waste (MSW) can be used as a great sustainable mineral additive to cement. Corinaldesi (2004) showed that MSW ash have similar chemical and physical properties to coal fly ash and can be effectively used as substitute where coal fly ash is not locally available. Same study compared compressive strengths of SCC with the mix of rubble ash, MSW ash and recycled concrete aggregate to conventional concrete mix. The study found that SCC had lower early compressive strength compared to conventional concrete, but still able to achieve strength over 5 ksi after 28 days. When the mixes were examined by ultrasound pulse to check for aggregate segregation, conventional concrete showed higher deviation in ultrasound pulse velocity. The study concluded that conventional concrete shows higher level of aggregate segregation than self-consolidating concrete

Recent studies (Tu, 2005; Ali 2010) investigated the effect of using recycled concrete aggregate in self-consolidating concrete. Both studies reported that replacing coarse aggregate with recycled concrete aggregate will not significantly change structural properties of the concrete.

#### **1.2.4. Insulated Concrete Form Wall (ICF) as Shear Wall**

The shear wall is a structural element that resists lateral loads parallel to the plane of the wall. Generally there are two types of shear walls. The types are distinguished based on wall's height (H) to length (L) ratio. If the  $L/H < 0.5$  the wall is considered to be squat or short wall, while if the  $L/H > 2$ , the wall is considered to be slender wall. When  $L/H$  is between 0.5 and 2, this wall is considered to be something between slender and short wall (International Building Code, 2006).

Recognizing the need and the value of energy efficient residential structures, U.S. Department of Housing and Urban Development developed a guideline, Prescriptive Methods for Insulating Concrete Forms<sup>2</sup>, for the construction of one- and two-family residential dwellings using insulating concrete form (ICF) systems. The guideline's requirements were based on multiple structural codes: Building Code Requirements for Structural Concrete, Minimum Design Loads for Buildings and Other Structures, International Building Code and the International Residential Code.

The Prescriptive Methods were developed so ICF systems can be effectively used as structural lateral resistant systems (shear wall) in residential construction.

Wall's geometry also determines walls behavior. Flexural capacity (flexural deformations) governs behavior at slender walls, while shear capacity (shear based deformations) governs behavior at short wall. Additionally, when L/H ratio is between 0.5 and 1, diagonal shear cracking is the predominant shear mode failure (Cardenas, 1980).

Due to the nature and esthetics of residential construction it is highly unlikely that any exterior wall in the structure will not have some kind of sizeable opening (doors, windows, sky – lighting). Since the geometry dictates walls mechanical behavior, introducing wall opening into the wall geometry will additionally complicate wall's structural response to loading.

Taylor (1998) reported that openings that are relatively small to the wall's overall dimension can be neglected since they do not produce any significant effect to wall's shear or moment capacity. However, position of the opening will affect wall's performance. Alli and

---

<sup>2</sup> In further text Prescriptive Methods for Insulating Concrete Forms for simplification reasons are going to be referred as Prescriptive Methods

Wight (1990) reported that even narrow wall openings placed close to the wall's boundaries can significantly decrease slender wall's shear capacity.

Mehrabi (1999) conducted a series of tests on lateral resistance of residential insulated concrete wall panels, wooden and steel frames. One of the tested specimens was flat wall panel 4" thick with insulation from both sides. The wall was designed for wind up to 70 mph. The wall panel's horizontal reinforcement consisted of three horizontal bars, one on the top of the wall and two at about 1/3 of the wall height from the bottom while vertical reinforcement was provided with three vertical # 4 bars, spliced with foundation dowels. The results showed that concrete wall panel resisted about twice as much load as the maximum strength of a wood- and steel-frame wall panels without exhibiting any sign of damage or distress. This study acknowledged that the ICF wall systems are highly advantageous over other types of the commonly used wall systems in residential construction.

There are very few studies that have tested shear strength of cement mixes with recycled aggregate. Sogo (2007) tested shear strength of recycled aggregate beams with and without reinforcement. The study showed that when reinforcement is not used the shear strength of the beams with recycled aggregate is 10-30 % lower compared to natural aggregates. When shear reinforcement is used no significant difference is observed in shear strength of the specimens. However, there is a lack of research on using recycled aggregates in shear walls or using self-consolidating concrete in shear walls. .

Prescriptive Methods addresses characteristics of concrete mix that should be used in ICF wall panels. Recommended maximum slump of 6" (Prescriptive Methods, Section 2.2.1) is in the range of commonly used ready mix concretes. Prescriptive Methods does not stipulate use of self-consolidating concrete in ICF walls, however, it does approve that exception can be made

when maximum slump requirements may be exceeded for approved concrete mixtures resistant to segregation as long as minimum compressive strength requirement is met.

When choosing the insulated forms for the wall system one has to make sure that forms has to be strong enough to keep concrete in place during casting and to satisfy fire resistant conditions. Flame-spread rating of ICF forms that remain in place shall be less than 75 and smoke-development rating of such forms shall be less than 450, tested in accordance with ASTM E 84.

Prescriptive Methods also addresses minimum horizontal and vertical reinforcement in the wall and around openings. It was required that all opening reinforcement placed horizontally (one #4 bar) above or below an opening shall extend a minimum of 24 inches (610 mm) beyond the limits of the opening, while for the vertical reinforcement around opening it was required one #5 bar along the full height of the wall story within 12 inches (305 mm) of each side of the opening (Prescriptive Methods Section, Section 5.2). Both vertical and horizontal wall opening reinforcements will be added to already put wall's reinforcement. Prescriptive Methods also addresses connection between the footing and the wall stipulating that the dowels should be installed across the joint between the foundation wall and the footing at 48 inches (1.2 m) on center (Prescriptive Methods, Section 6.1). Foundation footing should be checked for one way shear, flexural strength and development length of reinforcing bars.

Building code for structural concrete (ACI 318-08) stipulates minimum vertical and horizontal shear reinforcement in the wall section (ACI 318-08, Sections 11.9.9.2 and 11.9.9.4). When designing the wall section, it has to be taken into the consideration that vertical shear reinforcement ratio- $\rho_l$  to gross concrete area of horizontal section (length of the wall( $lw$ ) \* width of the wall ( $ww$ )), should not be less than whichever is greater between 0.0025 or  $\rho_l$ . Equation

1.1. from the ACI 318-08 (11.9.9.2) code was used to calculate vertical shear reinforcement ratio.

$$\rho_l = 0.0025 + 0.5 \left( 2.5 - \frac{hw}{lw} \right) * (\rho_t - 0.0025) \quad (\text{Equation 1.1.})$$

Where,  $lw$  is overall length of the wall and  $hw$  is overall height of the wall. Spacing the vertical shear reinforcement shall not exceed the smallest of  $lw/3$ ,  $3h$  and 18 in.

Additionally, code stipulates minimum horizontal reinforcement in the wall section. Ratio of horizontal shear reinforcement to gross concrete area of vertical section  $\rho_t$  shall not be less than 0.0025 and the spacing shall not exceed the smallest of the  $lw/5$ ,  $3h$  and 18 in.

Both codes (Prescriptive Methods and ACI 318-08) do not provide exact design guidelines for the walls with openings. However, ACI 318-08 stipulates that any shear wall that is subject to lateral in plane loading shall be designed with shear provisions for the beams (ACI 318-08, Section 11.9.2). In addition to the minimum reinforcement ACI 318-08 code requires minimum of two #5 bars in walls having two layers of reinforcement in both directions and one #5 bar in walls having single layer of reinforcement to be placed around opening in both direction vertical and horizontal (ACI 318-08, Section 14.3.7). Prescriptive Methods has similar requirement for the walls designed for wind speeds greater than 110 mph. Prescriptive Methods stipulates placing two #4 bars or one #5 bars for the full height of the wall story within 12 inches on each side of the opening (Prescriptive Methods, Section 5.2, Table 5.6).

Additionally, Prescriptive Methods requires that flat ICF wall systems shall have a minimum concrete thickness of 5.5 inches (140 mm) for basement walls and 3.5 inches (89 mm) for above-grade walls (Prescriptive Methods, Section 2.1.1). Conversely, there is one rather strange stipulation in the Prescriptive Methods regarding minimum wall thickness around

openings. Prescriptive Methods requires that minimum depth (thickness) of concrete over the length of the opening for flat ICF walls to be 8 inches. Considering the nature of residential construction (pace and simplicity), in order to honor this stipulation all exterior wall profiles are going to be built with 8" thickness regardless of the wall opening.

### **1.3. Study Objectives**

#### **1.3.1. First Objective – Concrete Mixes**

The first objective of this study is to compare in plane shear strengths of the concrete shear walls that are made of two different concrete mixes. First concrete mix is the mix that is commonly used in residential construction. This mix is control mix.

The second mix (experimental mix) is the mix that had coarse aggregate replaced with recycled concrete aggregate, 20% of cement by mass replaced with fly ash, and Portland cement replaced with IPF cement.

#### **1.3.2. Second Objective –Determining Representative Residential Shear Wall**

##### **Model**

The second objective of this study is to determine representative residential shear wall model that is going to be build and tested. The walls are designed to withstand lateral loads caused by high velocity winds. These wind loads are custom for tornado and hurricane prone areas of the U.S.

In addressing the second objective, the study proposes developing numerical models of in-plane shear resistance of the walls with varying thickness and wall openings. Finite element

analyses of the models were performed in order to determine stress distribution throughout the wall profile. Based on F.E. analysis the most representative wall model will be constructed and tested for shear resistance.

The accuracy of the numerical ICF wall model will be validated with in-plane shear testing of full scale ICF wall.

### **1.3.3. Third Objective- Sustainability and Cost Comparison**

The third objective of this study is to incorporate sustainability concept into the construction of ICF walls. In addressing this objective, the study proposes development of a sustainable, cost-competitive job-built ICF system that can be easily transported, stored, and rapidly installed on site. The proposed job built ICF system will not require trained crew for installation and building, and all materials needed for construction would be locally available and easily accessible.

## **1.4. Hypothesis**

This section of the chapter lists working hypothesis in this study. Hypothesis will be tested analytically and experimentally.

**Hypothesis #1:** Test results for the shear wall made of experimental concrete mix will not be significantly greater than test results for the shear wall of regular concrete.

**Hypothesis #2:** Test results gotten from the testing a residential shear wall with control mix (SW1) will not be significantly greater than results gotten from the testing a residential shear wall with experimental mix (SW2)

**Hypothesis #3:** The cost of the construction of the job build insulated concrete form walls is not going to be significantly more expensive than the cost of construction of a precast insulated concrete form walls.

## **CHAPTER 2. METHODOLOGY OF EXPERIMENTAL ASSESMENT**

This chapter this chapter defines materials and concrete mix designs used in building insulated concrete form walls. It also lists instrumentation used to test flexural and compressive strength of concrete specimens.

Additionally, it presents the mathematical models used for analyzing effects of different wall opening, thickness and reinforcement on the wall shear capacity. It also lists methodology, instrumentation and experimental setting for testing wall's shear strength

Finally, it describes sustainable methods approach in building insulated concrete form walls.

### **2.1. Materials and Material Properties**

This section of the chapter describes concrete mixes and materials used in the study. Additionally it lists material properties and instrumentation used in testing concrete mixes.

#### **2.1.1. Concrete mix materials**

The materials used in the concrete mixes were: Portland cement type I, IPF cement, river sand, crushed limestone, recycled concrete aggregate, Nebraska fly ash class C, super-plasticizers admixture (glenium 3030).

#### **2.1.2. Concrete Mix Design**

This section of the chapter presents description of the mix designs used in the study. Two different mixes were used in this study.

1. Control concrete mixed presently used in residential construction (CC)

## 2. Experimental concrete mix consisting of self-consolidating recycled concrete (SCRC)

### 2.1.3. Control Concrete Mix

The control concrete mix contains sand (4110 and S47B) as fine aggregate, crush lime stone (C67 5S) as a coarse aggregate, water and Portland type I cement.

Quantities of natural aggregate concrete were optimized to achieve flow-ability and slump of 6" with air entrainment 5% and water/cement ratio of 0.427. The unit weight of the mix is 143.06 lb/ft<sup>3</sup>. For testing purposes, mixing took place in a mixing truck to simulate actual construction conditions. The material quantities used in the mix are presented in Table 2.3.

**Table 2.1. Concrete Control Mix Specifications**

<u>Material</u>	<u>Quantities</u>	
	<u>Proportion (%)</u>	<u>Batched (lb/cy)</u>
Portland Cement Type I	15.79	610
Water	6.75	260.8
Coarse Aggregate	69.79	2696
Fine Aggregate	7.66	296
Air entrainment additive (oz)-AAE90	0.01	2

Designed strength of the mix is designed to be 4 ksi at 28<sup>th</sup> day.

### 2.1.4. Experimental Concrete (SCRC) Mix

Experimental concrete mix (SCRC) contains recycled concrete as a coarse aggregate, graded sand (4100 and 47B) as fine aggregate, water, IPF cement and Nebraska class C fly ash. Twenty percent (20%) of IPF Duracem D cement by mass is replaced with Nebraska class C fly ash. Unit weight of the mix is 138 lbs/ft<sup>3</sup>. Self-consolidating agent Glenium 3030 (6 oz/cwt) is

used to achieve flow-ability and slump greater than 18” and air entrained agent Daravair 1400 is used to achieve air entrainment of 5%. The mix has water to cement ratio of 0.53 and water to cementitious paste (cement + fly ash) ratio of 0.42. Designed strength of the mix is 4 ksi at 28<sup>th</sup> day. The material quantities used for the mix of the concrete are presented in Table 2.4.

**Table 2.2. Experimental Mix Specifications**

<u>Material</u>	<u>Quantities</u>	
	<u>Proportion (%)</u>	<u>Batched(lb/cy)</u>
IPF Cement (75% of cementitious paste+25 fly ash class D)	16.11	600
Water	8.46	315
Recycled Coarse Aggregate (100%)	53.69	2000
Fine Aggregate-(Sand 4110)	7.79	290
Fine Aggregate (47 B sand gravel)	9.93	370
NE Fly Ash Class C	4.03	150
SC Agent- Glenium 3030 (oz/cwt)	0.01	9 <sub>(oz/cwt)</sub>
Air entrainment additive- Daravair 1400 (oz)	0.001	0.060

### 2.1.5. Natural aggregate

Natural aggregate used in this study consists of gravel sand (47B), fine sand (4110), and crushed limestone (C67 Class 5S). The gravel sand (47B) was classified as poorly graded sand (SP). Sample’s physical properties are shown in Table 2.5.

**Table 2.3. Physical Properties for Gravel Sand 47B Aggregate**

<b>TEST DESCRIPTION</b>	<b>TEST METHOD</b>	<b>RESULT</b>
Organic Impurities	ASTM C40	lighter std.
NaSO <sub>4</sub> soundness % loss (5 cycles)	ASTM C88	1.3
L.A. Abrasion % wear	ASTM C131	29.6
Min. Index Density pcf	ASTM D 4254	110.9
Max. Index Density pcf (WET)	ASTM D 4253	124.5
Max. Index Density pcf (DRY)	ASTM D 4253	128.6
Dry Unit Weight pcf	C 128	116.5
Bulk Specific Gravity SSD	C128	2.62
Permeability of Granular Soils cm/sec	ASTM D2434	0.0776

The fine sand (4110) was also classified as poorly graded sand (SP). Sample's physical properties are shown in Table 2.6.

**Table 2.4. Physical Properties for Fine Sand 4110 Aggregate**

<b>TEST DESCRIPTION</b>	<b>TEST METHOD</b>	<b>RESULT</b>
Organic Impurities	ASTM C40	lighter std.
NaSO <sub>4</sub> soundness % loss (5 cycles)	ASTM C88	1.3
L.A. Abrasion % wear	ASTM C131	29.6
Min. Index Density pcf	ASTM D 4254	107.2
Max. Index Density pcf (WET)	ASTM D 4253	119.5
Max. Index Density pcf (DRY)	ASTM D 4253	123.1
Dry Unit Weight pcf	C128	116.1
Bulk Specific Gravity SSD	C128	2.615
Absorption %	C128	0.3
Permeability of Granular Soils cm/sec	ASTM D2434	0.0434

loss was 0.7. Sample's grading curve is shown in Figure 2.13.

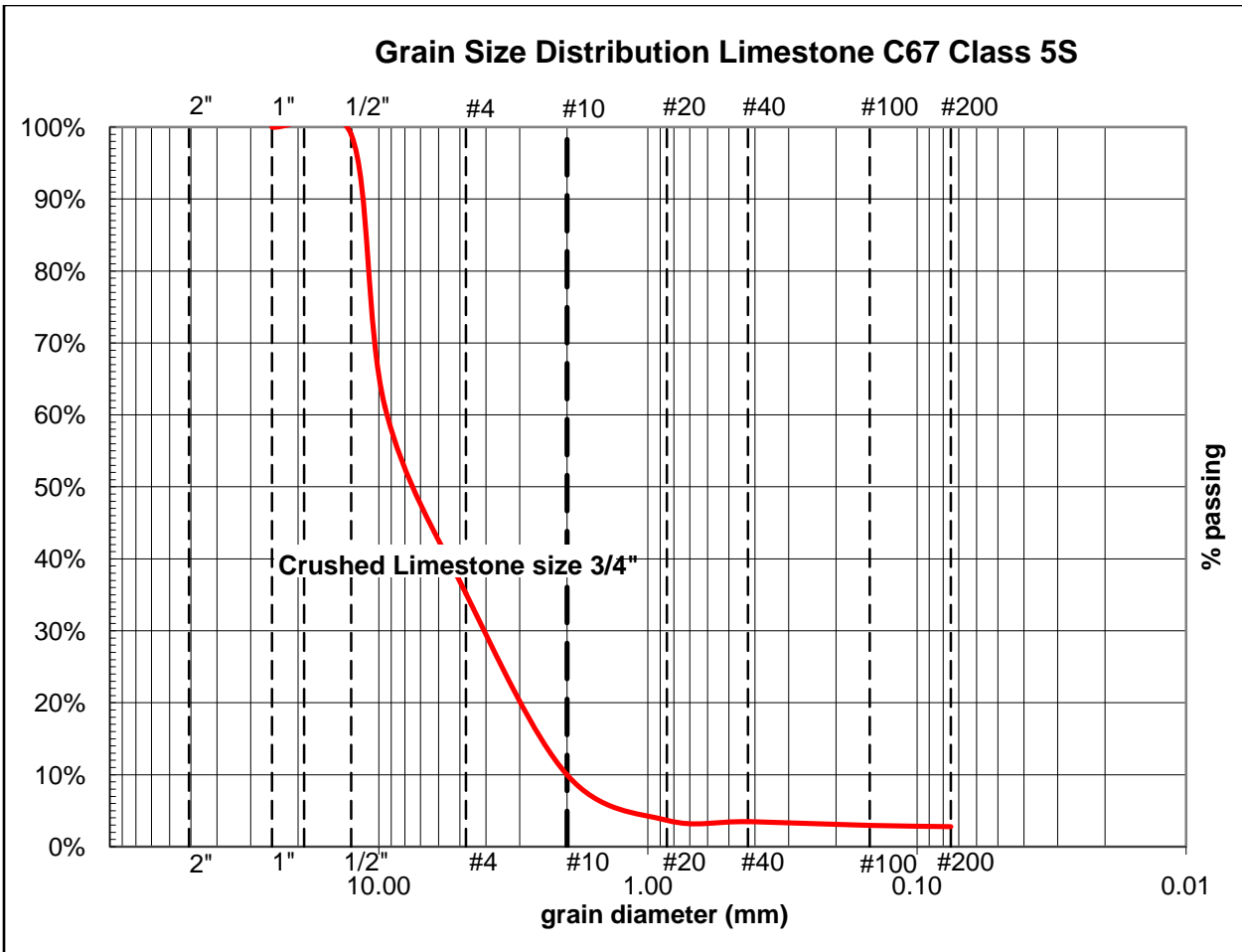


**Figure 2.1. Gradation Curve for Limestone C67 Class 5S**

### 2.1.6. Recycled concrete aggregate

Recycled concrete aggregate used in this study is supplied by the local distributor. The maximum size of aggregate is  $\frac{3}{4}$ ". This size was also recommended for use in self-consolidating concrete mixes. Recycled concrete aggregate was tested in accordance with P-207 Local Material Crushed Rock Base Course. The results are presented in Table 2.7.

**Table 2.5. Recycled Concrete Aggregate Physical Properties**

<b>TEST DESCRIPTION</b>	<b>TEST METHOD</b>	<b>RESULT</b>
<b>Specific Gravity and Absorption</b>		
Bulk Specific Gravity	ASTM C128	2.271
Bulk Specific Gravity SSD	ASTM C128	2.392
Apparent Specific Gravity	ASTM C128	2.584
Absorption (%)	ASTM C128	5.4
<b>Quality Tests</b>		
L.A. Abrasion (% wear)	ASTM C131	52.6
Freeze Thaw Soundness (% loss)	NDOR T103	10.1
Liquid Limit	ASTM D4318	NP
Plasticity Index	ASTM D4318	NP
Soundness of Aggregate ( % loss)		4.5

The recycled aggregate was classified as well graded sand (SW) with coefficient of curvature ( $C_c$ ) of 1.75 and Coefficient of uniformity ( $C_u$ ) of 18.48. The aggregate distribution curve is shown in Figure 2.14.

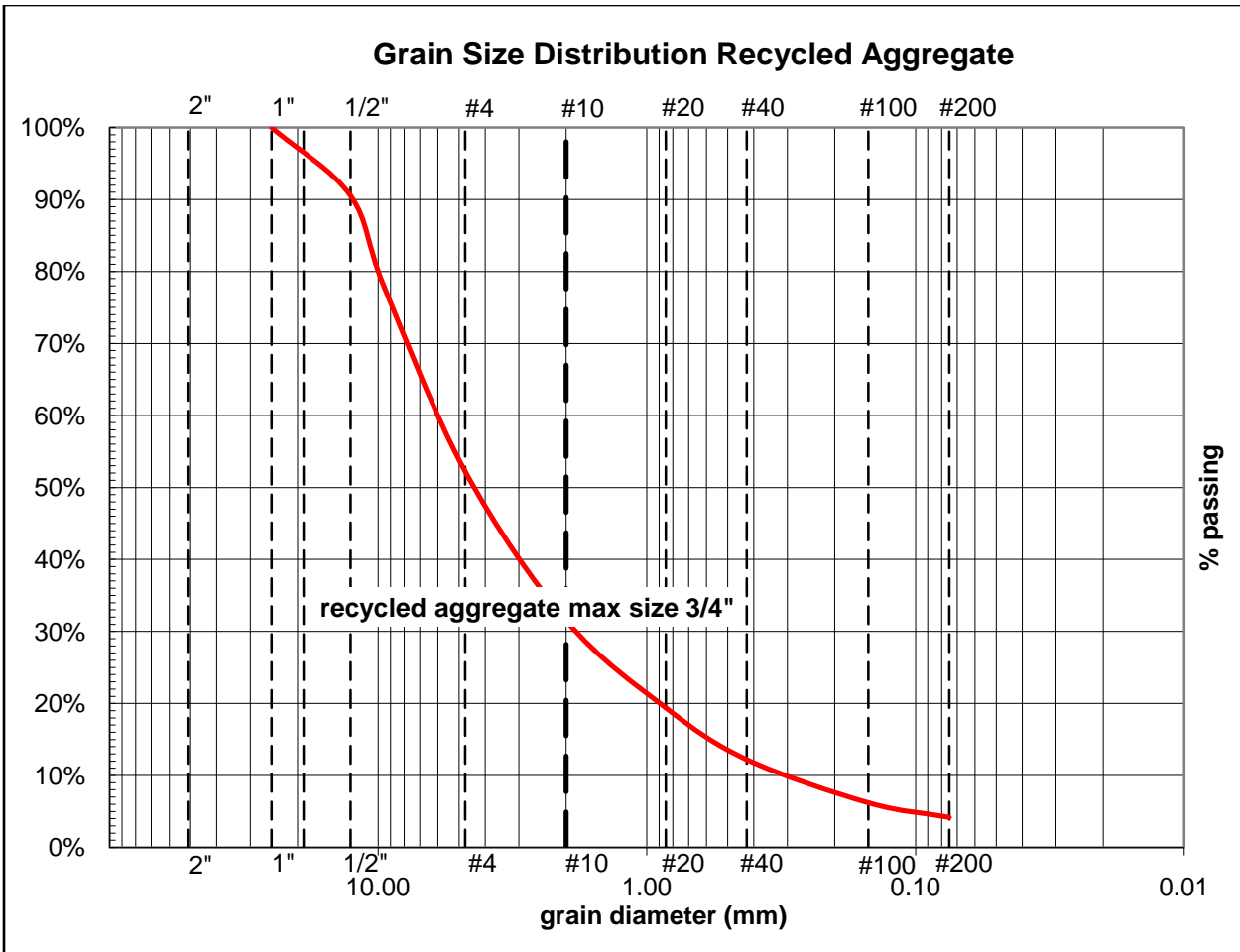


**Figure 2.2. Gradation Curve for Recycled Concrete Aggregate**

### 2.1.7. IPF Cement

IPF Duracem F is subtype of Portland cement that is mixed with 25% Class F fly ash. This cement is recommended to use in high performance concrete mixes. This type of concrete was produce to address metal mitigation problems (silica reactivity) of previously fly ash based concrete mixes and to increase concrete's sulfate resistance. Additionally, IPF cement is advertised to improve flexural and compressive strengths of concrete mixes.

### 2.1.8. Nebraska Fly Ash Class C

Nebraska Fly Ash Class C is cementitious additive used in the concrete mix. Fly ash is fine residue that is a byproduct of coal combustion in thermal power plants. Fly ash reacts with calcium released by cement hydration forming cement compounds. It is added to concrete to increase strength and reduce permeability. Nebraska Fly Ash Class C comes from the coal power plant in Nebraska City. Physical and chemical properties of Nebraska Fly Ash Class C are given in table below (Table 2.8. and 2.9.).

**Table 2. 6. Chemical Composition Nebraska Fly Ash Class C**

<b>Chemical Composition (mass %)</b>	
Silicon Oxide (SiO <sub>2</sub> )	35.4
Aluminum Oxide (Al <sub>2</sub> O <sub>3</sub> )	19.1
Iron Oxide (Fe <sub>2</sub> O <sub>3</sub> (T))	5.5
SUM (SiO <sub>2</sub> +Al <sub>2</sub> O <sub>3</sub> +Fe <sub>2</sub> O <sub>3</sub> (T))	60
Sulfur Trioxide (SO <sub>3</sub> )	2.3
Calcium Oxide (CaO)	25.5
Magnesium Oxide (MgO)	5
Moisture Content	0.1
Loss on Ignition	0.6

**Table 2.7. Physical Properties Nebraska Fly Ash Class C**

<b>Physical Properties</b>	
<i>Fineness</i>	
Retained on a 45- $\mu$ m sieve, (%)	14.7
<i>Strength Activity Index</i>	
With Portland Cement, (%)	
Ratio to Control @ 28 days	99
Ratio to Control @ 7 days	91
Water Requirement, (% of Control)	95
<i>Soundness</i>	
Autoclave Expansion, (%)	0.05
Density (grams per cubic cm)	2.56

### 2.1.9. Reinforcement materials

Steel #4 (0.5" diameter) bars size were meshed and used for longitudinal and transversal reinforcement to provide strength and serviceability. Reinforcement steel has modulus of elasticity of 29,000 ksi and yielding strength of 60 ksi.

### 2.1.10. Formwork materials

The materials used in building of a formwork were: expanded polystyrene panels (Table 2.10), plywood panels (thickness  $\frac{3}{4}$ "), lumber boards (dimensions 2"x4"x 8'), steel ties (diameter  $\frac{1}{2}$ ", length 72") and plastic tubes (diameter  $\frac{3}{4}$ ", length 6').

**Table 2.8. Foamular-250 Properties**

Density (lb/ft <sup>3</sup> )	Thermal Resistance R per 1" thickness (40°F)	Compressive Strength (psi)	Flexural Strength (psi)	Water Vapor Permanence of 1.0" thickness	Water Absorption (max volume %)
3	5	60	75	2.5	2

## 2.2. Concrete Sample Testing and Instrumentation

The unconfined compression test and flexural test were conducted to determine structural properties of the concrete specimens. All strength tests performed followed the specifications of American Standards for Testing Material (ASTM) Specifications.

### 2.2.1. Compressive strength test

To determine concrete compression strength compression tests (ASTM C 39) are conducted at 7, 14 and 28<sup>th</sup> day.

For compressive strength tests, 4“diameter, 6” long cylindrical specimens were casted for testing. Each concrete mix was tested at 7, 14 and 28 days. A compression testing machine (Manufacturer – Forney. Model : QC-400C-D2) was used for conducting compression test.

### **2.2.2. Flexural strength test**

To determine concrete flexural strength and it's modulus of rupture, the third-point loading flexural test (ASTM C-78) was performed using hydraulic flexure testing machine. For flexural tests prismatic beam specimens of dimension of 6 “x 6 “x 20 were casted. The load was applied at until sample's rupture. The maximum stress at the middle of the span is computed and reported as concrete flexural strength.

Since flexural capacity of normal concrete is well documented, only recycled concrete mix specimen was tested for flexural strength at 28th day. A universal flexural testing machine (Manufacturer– Tinius Olsen) was used in testing flexural strength of concrete.

### **2.3. Developing Numerical Models for Finite Element Analysis (FEA)**

This section presents steps carried out in developing numerical model for the Finite Element Analysis. The sections start with defining the model used for calculation of the wind load. The wind load is then converted into the single point load applied at the top of the wind wall. This load corresponds to in-plane lateral load applied to top of the shear wall. Once the lateral load is determined the model of the shear wall is modeled in the finite element software SAP2000 (Computers and Structures, Inc). The FEA is carried out and the stress distribution throughout the shear wall is determined. The capacity of the shear wall is compared to the demand and reinforcement, if needed, is designed. Subsequently, reinforcement design is compared to the ACI 318-08 code requirement and further analyzed.

### 2.3.1. Wind Load Structure Profile

According to the U.S. Census Bureau 2011, one-story residential homes account for 47% of all residential units build in the last 20 years. In 2010, the average single-family house was 2,392 square feet, while the average floor height is 8 ft. Based on the average square footage and average wall height, the study's structure profile used for calculation of the wind load is a wall 50 ft x 48 ft long and 8 ft high with roof height of 15 ft and slope of 15° (Figure 2.3). The length of the profile represents the average side of the single family one-story residential unit, while the profile's height represents average residential wall height. The roof height and roof slope are derived from the dimensions of the structure and they follow the provisions of the International Residential Code for One and Two Family Dwellings (IRC 2012, Section R301.3 Story height).

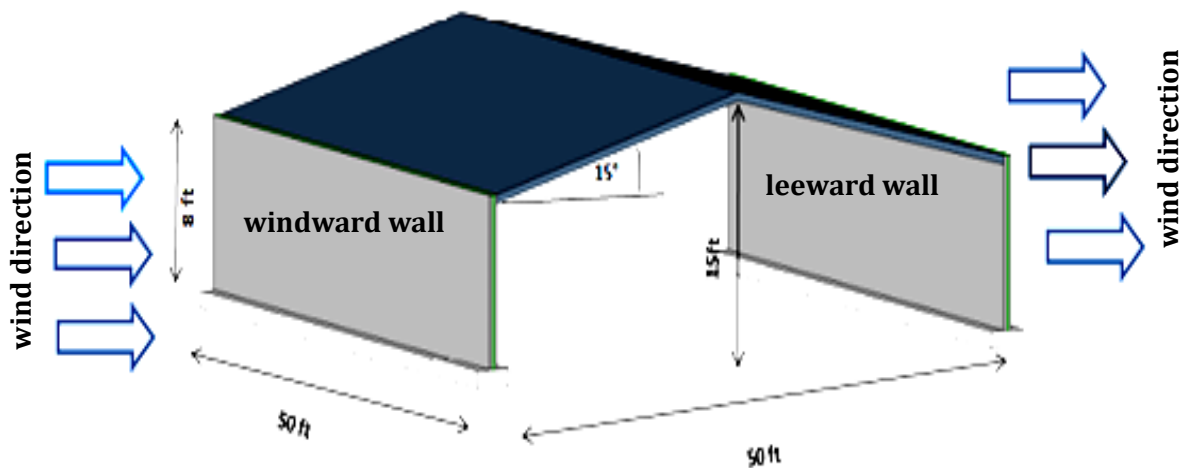


**Figure 2.3. Wind Load Profile Structure**

### 2.3.2. Wind Load Calculations<sup>3</sup>

The study used analytical procedure detailed in ASCE 07-10 for calculating wind loads. All equations used in the analytical procedure are referenced accordingly (Figure 2.4.).

According to Southeast Regional Climate Center map, majority of the tornados in Florida were type F2 (Fujita scale) with wind speeds of 113 -157 mph. The wind speeds greater than 155 mph corresponds to hurricane Category 5. Since the study assumes future application of the concrete shear walls in the tornado and hurricane prone areas, it was proposed that designed basic wind speed ( $V$ ) be 170 mph which correspond to basic wind speed from the ASCE 07-10 map for southern Florida.

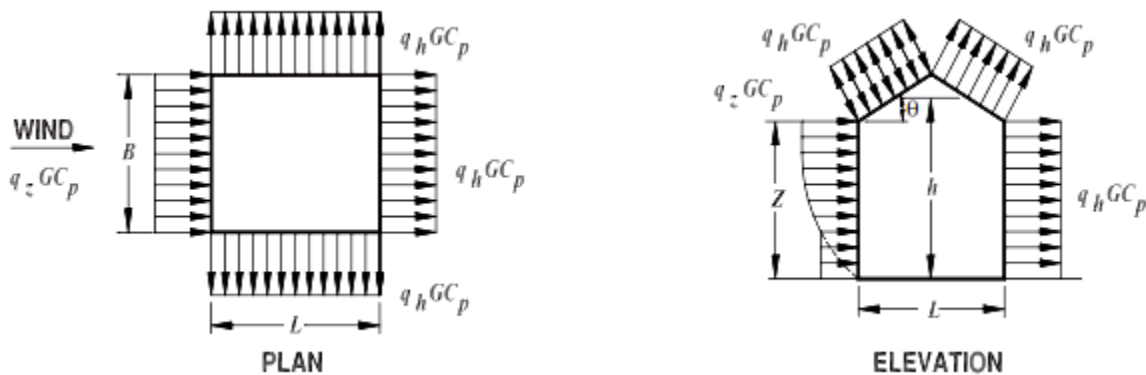


**Figure 2.4. Graphical Representation of Procedure for Calculating Wind Loads on the Structure (ASCE 07-10. Figure 27.4-1).**

a) *Wind Velocity Pressure Coefficient ( $q_z$ )*

Wind velocity pressure coefficient ( $q_z$ ) is calculated using code ASCE 07-10, Section 27.3-1, Equation 2.1.

<sup>3</sup> For detailed wind load calculations procedure go to Appendix A-1

$$q_z = 0.00256 K_z K_{zt} K_d V^2 I \quad (\text{Equation 2.1.})$$

$$q_z = 53.45 \text{ psf}$$

Since the total height of the building is  $\leq 15$  ft (wall + roof), therefore

$$q_z = q_h$$

where  $q_h$  is velocity pressure calculated at mean roof height from Equation 2.1. (ASCE 07-10, Section 27.3-1).

$$q_h = 53.45 \text{ psf}$$

*b) Internal Pressure Coefficient ( $GC_{pi}$ )*

Internal pressure coefficient is constant value for enclosed structures.

$$GC_{pi} = \pm 0.18$$

*c) External Pressure Coefficient ( $GC_p$ )*

The structure is considered rigid, with a gust factor,  $G=0.85$  (ASCE 07-10, Section 26.9.1). While pressure coefficient  $C_p$  for the walls is determined from ASCE 07-10 Table 27.4-1. External pressures for windward and leeward walls and roofs are calculated (Table 2.9)

**Table 2.9. Summary of External Pressure Coefficients**

Wall Orientation	External Pressure Coefficient
Windward wall	0.68
Leeward wall	0.425
Roof windward	-0.595
Roof leeward	-0.425

d) *Design Pressure (p)*

Wind Pressure Equation used (Equation 2.2) for calculating the pressure design ( $p$ ) combines internal and external design pressures ASCE 07-10, Section 27.4-1.

$$p = qGC_p - q_i(GC_{pi}) \quad (\text{Equation 2.2})$$

Design pressure ( $p$ ) is broken down into two wind load pressures: wall pressure ( $p_w$ ) and roof pressure ( $p_r$ ) (Figure 2.5).

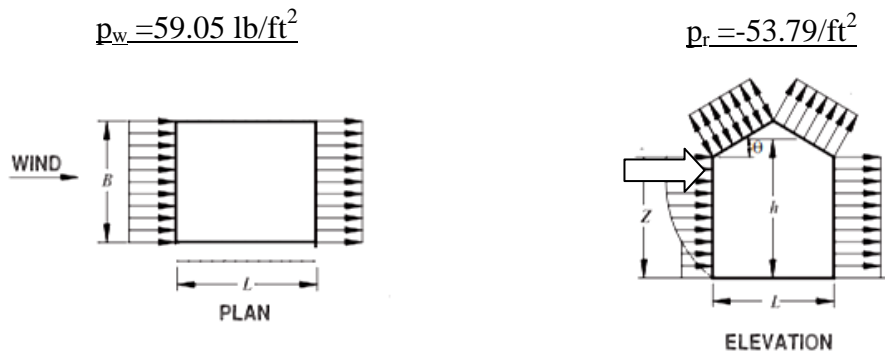


**Figure 2.5. Wind Wall Pressure ( $p_w$ ) and Roof Pressure ( $p_r$ )**

e) *Total Wind Load (W)*

Total wind loads acting on the structure come from the wind wall pressure and from the roof's wind pressures.

Total wind load acting on structure is calculated to be  $\underline{W = 848.93 \text{ lb/ft}}$ .

f) *Lateral Wind Force ( $P_w$ )*

Lateral wind force ( $P_w$ ) on wall is calculated from the total wind load ( $W$ ) acting parallel to the shear wall (Figure 2.6.).

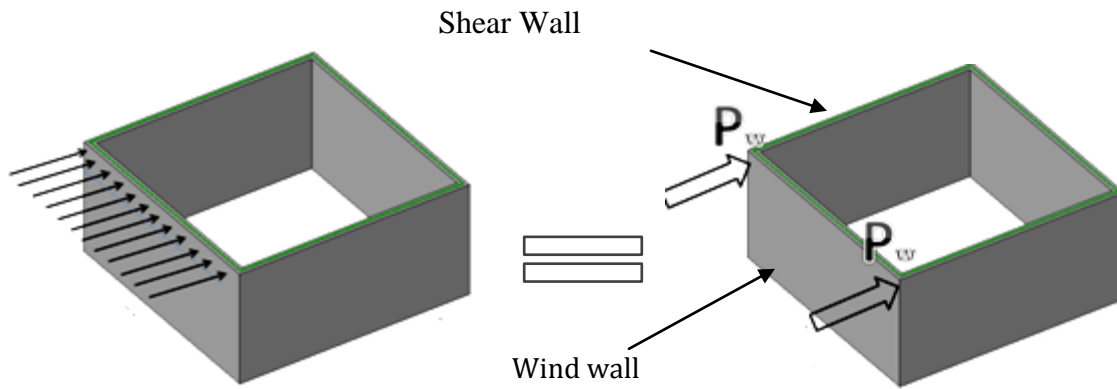


**Figure 2.6. Schematic Computation of Lateral Wind Force ( $P_w$ )**

Lateral wind force was calculated to be  $P_w = 21.22$  kips. This force was used as design shear force  $V_{\max}$  ( $V_u$ ) in computer models in order to analyze behavior and stress distribution of the shear walls.

### **2.3.3. Computer Models for Finite Element Analysis**

This section describes procedure used in developing F.E. models of residential shear walls.

#### **2.3.3.1. Preliminary calculations for sizing the shear wall**

Since the lateral forces on residential structures are relatively small compared to commercial structures, it was proposed that lateral wind (shear) force should primarily be resisted by concrete. However, designing the whole structure's length (48ft) as a shear wall was determined to be impractical and rather wasteful. Consequently, the length of 14 ft was calculated to be appropriated length for the shear wall analysis<sup>4</sup>.

<sup>4</sup> Detailed procedure and calculations for initial length of the shear wall is given at Appendix A-2

### **2.3.3.2. Determining the Opening Size and Additional Wall Thickness of Models for Finite Element Analysis (F.E.A)**

The length and the size of the openings should replicate commonly used wall features in residential construction. The minimum residential wall thickness required by International Code is 4" (Prescriptive Methods would allow minimum flat wall thickness of 3.5" in certain cases).

In order to keep a number of F.E. models relatively reasonable, it was decided that additional 5" and 6" wall thickness will be analyzed. Analyzing the 10" wall thickness was ruled out since by the ACI 318-07 code requirement, 10" thick wall would need minimum of 2 layers of reinforcement, which in this case would complicate comparison, and it was foreseen as highly over-conservative design. Prescriptive Methods stipulate that concrete thickness (depth) over the size of the opening has to be minimum 8" so this wall thickness is also included in the analysis.

The total of 12 finite element models are developed and analyzed. The following is breakdown of the finite element models:

- a) Group 1:- Three single window opening (2ft x 4 ft) with wall thickness of 4, 5, 6 and 8 inches,
- b) Group 2: - Double-door opening (6 ft x 6.8 ft) with wall thickness of 4, 5, 6 and 8 inches,
- c) Group 3: -Large double window opening (6ft x 5.8 ft) with wall thickness of 4, 5, 6 and 8 inches.

To minimize model variability total area of the wall openings for all 3 groups was kept relatively close to 20-30% of the total wall area.

When determining wall openings, additional look was given to the orientation and symmetry of the openings in respect to the wall's dimensions.

### 2.3.3.3. Modeling and Analyzing F.E. Wall Models in SAP2000

All shear wall models are modeled and analyzed in SAP200 finite element analysis software in order to determine best wall candidate. The maximal shear stress and maximal deflection for each model are calculated and presented in Table 2.10<sup>5</sup>.

**Table 2. 10. Maximum Shear Stress and Deflection for F.E. Shear Wall Models**

<b>F.E. Model</b>	<b>Wall Thickness (in)</b>	<b>Maximum Shear Stress (psi)</b>	<b>Maximum Deflection (in)</b>
Three single window - Group 1	4	-141.1	-0.0194
Three single window - Group 1	5	-113.06	-0.0156
Three single window - Group 1	6	-94.22	- 0.013
Three single window - Group 1	8	-70.66	-0.097
Double-door – Group 2	4	-129.38	-0.025
Double-door – Group 2	5	-103.55	-0.02
<b>Double-door – Group 2</b>	<b>6</b>	<b>-98.92</b>	<b>-0.0165</b>
Double-door – Group 2	8	-74.19	-0.0121
Large double window – Group 3	4	-149.5	- 0.027
Large double window – Group 3	5	-119.2	-0.0185
Large double window – Group 3	6	-99.55	- 0.015
Large double window – Group 3	8	-74.66	- 0.0114

<sup>5</sup> Detailed calculations for FEA models are presented in Appendix A-3

After detailed analysis of F.E. models it was decided that numerical model 6" thick wall from Group 2. is the best candidate to be a tested as representative residential shear wall. The main reason why it was decided Group 2. was the best model for testing is that the deflection failure mode pattern seems to be the most critical at this group. Deflection pattern of the beam that connects two solid panel sections of the wall could be the easily observed and confirmed (Figure 2.7).

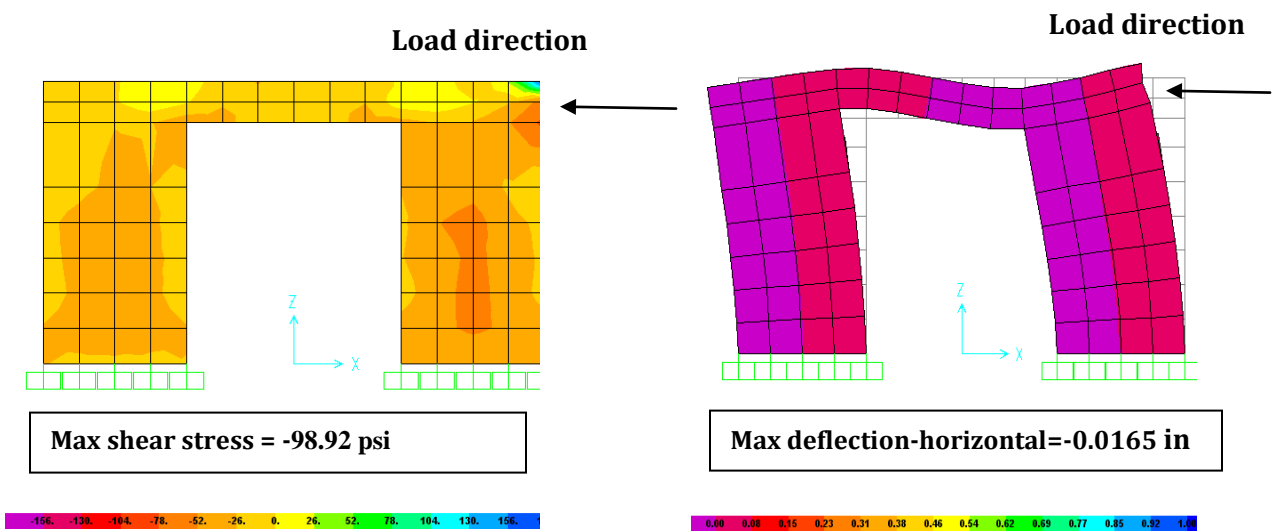


**Figure 2.7. F.E. Model of 6" Thick Shear Wall with Double Door Opening**

## 2.4. Shear Wall Testing

This section of the chapter describes finalized shear wall design including wall dimension and reinforcement detailing. Additionally this section presents testing procedure and instrumentation used in testing the wall specimen.

### 2.4.1. Shear Wall Dimensions

The study proposed building concrete wall that is 8 ft (96in) high, 14 ft (168in) long and 6 in thick, with the double door opening in the middle of the wall that is 6.83 ft (82 in) high, 6 ft (72 in) long (Figure 2.8.).

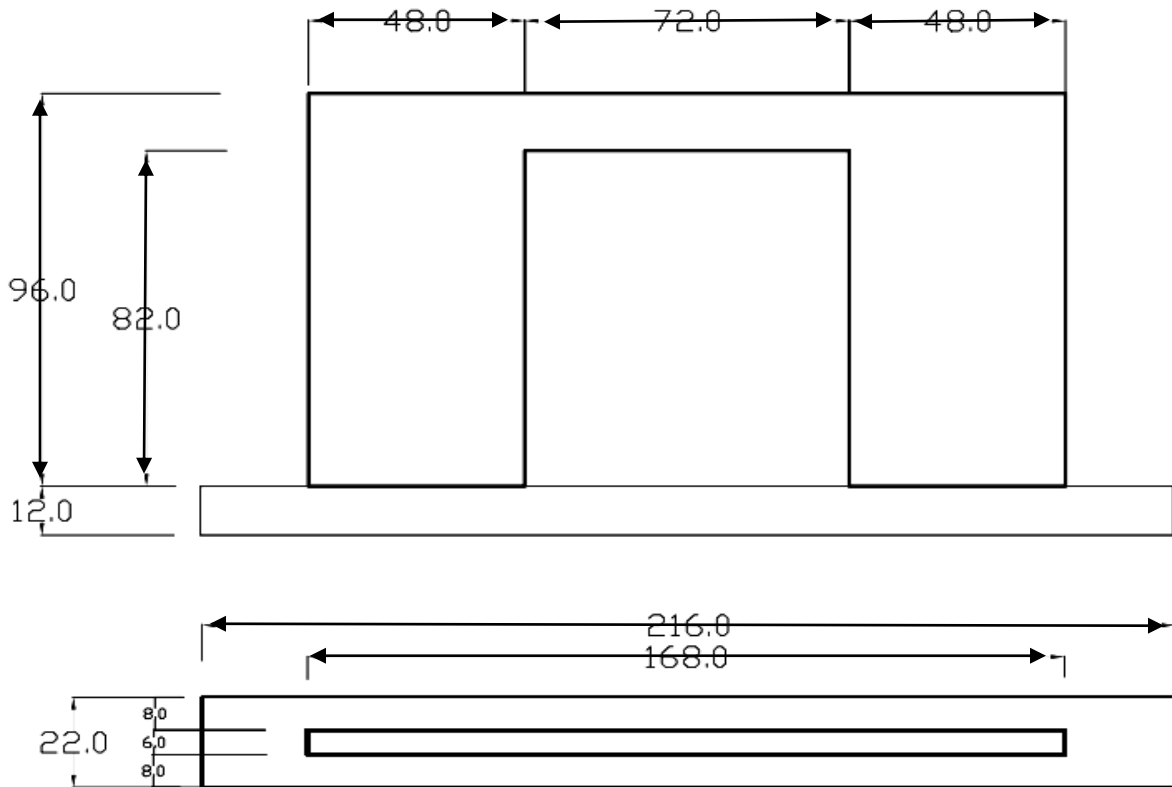


**Figure 2.8. Shear Wall Dimensions**

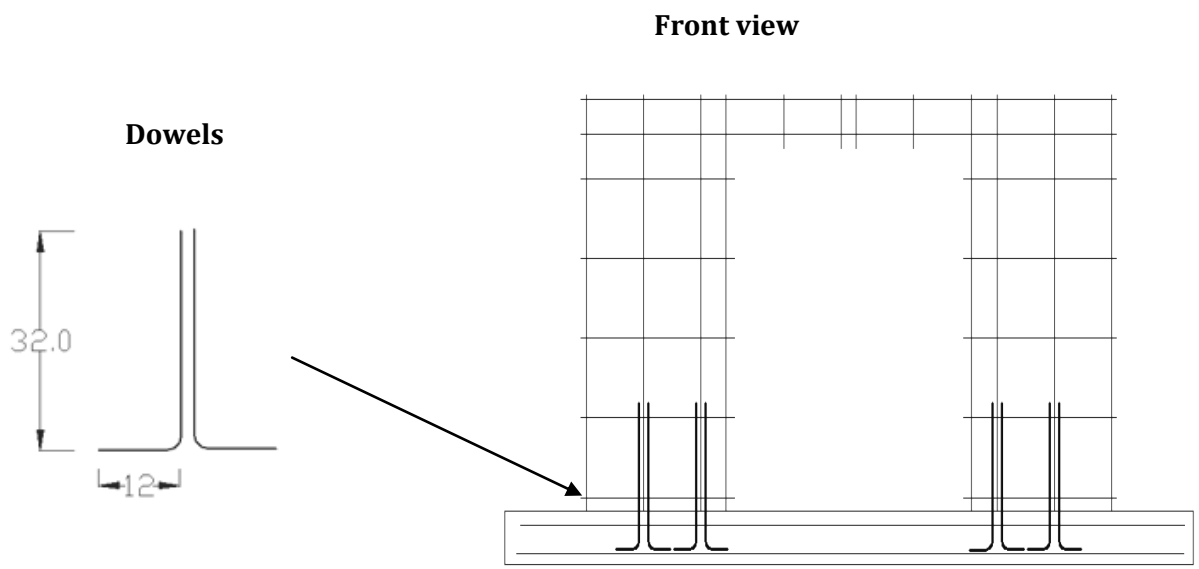
The wall is sandwiched between 2" thick insulation panels and placed over concrete footing that is 18 ft (216 in) long, 1.83 ft (22 in) wide and 1ft (12in) high (Figure 2.9).



**Figure 2.9. Insulated Concrete Form Walls**

### 2.4.2. Footing –Wall Connection

Shear wall footing was designed to mimic cast in place residential footings. Footing concrete strength was designed for  $f'c=8$  ksi. Footing reinforcement<sup>6</sup> was designed to withstand flexural loads coming from the self weight and walls weight while being lifted and transported to testing position. Footing's dowels (footing-wall connections) consist of four #5 bars spaced 18" on center. Total length of the dowel is 32". Dowels are spliced with vertical reinforcement.



<sup>6</sup> Footing detailed reinforcement is presented in Appendix A-4

### 2.4.3. Shear Wall Reinforcement Detailing

During preliminary design it was determined that wall has enough shear capacity in concrete and that it needs only minimum reinforcement (Appendix A-2). Minimum reinforcement for the shear wall is designed as vertical and horizontal mesh of #4 bars ( $A_s = 0.2 \text{ in}^2$ ). ACI 318 -07, Section 11.9.2 stipulates spacing limits for minimum vertical reinforcement, which is a minimum of the following:

a)  $l_w/5$ , where  $l_w$  is length of the wall

$$l_w/5 = 168/5 = 33.6 \text{ in}$$

b)  $3h$ , where  $h$  is thickness of the wall

$$3h = 3 \times 6 = 18 \text{ in}$$

c) 18 in.

Spacing limits for horizontal reinforcement is a minimum of the following

a)  $l_w/3$ , where  $l_w$  is length of the wall

$$l_w/3 = 168/3 = 56 \text{ in}$$

b)  $3h$ , where  $h$  is thickness of the wall

$$3h = 3 \times 6 = 18 \text{ in}$$

c) 18 in.

Additional stipulation requires one #5 bar, in walls having single layer of reinforcement to be placed around opening in both direction vertical and horizontal (ACI 318-08, Section 14.3.7). However, Prospective Methods in the commentary acknowledges that adding # 5 bars that even though recommended, it is considered over designed and impractical for construction purposes (C 5.2.). International Building Code (IBC) suggests that one #4 bar from each side of the opening is enough to satisfy loading conditions as long as vertical #4 bar has continues span

from support to support. The final reinforcement design is a mesh of #4 bars spaced at 18" in both directions with added bars around opening (Figure 2.10).

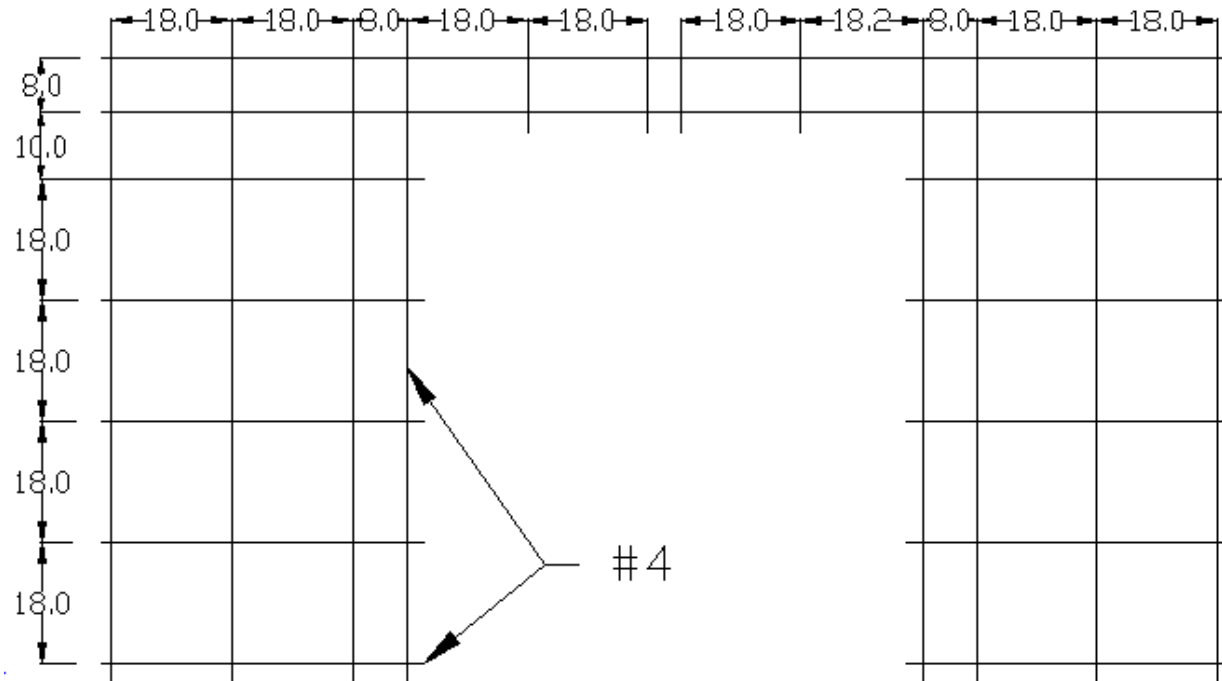


**Figure 2.10. Reinforcement Mesh Design**

#### **2.4.4. Shear Wall Testing Procedure**

Shear wall testing has taken place in the University of Nebraska–Lincoln Structural Lab at PKI. Tests were conducted after concrete's curing period of 28 days. The shear walls were tested in vertical position. Overturning restraint connections that were attached at the leading edge and at mid-span of the footing are preventing overturning failure of the specimen. These hold-down connections are anchoring footing to the structural lab strong floor. Shear wall sliding was prevented by 12"x 12" x 2" steel plate that was anchored to a strong floor while bearing on in-plane back edge of the shear wall's footing (Figure 2.11).

In order to mimic innovative single story residential construction, testing setup for ASTM E 564 - 2000 needed to be modified to better serve testing purpose. Testing setup provisions for ASTM E 564 (Section 5.4) suggest that loading condition should be uniformly distributed along top edge of the wall to simulate roof or floor members that will be used in building construction. Merhabi (1999) and NAHB Research Center (2002) used cast in place concrete beams to distribute later loads from an actuator to the top edge of the wall. Cast in place beams are used to replicate cold joint between ICF walls and floor slab. However, given that this study proposes using efficient job build ICF formwork systems, that allows concrete placement rate of over 15 ft/h, it is assumed that building's floor-wall system would be cast at once, and no cold joint would be needed. This innovative design would significantly lower construction cost and shorten construction time. Knowing this, it was proposed that lateral load from the actuator is applied directly to the upper edge of the shear wall.

Before data collection, a small initial load (10 % of the theoretical ultimate load) was applied to a testing wall. The load was held for a few minutes to seat the connections between the wall and footing. The initial load was then removed. After data acquisition system is initialized, testing procedure started with lateral load being increased gradually. Lateral load is applied at a rate of 0.2 in/ min. A 100,000 lb load cell was attached to the end of the actuator to facilitate data acquisition.

Seven, linear variable differential transducer (LVDT), were used to measure the displacement of the wall during the tests. Additional control markings were placed at the bottom edge on the out of plane face of footing and at the bottom edge on in-plane face of the footing. These markings are to measure horizontal slip and uplift of the footing. Four strain gauges are placed on the compression sides of the wall to detect strain deformation on the concrete surface.

The static lateral loading test was conducted until displacement of the top of the wall reaches 2", or until wall shear strength had been considerably reduced from the maximal value, due to significant structural damage in the specimens. Data from the load cell, strain gauges and LVDTs are collected at 2 times per second. Additionally, shear wall's crack development and crack propagations are observed and marked during testing. Whole procedure is video-taped with digital camera.

#### **2.4.4.1. Footing hold-down connection design**

In order to reach wall's full shear capacity it is imperative to prevent overturning, or sliding failure of the wall. To prevent wall's overturning footings are anchored to the strong floor with two 2" in diameter, 24" long, treaded steel bolts. Each bolt is penetrating through 12" deep concrete footing through pre-casted, specially designed holes. Before concrete footing is casted, two 3" diameter hollow plastic tubes were placed inside the formwork, at specially designated position and left until concrete is harden. The holes' positions in the footing are mirroring strong floor anchoring holes. After concrete was hardened plastic tubes were taken out and steel bolts were put through the footing and screwed into anchoring hole. The 12" x 12" x 2" steel plate was put over the steel bolt and laid on the top of the concrete footing. The steel heavy duty nut is screwed on steel bolt and secured steel plate preventing overturning of the whole structure. At the back edge of the footing 12" x 12" x 2" steel plate is anchored directly into the strong floor with one side bearing onto the footing preventing sliding motion of the structure ( Figure 2.11).

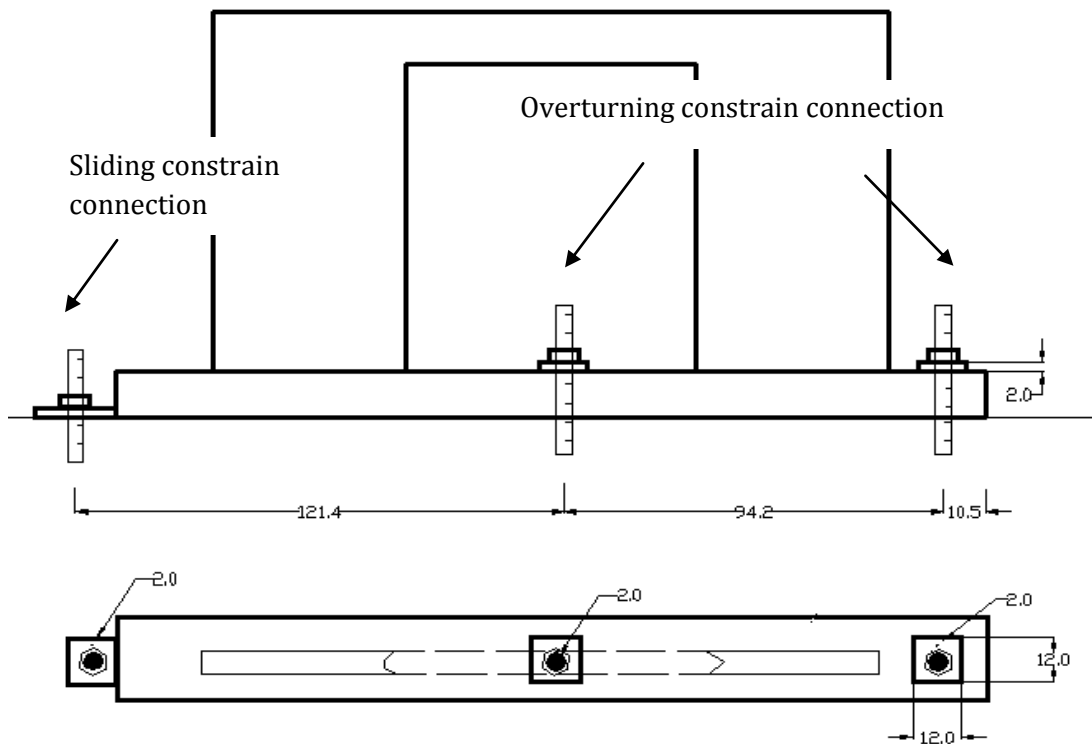


**Figure 2.11. Testing Constrain Connections– Overturning and Sliding Constrain Connections**

#### **2.4.4.2. Shear Strong Wall**

Shear Strong Wall is 25 ft high, 6 ft long and 6.5 ft deep ft anchoring wall that is used in testing of shear capacity.

Shear Strong Wall is heavily reinforced high strength concrete structure with 3” anchoring wholes spaced at 23” at center along the height of the wall.

#### **2.4.4.3. Hydraulic Actuator and Hydraulic Actuator Supporting Frame**

A hydraulic actuator is a testing machine with 23” long loading jack with outer diameter of 7” with push-out range of 10 in and capacity of 120,000 lb (Figure 2.12). A hydraulic actuator is attached to a support frame that is anchored to lab’s strong wall. Support frame is a

steel structure designed to hold actuator in place. Support frame consists of two 3.5" x 3.5" x 0.2" steel channels connected at top with 14"x 6"x 0.5" steel plate. Actuator anchoring steel plate is connected to steel channels and support steel plate with 7/8" bolts and firmly tightened. Frame is anchored to a strong wall with 1" in diameter treaded steel rod that is tightened to a steel plate.

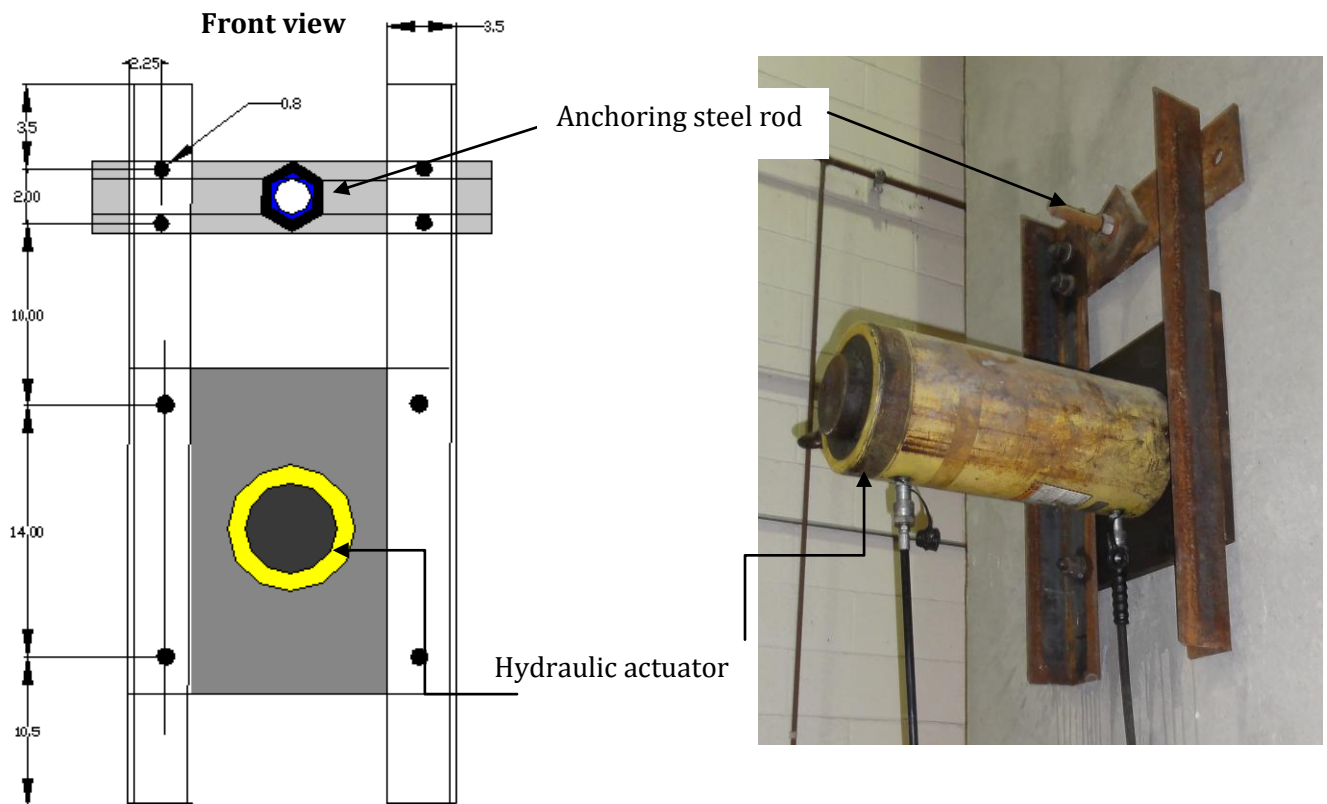


**Figure 2.12. Hydraulic Actuator and Hydraulic Actuator Supporting Frame**

#### 2.4.4.4. Strain Gauges

The total of four PL-60 wire strain gauges were used to measure strain on the in-plane compression face of the wall (Figure 2.13).

- a) First strain gauge (s1) and third strain gauge (s3) are placed 24" above the footing.
- b) Second strain gauge (s2) and fourth strain gauge (s4) are placed at 72" above the footing

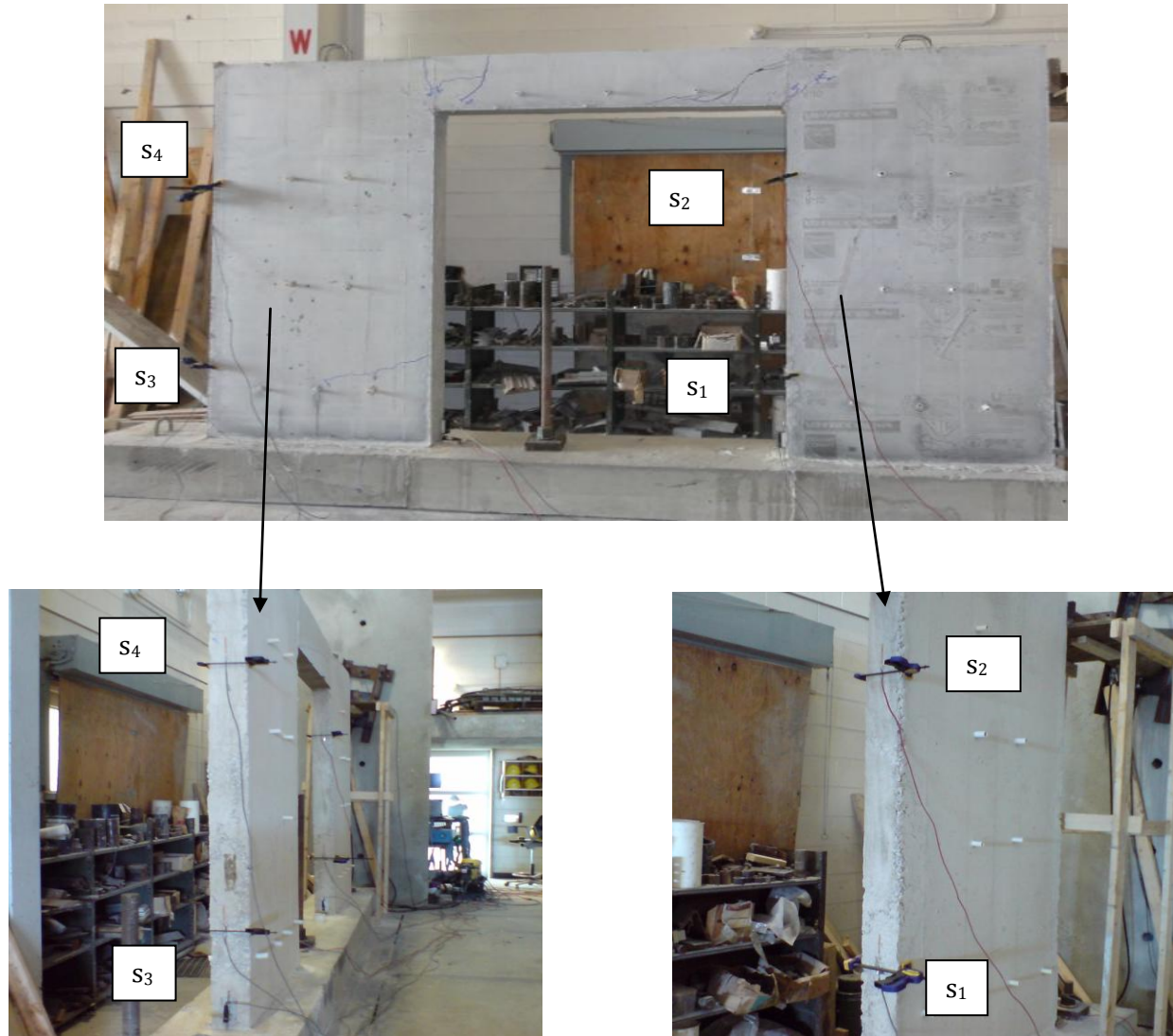


**Figure 2.13. Strain Gauge Placement Position**

#### **2.4.4.5. Deflection Gauges -Linear Variable Differential Transducers (LVDT)**

Wall deflections under lateral loading were measured using Linear Variable Differential Transducers LVDT. First transducer -LVDT1 was connected at the top leading corner on out of

plane face of the wall. LVDT1 is measuring horizontal displacement of the top of the wall. Second transducer -LVDT2 is placed at the bottom leading corner of the wall LVDT2 measures horizontal displacement of the bottom of the wall (wall slipping). Third transducer-LVDT3 is placed at the bottom leading edge on the in-plane face of the wall. LVDT3 measures uplift displacement of the wall relative to the footing. Fourth transducer LVDT4 is placed at the bottom of the back edge on in plane face of the wall. LVDT4 measures vertical displacement of the wall's outer compression face (Figure 2.14). Fifth transducer LVDT5 is placed at the bottom corner of the trailing wall panel on tension side.

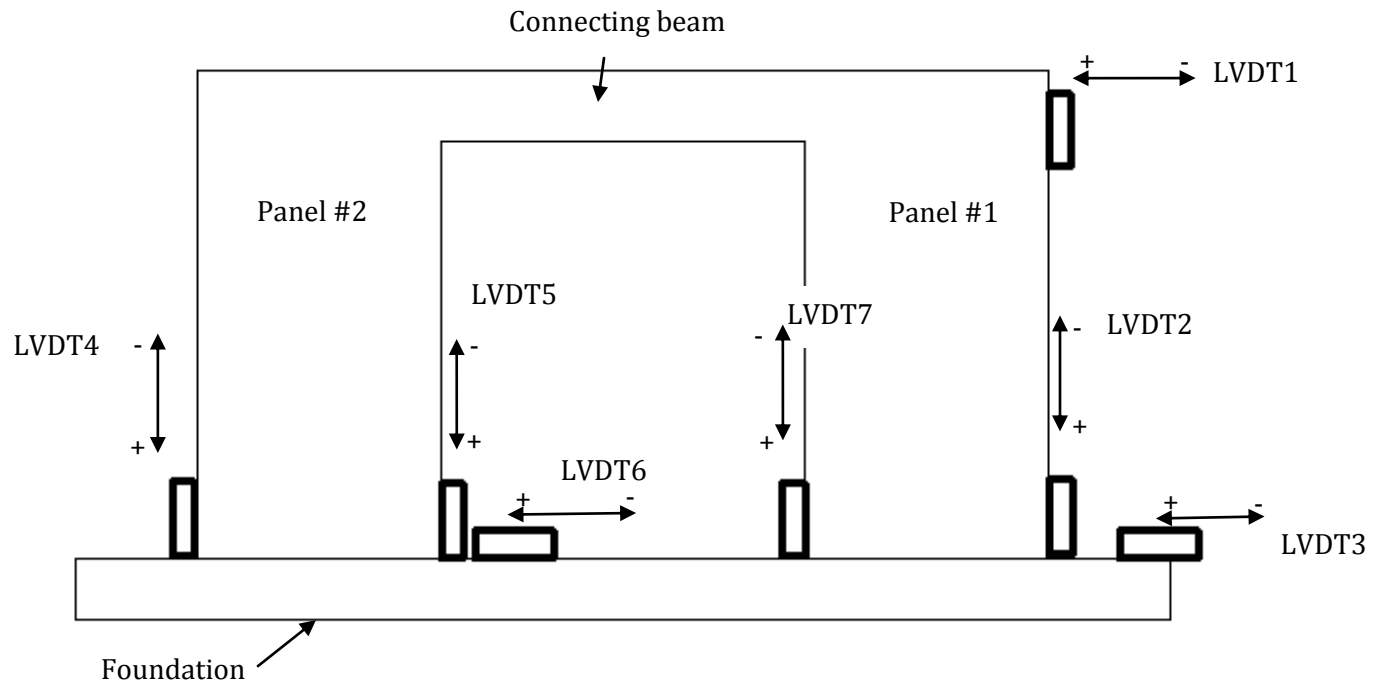


**Figure 2.14. Deflection Transducers Placement and Directional Orientation**

Sixth transducer- LVDT6 is placed at the bottom trailing edge on the in-plane face of the trailing wall's panel. Seventh transducer LVDT7 is placed at the bottom of the trailing edge on in plane face of the wall's first panel.

## **2.5. Sustainable Construction Methodology in Building Insulated Concrete Wall**

This section describes the sustainable principles and construction methods used in building insulated concrete form walls. Additionally, it presents design of efficient and economical job built formwork system for insulated concrete form wall.

### **2.5.1. Sustainable Principles in Building Process**

The study adopted four major sustainable principles in building process of insulated concrete form walls: conservation, waste reduction, energy savings and local availability.

1. In order to conserve the environmental resources, recycled materials should be used in the construction process. To achieve this goal the study proposed replacing all coarse aggregate with recycled concrete aggregate in the concrete mix. Additionally, salvaged construction materials (boards, plywood, nails, steel treaded ties, and plastic tubes) from old construction projects were to be re-used for construction of formwork for ICF walls.

2. In order to reduce construction and industrial waste, 20% of cement by mass is replaced with fly ash. Additionally, new “green” cement type (IPF) was used in concrete mix. All boards and plywood dimensions used in construction of the formwork are carefully designed and cut in a way that could be re-used for other construction projects, with minimum waste generated. To simplify handling process of the wooden materials only two profiles were used:  $\frac{3}{4}$ ” plywood and 2 x 4 boards. Finally advanced planning and scheduling plays important role in minimizing construction waste. For example materials used in building footing formwork, was reused for building walls formwork. The boards and plywood were cut only once with minimum waste generated and minimum damage inflicted. The tie holes drilled in plywood for footing were used as tie holes in the wall.

3. Energy savings plays a big role in building efficient and sustainable structures. In order to achieve this goal the study proposed building ICF walls with total thermal resistivity of  $R=20$ . This value is about 10 times greater when compared to regular concrete walls, or more than twice when compared to regular, insulated wooden frame residential wall (Recommended Levels of Insulation, Energy Star 2012).

4. In order to reduce environmental impact (carbon footprint) of transporting construction supplies, all materials used in the study needed to be locally manufactured or locally available. Recycled concrete aggregate came from the local plant that used concrete acquired from local demolishing/ renovation projects. Fly ash that was used in concrete mix is Nebraska Class C fly ash and came from the local coal power plant. All wooden materials (boards and plywood) came from the local Home Depot store. Special consideration was given to the insulation material used in the study. Initial idea was to use any EPFB (Expanded Polystyrene Foam Boards) for the insulation; however, very few companies have country wide manufacturing centers. After careful investigation it was decided that Foamular-250 was the best candidate. Company that supplies these panels has nation-wide manufacturing centers and distribution contract with Home Depot, making this brand widely and easily available. Worth mentioning is that the Foamular-250 was originally not meant to be used as wall insulation or as a building block the ICF walls, but as attic and basement insulation.

## 2.5.2. Construction Methods in Building ICF Walls

Construction methods are the procedures and techniques employed during construction. In order for construction methodology to be widely accepted, it has to be applicable and conductible. All materials used in the study were picked in a way that the construction process can be replicated almost anywhere in the USA.

### 2.5.2.1. Formwork Design and Construction

The unit weight of  $150 \text{ lb/ft}^3$  and average placement rate of  $15 \text{ ft/h}$  were used as parameters in calculating concrete lateral pressure<sup>7</sup>.

Expanded Polystyrene Panels (EPP) are used as permanent formwork sheets. EPPs are supported by plywood sheets, studs and wales and secured by treaded ties.

In ordered to simplify building procedure 2x4 lumber boards are chosen for both studs and wales. Studs supported plywood, while wales were resting on flat side of 2x4 boards. Based on the lateral pressure imposed on the studs and wales tie spacing was calculated. Tie spacing was governed by the same deflection limits as it was for wales and stud spacing.

**Table 2.11. Formwork Spacing Limits**

<b>Limit spacing</b>	<b>Designed (in)</b>	<b>Build (in)</b>
Studs	8.03	7.5
Wales	19.5	18.0
Ties	17.7	12.0

---

<sup>7</sup> Detailed formwork calculations are presented in Appendix A-5

EPP were connected with hollow plastic tubes (leftovers from a plumbing projects) to hold insulation in place and to provide the bond between EPP and concrete.

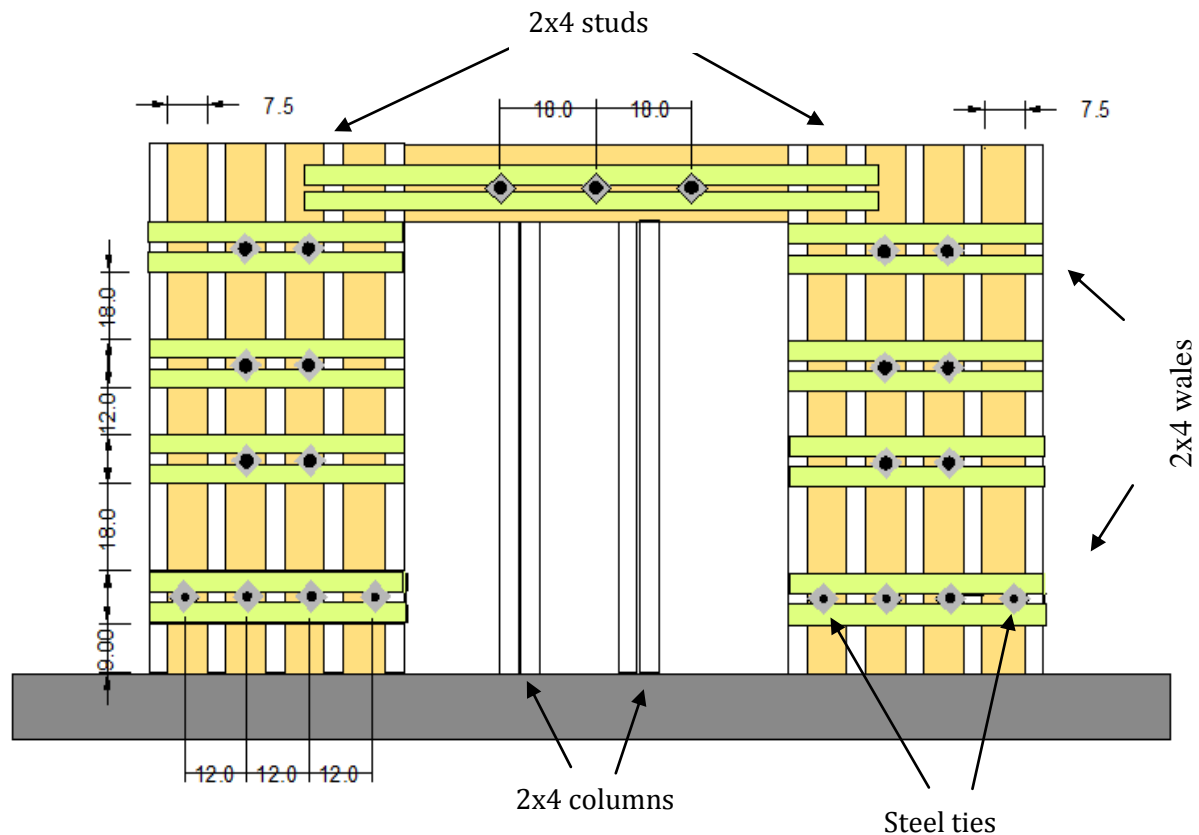


**Figure 2.15. Formwork Design**

Ties were placed inside plastic tubes and connected to the wales. Low strength steel treaded tie with minimum capacity of 3,500 lb was used as a tie. Once concrete is hardened and made a bond with EPP, ties were removed from the plastic tubes and reused. Additionally, bearing stress that ties induced on the washers and bearing stress that washers induced on the wales was checked and confirmed that all stress are under allowable limits. Final formwork design is presented in the Figure 2.15 and Table 2.11.

#### **2.5.2.2. Concrete Placement**

In order to replicate real work situation concrete is mixed and delivered in the mixing trucks. Before concrete is placed into the formwork, air entrapment test was performed in order to confirm 6% air entrapment. After entrapment test had satisfying result, slump test was performed on the concrete sample. After successful verification that slump test is 6" for the control mix and >18" for the experimental mix (self-consolidating concrete), concrete was poured in 0.5 yd<sup>3</sup> concrete buckets. Concrete samples for the compression and flexure tests were taken from the concrete buckets. Following sampling procedure, concrete is elevated and dropped from the 2-3 ft from the top edge of the formwork. Concrete was place at rate of 15 ft/hr.

### **2.6. Construction Cost Comparison**

In order for ICF system to be market competitive it has to be cost effective and labor friendly. To analyses construction cost it was decided to compare material and labor costs between industry standard pre cast ICF walls and sustainable job built ICF walls.

ICF industry reported data on materials and labor are used to obtain average cost data for precast ICF wall systems. Project's material purchases were used to calculate material costs for job build ICF wall system and sustainable job build ICF wall system.

The cost of exterior wall framing per square foot was used for estimating labor cost for job build ICF walls. It was noticed that handling re-used construction material would take more time, therefore 15% higher labor cost was used for estimating sustainable job build ICF labor costs.

## **CHAPTER 3. RESULTS**

This chapter lists shear resistance (pushover) test results and material testing results for control concrete mix (SW1) and experimental concrete mix (SW2). Additionally, this chapter list comparative cost analysis between precast industry standard ICF walls and sustainable construction job build ICF walls.

### **3.1. Material Testing Results**

All test results in Material Testing Results section were obtained averaging two test trials.

#### **3.1.1. Compression Strength for Control Concrete Mix (Natural Aggregate)**

Compression test results for Control Mix were presented in the Table 3.1. Control Mix was successfully designed and testing specimen were properly cured.

**Table 3.1. Compression Test Results for Control Concrete Mix**

<b>Compression tests</b>	
<i>day</i>	<i>psi</i>
7	3,329
14	3,533
21	4,033
28	4,565

#### **3.1.2. Compression Strength for Experimental Concrete Mix (Recycled Aggregate)**

Compression test results for Experimental Mix were presented in the Table 3.2 and Table 3.3. After 14<sup>th</sup> day testing revealed that concrete specimen were not gaining any strength. Inspection of a specimen interior after a break revealed that cement paste inside a specimen was still being wet, indicating that no hydration was taking place (Figure 3.1).

**Table 3.2. Compression test results for experimental mix (wet cured)**

<b>Compression tests (<i>wet cured</i>)</b>	
<i>day</i>	<i>psi</i>
7	254
14	420
21	293
28	678

**Figure 3.1. Experimental Mix Compression Test**

Since Experimental Mix was not curing properly it was decided to take 6 testing cylinders out of curing room, and to cure it at lab temperature where the shear walls were built. It seems that samples did gain some extra strength by being cured. The lab cured sample gained twice the strength of wet cured sample (1,164 psi vs. 678 psi). However, strength gain quickly leveled off, and further strength gain was stopped at 35th day. After failing to gain more strength it was decided the wall with experimental mix should be tested. Measured strength after 21<sup>st</sup> (35<sup>th</sup>) day of dry curing (1,158 psi) was way under designed compression strength of 4,000psi.

**Table 3.3. Compression tests (lab cured)**

<b>Compression tests (<i>lab cured</i>)</b>	
<i>day</i> <sup>8</sup>	<b>psi</b>
7 (21)	670
14 (28)	1,164
21 (35)	1,158

### 3.1.3. Flexural Strength of Experimental Concrete Mix (Recycled Aggregate)

Third point loading test was used to determine breaking load,  $P = 28,788\text{lb}$  (Figure 3.2).

After breaking load was determined from the flexure test, flexural strength was calculated using Equation 3.5

$$R = \frac{PL}{bd^2} \quad (\text{Equation 3.1})$$

where  $L$  is effective length of specimen = 18in;

$b$  is width of the specimen = 6 in;

$d$  is depth of the specimen = 6in.

$$R = 2,399\text{psi}$$



**Figure 3.2. Flexural Strength Testing for Experimental Concrete Mix**

<sup>8</sup> First number is lab cured day, second number (in parenthesis) is actual day after samples are casted

## 3.2. Shear Wall Testing Results

This section of the chapter lists results obtained from the static shear pushover test. Following data are collected and analyzed: ultimate load capacity, load-displacement analysis, wall shear stiffness, load-strain distribution, and crack formation, growth and progression.

### 3.2.1. Shear Wall Testing Result for Control Concrete Mix (SW1)

The SW1 wall was tested on 42th day after the concrete was casted. The lateral load was applied at approximately 2000lb/s. The load is transferred from the actuator to the wall over 7"x7"x2" steel plate. In this way load is distributed over effective concrete area of 42 in<sup>2</sup>, greatly reducing chance of concrete bearing failure. The maximum lateral load achieved before wall's structural failure was **40,555.87 lb** (Figure 3.3).



**Figure 3.3. Control Wall Structural Failure**

### 3.2.2. Load Displacement Analysis for SW1

Load-displacement analysis is based on evaluation of load displacement curves. Load displacement curves are plots of load versus displacements obtained from deflection transducers (LDVT). Most commonly displacements are represented as shear displacement ( $\Delta_s$ ) and lateral

displacement ( $\Delta_1$ ). Additional wall's behaviors such as uplift, slipping, rotation ("toe" crushing) can be analyzed from load displacement curves.

Shear displacement is calculated from displacement transducers using Equation 3.1.

$$\Delta_s = \Delta_1 - \Delta_2 - (\Delta_3 - \Delta_4) * \frac{a}{b} \quad (\text{Equation 3.2.})$$

where,  $\Delta_1, \Delta_2, \Delta_3, \Delta_4$  are data obtained from LDVT1, LDVT2, LDVT3 and LDVT4,

$a$  is height of the wall,

$b$  is overall length of the wall.

Maximal shear displacement ( $\Delta_{s \max}$ ) was obtained at failure load ( $L_{\max}$ ).

$$\Delta_{s \max} = 0.72 \text{ in}$$

$$L_{\max} = 40,555 \text{ lb}$$

Load–shear displacement curve (Figure 3.4) shows shear wall's characteristic and expected response during the loading phase.

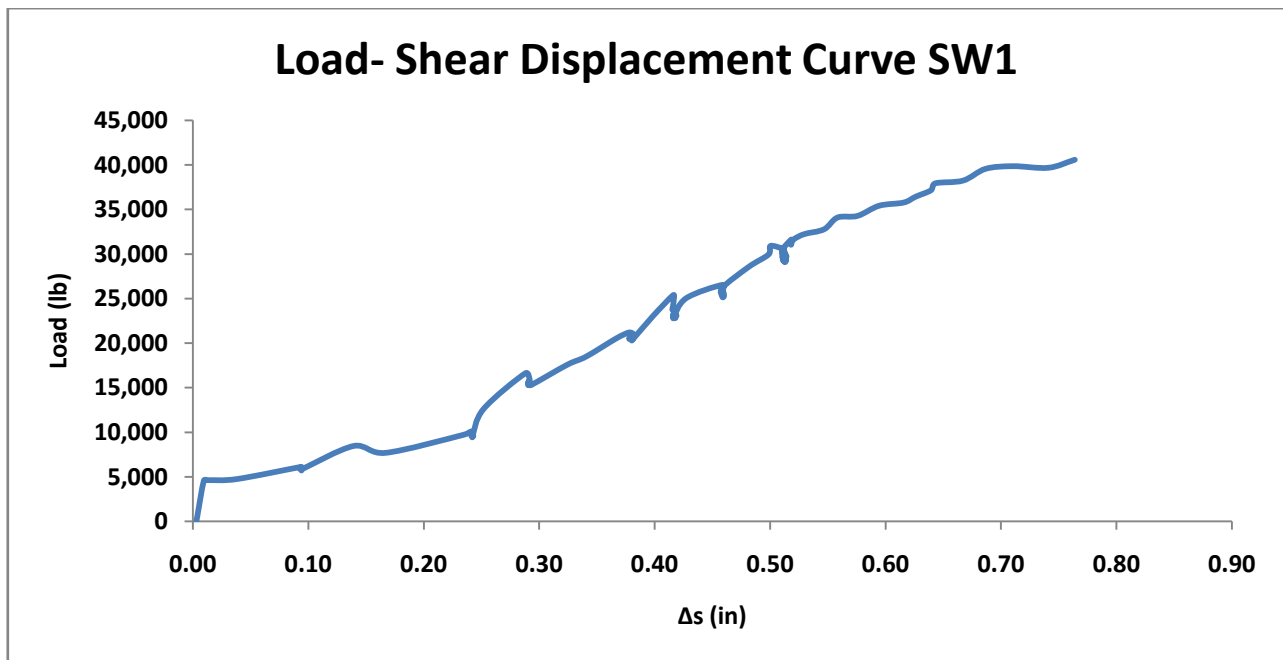


**Figure 3.4. Load-Shear Displacement Curve SW1**

The contribution of the each wall panel to the total shear deflection was analyzed comparing panel's individual shear deflections (Equations 3.2 and 3.3).

$$\Delta s_1 = \Delta_1 - \Delta_2 - (\Delta_3 - \Delta_7) * \frac{a}{b_1} \quad (\text{Equation 3. 3})$$

$$\Delta s_2 = \Delta_1 - \Delta_5 - (\Delta_6 - \Delta_4) * \frac{a}{b_2} \quad (\text{Equation 3. 4})$$

Where,

$\Delta s_1, \Delta s_2$  are shear deflections of panel #1 and panel #2 respectively

$b_1$  and  $b_2$  are lengths of solid concrete panels.

$$\Delta s_{1\max} = 0.84 \text{ in} \quad \Delta s_{2\max} = 0.82 \text{ in}$$

Shear deflection of the wall panel #1 very closely reassembles total shear deflection, while shear deflection of the panel #2 somewhat lags behind (Figure 3.5).

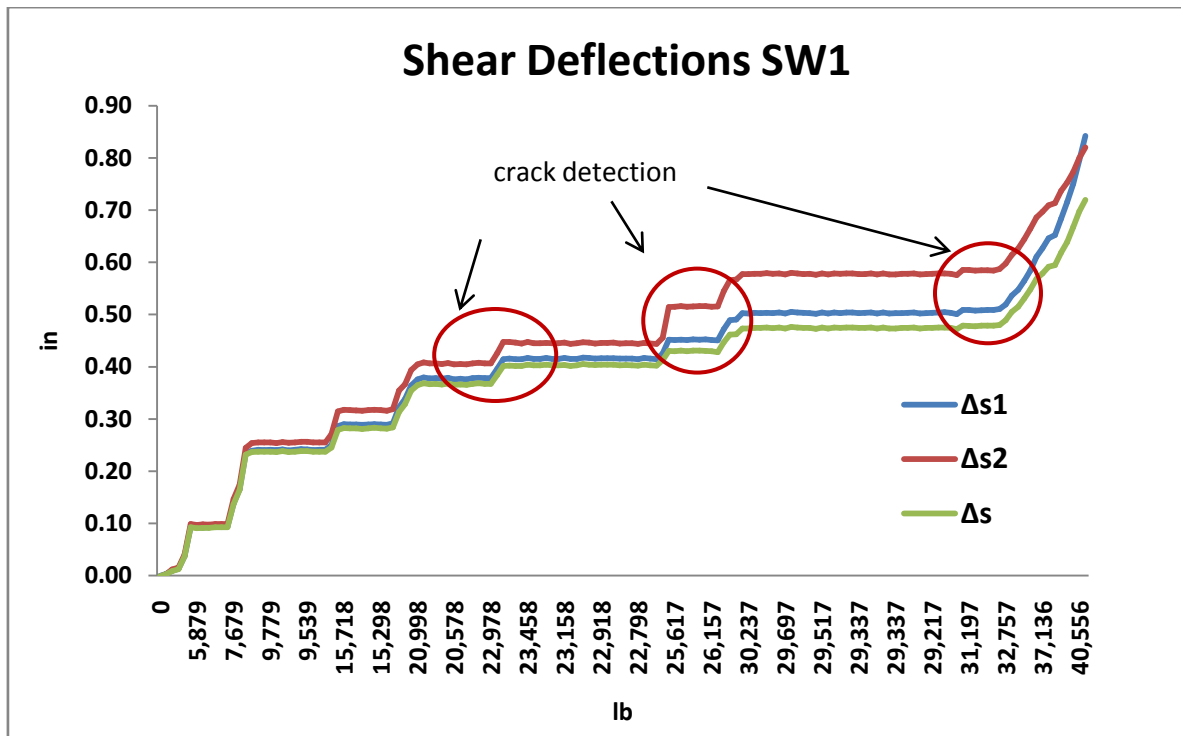
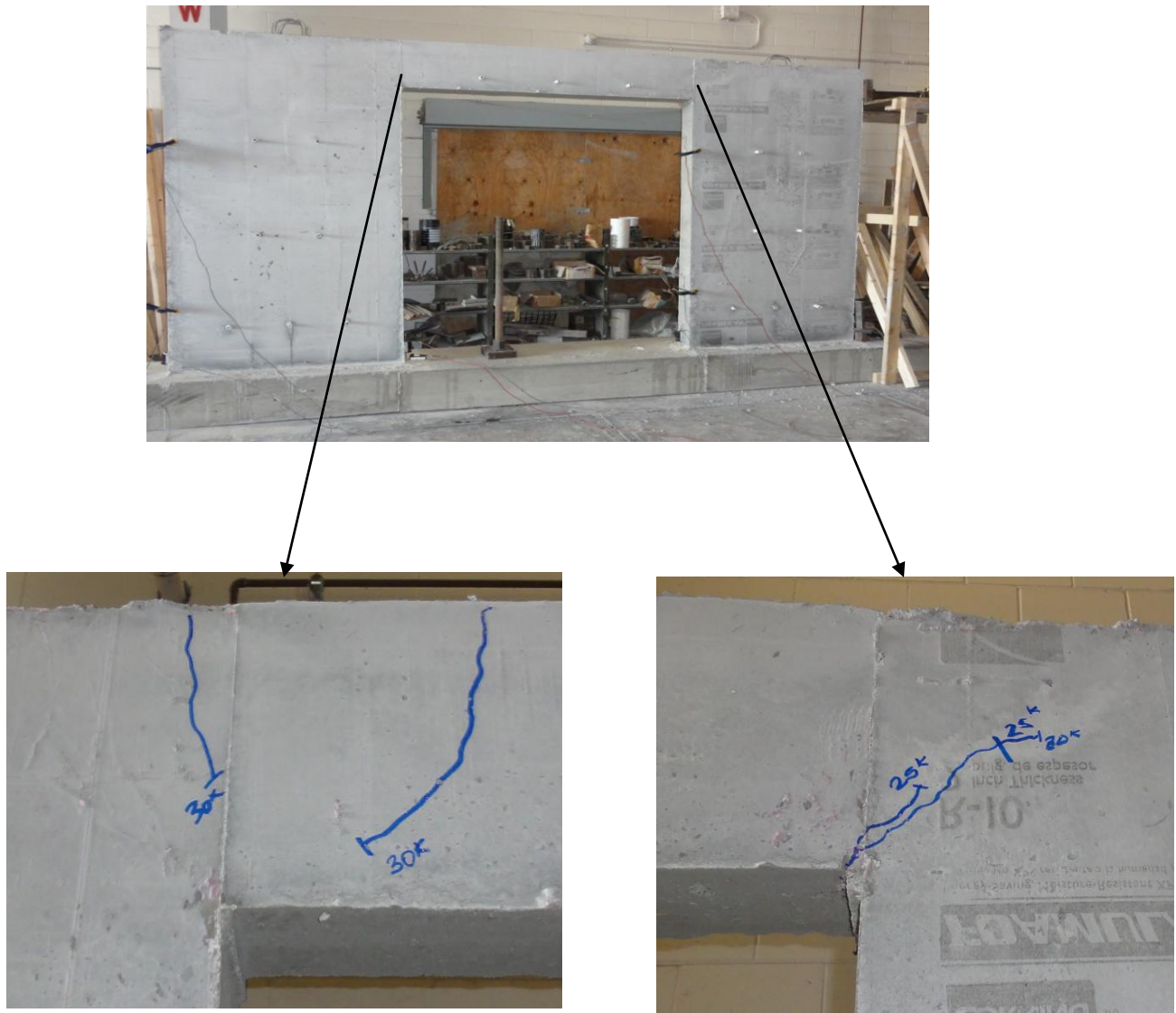


Figure 3.5. Shear Deflections SW1

The difference between two panels' shear deflections is attributed to the crack propagation at the joint between wall's connecting beam and the wall panels (Figure 3.6). First crack that is detected at load of approximately 20,000lb coincides to the first significant separation of shear deflection curves. Further crack propagation ( at loads of 25,000lb and 30,000lb) even more enhanced the separation between shear deflection curves.



**Figure 3.6. Crack Propagation at SW1**

Lateral displacement ( $\Delta_1$ ) is displacement obtained from LDVT1, which is transducer on the top of the leading edge of the wall.

When  $\Delta_s \approx \Delta_1$ , wall response is characterized as pure shear behavior. When  $\Delta_s \neq \Delta_1$ , wall's response can be attributed to multiple sources such as wall slipping or uplift due to inappropriate connection with footing, concrete crushing on the compression side or wall's torsional failure.

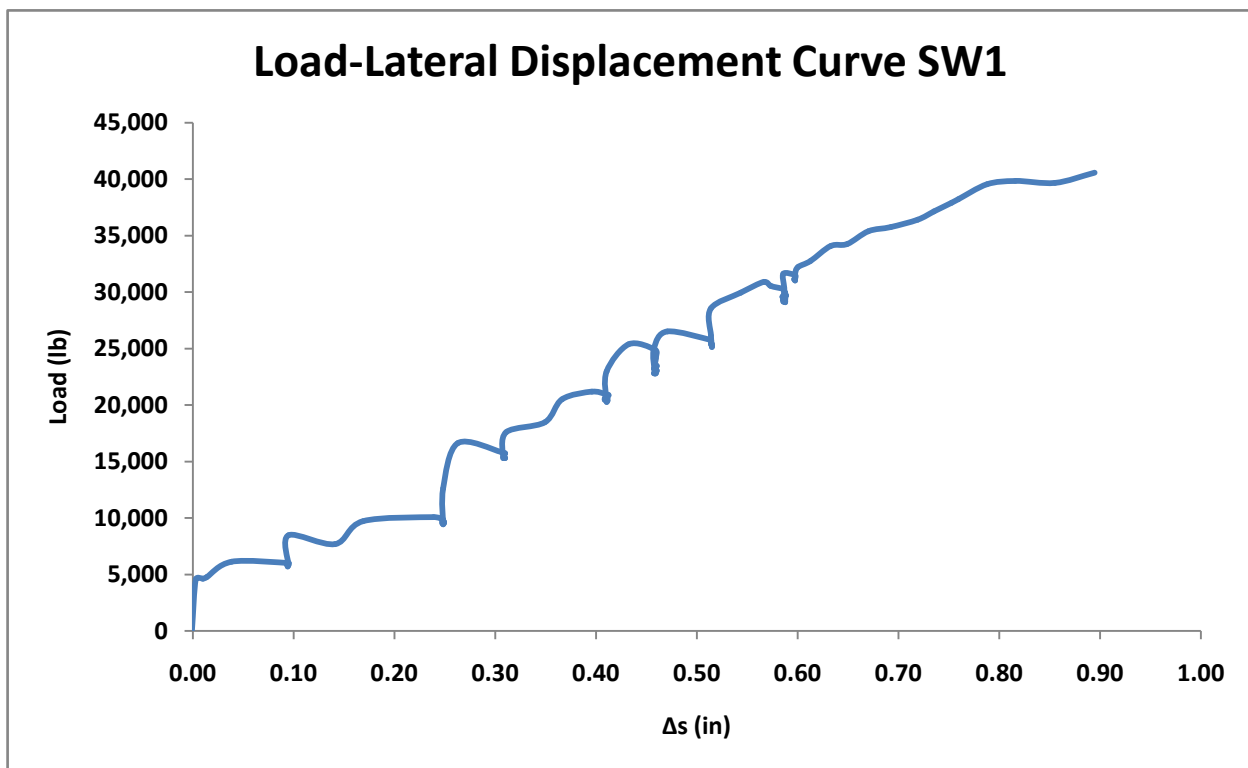


**Figure 3.7. Load–Lateral Displacement Curve SW1**

Maximal lateral displacement ( $\Delta_{1_{max}} = 0.93$  in) was obtained at the failure load.

The load-displacement curve (Figure 3.7) shows shear wall's linear response during the loading phase. Well defined proportional limit was easily detected on the load displacement curve.

Lateral displacement at the design load of 21.22 kips was 0.41 in.

In order to better understand walls behavior, contribution of the each transducer is individually analyzed. Figure 3.8 shows deflection history for seven transducers.

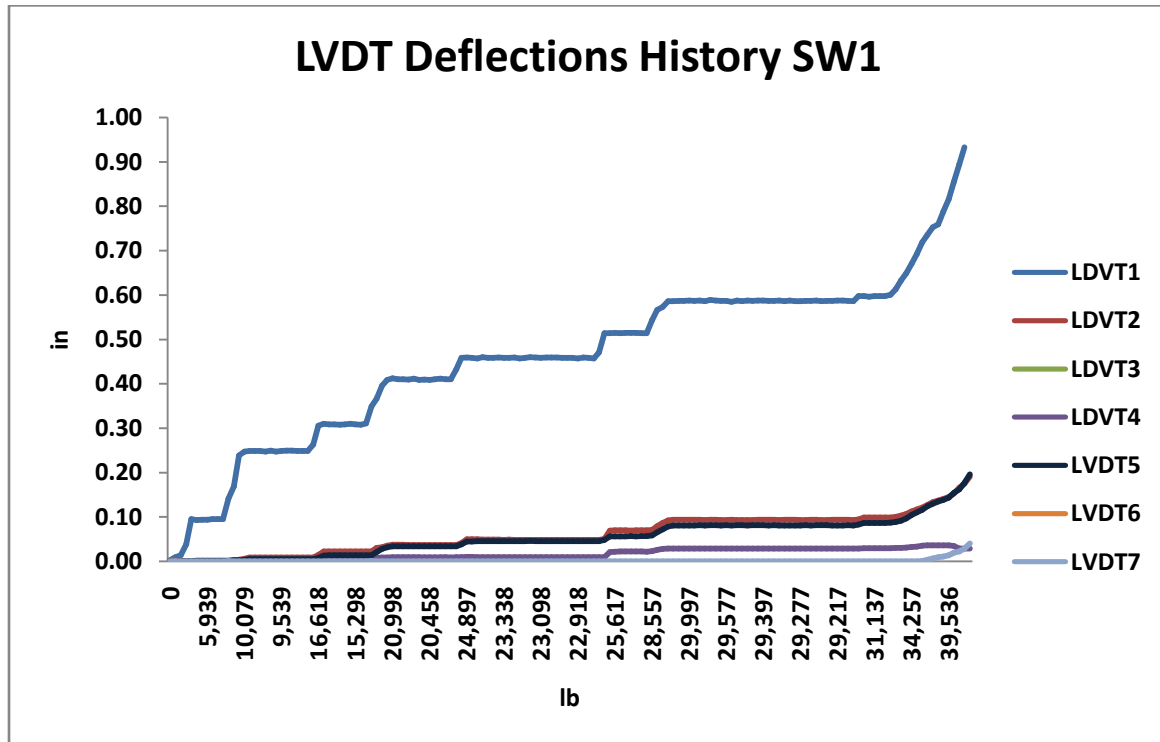


**Figure 3.8. LVDT Deflection History SW1**

As anticipated deflection history showed that upper part of the shear wall was deflecting linearly with load increments. Wall's bottom remained almost unaffected by load growth. Wall's uplift was minimal (LVDT2 and LVDT5), while slipping wasn't detected (LVDT3 and LVDT6). The footing to wall connection was effectively preventing wall's uplift and slipping.

The deflection behavior of the concrete panels was analyzed comparing matching deflection transducers on the concrete panels

- a) uplift deflection- LDVT2 vs. LDVT5 (Figure 3.9),
- b) slipping deflection- LDVT3 vs. LDVT6
- c) rotational deflection ("toe" crushing)- LDVT7 vs. LDVT4 (Figure 3.10).

Both concrete panels showed high resistance to the uplift force. Maximal uplift deflection for panel #1 was 0.191 in while for panel #2 was 0.196 in. Figure 3.9 shows that there is a very small difference (0.0145in) in panels' behavior when resisting uplift force.

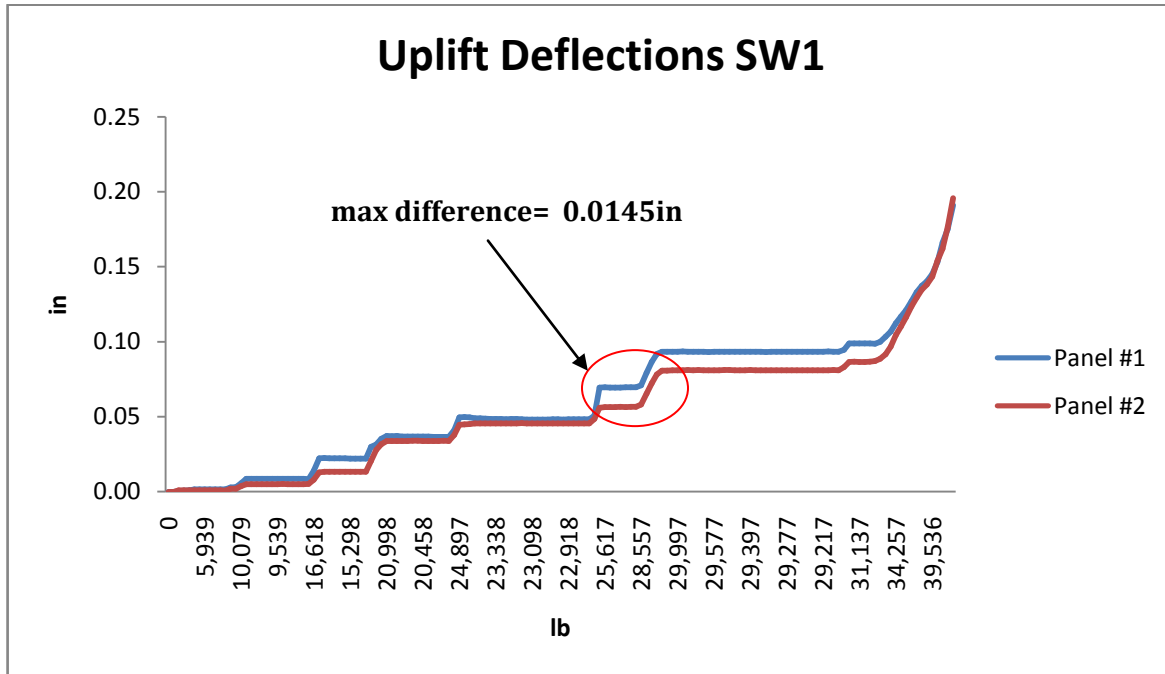


**Figure 3.9. Uplift Deflections SW1**

Both concrete panels showed very high resistance to the slipping force. Maximum slipping deflection for panel #1 -0.0098in while maximum slipping deflection for the panel #2 was -0.0125in. Negative sign means that actual slipping did not occur, but rather rotation at the wall-footing connections. Wall's slipping behavior is characterized by the same direction (sign orientation) of the lateral force and the bottom of the wall. Negative sign for both wall panels means that the wall panels moved in opposite direction than lateral force. However, the magnitude of the movement is insignificant when compared to the total quantity of lateral deflection (0.93 in or  $\approx 1.3\%$  of total lateral deflection).

When concrete panel is laterally loaded at the top, the bottom end has tendency to rotate inward, generating high compression (crushing) forces. Rotational analysis gives us very good

insight how crack formation directs panels' behavior. As seen from Figure 3.10 bulk of wall rotation is detected at the second panel. The first major spike in panel's rotation coincides with first crack detection at approximately 25,000lb. The second change in panels' response to lateral load occurred after massive crack progression at the joint between cross beam and panel #1. This event occurred at lateral load of 35,000lb. At this point there is an aggressive transfer in panel's rotation from panel#2 to panel#1, with simultaneous drop in deflection at panel #2. This drop at panel#2 could be attributed to hinge formation at joint between cross beam and panel#1.

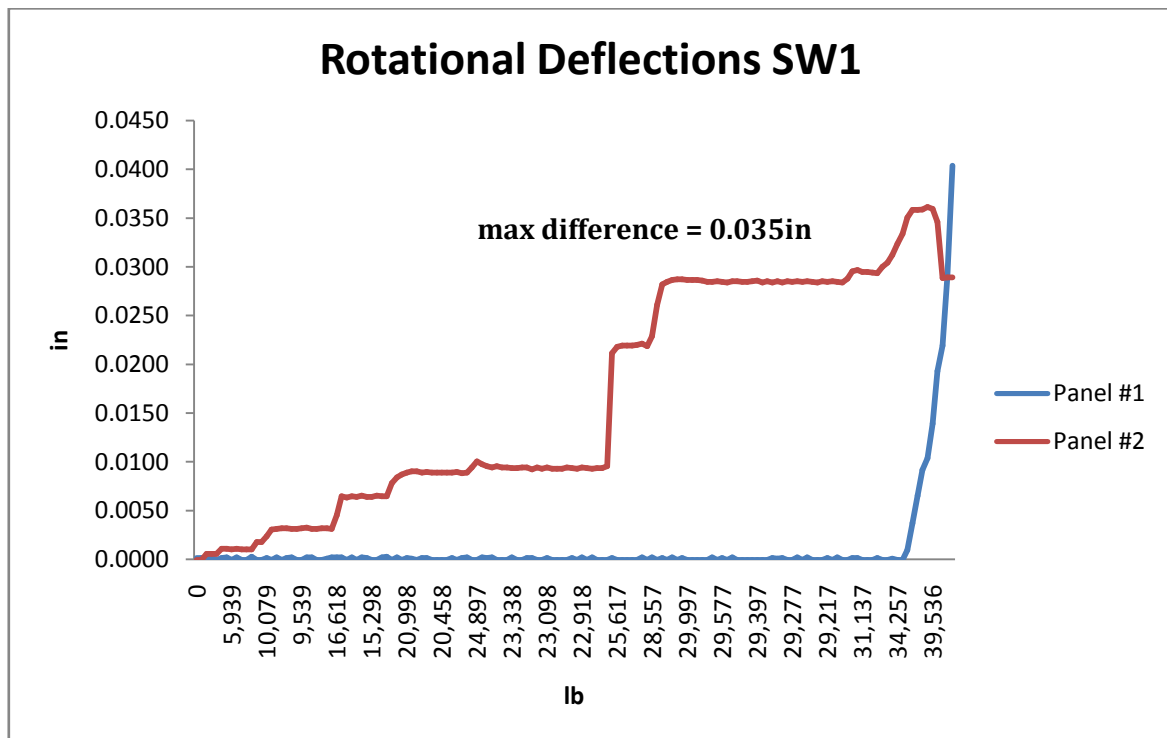


**Figure 3.10. Rotational Deflections (“toe” crushing) SW1**

The maximum deflection at panel#1 was 0.04in, while maximum deflection at panel#2 was 0.035in. Maximum difference in deflection between panels was 0.035in.

Load–deflection analysis summary is presented in Table 3.4.

**Table 3.4. Load –Deflection Analysis Summary SW1**

Load -Shear Deflection		Load-Lateral Deflection		Panel #1 Deflection (in)	Panel #2 Deflection (in)
$\Delta s_{\max} = 0.72$ in	$L_{\max} = 40,555\text{lb}$	$\Delta l_{\max} = 0.93$ in	$L_{\max} = 40,555\text{lb}$	uplift $_{\max} = 0.191$	uplift $_{\max} = 0.196$
$\Delta s_{1\max} = 0.84$ in	$L_{\max} = 40,555\text{lb}$	$\Delta l_{\text{sap2000}} = 0.21$ in	$L_{\text{sap2000}} = 21,2100\text{lb}$	slipping $_{\max} = -0.0098$	slipping $_{\max} = -0.0125$
$\Delta s_{2\max} = 0.82$ in	$L_{\max} = 40,555\text{lb}$	$\Delta l_{\text{design}} = 0.41$ in	$L_{\text{design}} = 21,2100\text{lb}$	rotational $_{\max} = 0.04$	rotational $_{\max} = 0.035$

### 3.2.3. Shear Stiffness (G) of SW1<sup>9</sup>

The shear stiffness is defined as wall's resistance to shearing strains. The shear stiffness correlates wall's deformation to an action of a force applied parallel to one of its surfaces while its opposite face experiences an opposing force. The wall's shear stiffness was calculated according to the equation recommended in ASTM E564.

$$G' = 8,423.60 \text{ lb/in}$$

### 3.2.4. Strain Analysis for SW1

Strain gauges were placed on the compression sides of the wall face. Gauges  $s_1$  and  $s_2$  are placed on the compression face of the panel#1, while gauges  $s_3$  and  $s_4$  are placed on the compression face of the panel#2. Maximal strain obtained for SW1 was  $-118 \mu\text{E}$ . Maximal strain was recorded at the maximal lateral load of 40,555 lb (Figure 3.11).

<sup>9</sup> Detailed shear stiffness calculations are presented in Appendix A-5

Load-Strain curve in Figure 3.11. shows linear dependency between lateral load and concrete strains on the compression sides. Shape irregularities displayed on the graph are attributed to the gauge's sensitivity to the testing conditions.

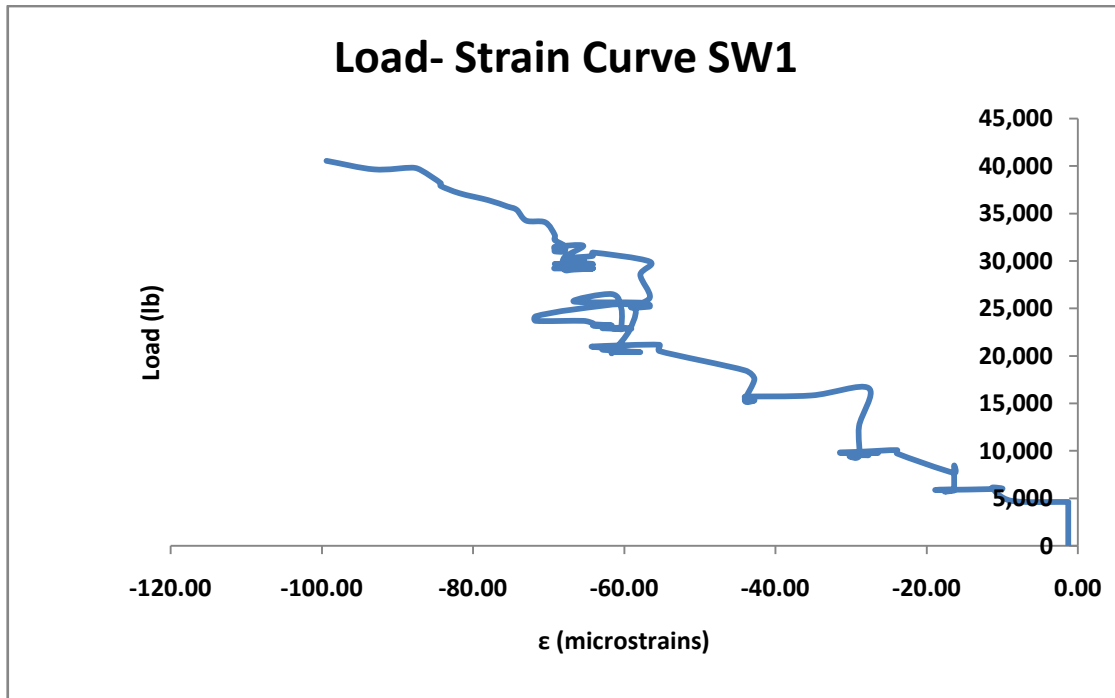


**Figure 3.11. Load-Strain Curve SW1**

### 3.2.5. Concrete Crack Analysis for SW1

Concrete crack analysis is visual observation of cracks development and cracks propagation while wall being under constant lateral loading. Once the cracks were detected, they were marked and photos were taken (Figure 3.12). Procedure is repeated until wall's structural failure.

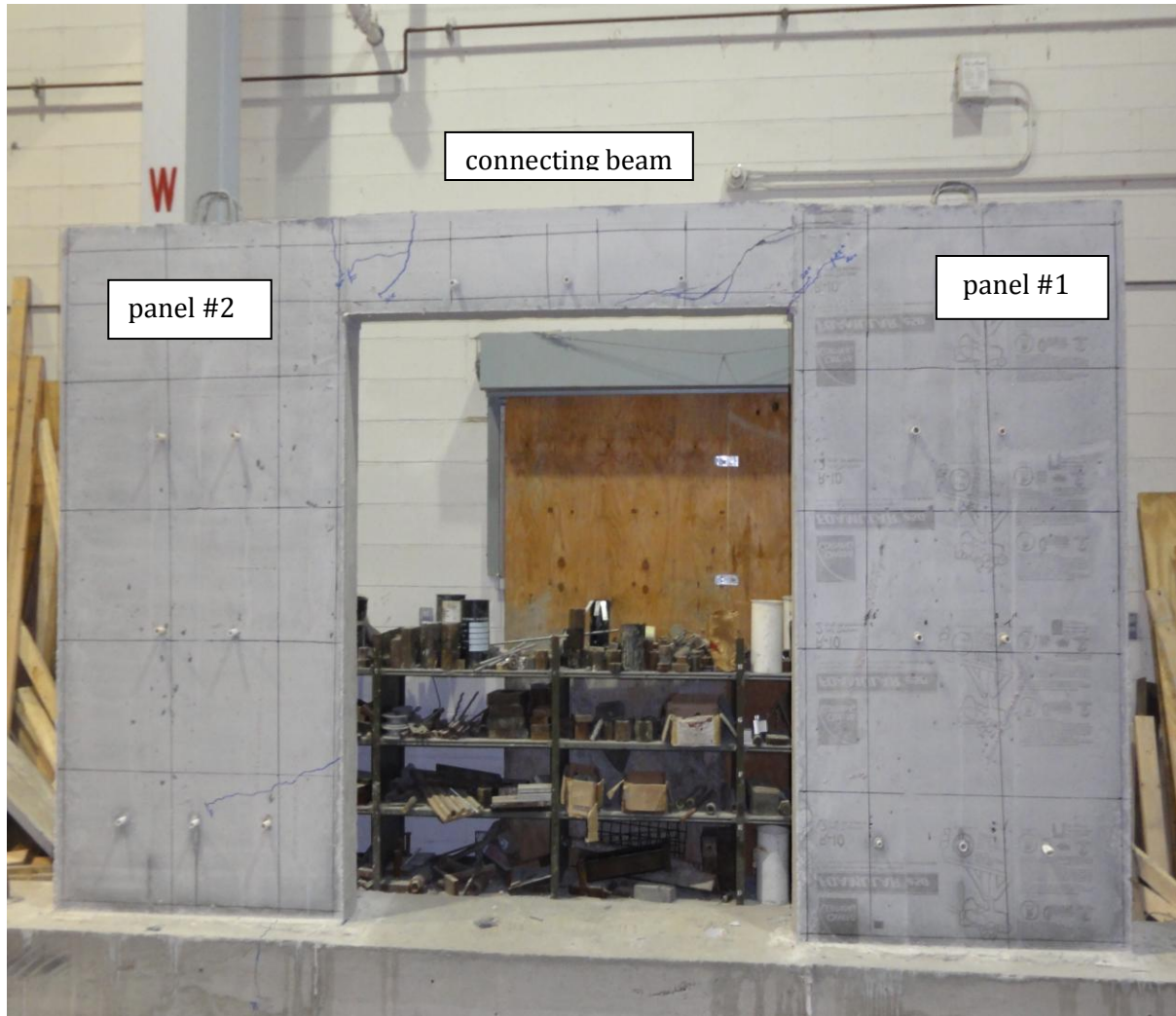


**Figure 3.12. Concrete Cracks Development<sup>10</sup>**

First cracks were observed at 25,000lb on the both sides (front and back) at the joint between connecting beam and panel#1 (Figure 3.13). At load of 30,000lb additional cracks showed on the both side at the joint between connecting beam and panel#2 (Figure 3.14). Cracks that were created at 25,000lb load further propagated diagonally. At failure load of 40,555lb concrete split at the base of the connecting beam 15” lateral from the joint with panel#1 (Figure

<sup>10</sup> Dark lines on the wall represent reinforcement position in the wall

3.15). Splitting crack was 0.25" wide and 19" long, diagonally spreading across the depth of the connecting beam.



**Figure 3.13. Cracks Generation at Load of 25,000lb (Front and Back Side)**



**Figure 3.14. Cracks Generation at Load of 30,000lb (Front and Back Side)**



**Figure 3.15. Cracks Generation at Failure Load (Front and Back Side)**

At the failure load cracks at the joint between connecting beam and panel#2 propagated further but no concrete splitting was detected. Additional new crack (22" long) was detected at the bottom section of the panel#2.

### 3.2.6. Shear Wall Testing for Experimental Concrete Mix (SW2)

The SW2 wall was tested on 35th day after concrete was casted. The lateral load was applied at approximately 1000lb/s. The load is transferred from the actuator to the wall over 7"x 4"x 2" steel plate. The load was distributed over effective concrete area of 28in<sup>2</sup>, which proved to be insufficient to prevent concrete bearing failure. The maximum lateral load, achieved before wall's structural bearing failure, was measured to be **27,657.18 lb** (Figure 3.16).

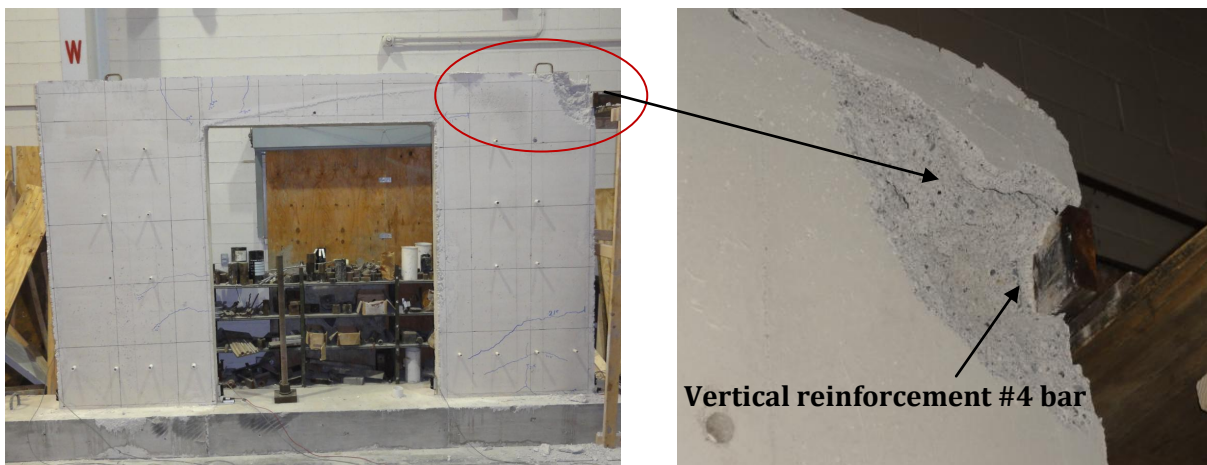


**Figure 3.16. Experimental Wall Bearing Failure SW2**

Further concrete penetration by hydraulic actuator was prevented by wall's vertical reinforcement (Figure 3.16).

### 3.2.7. Load Displacement Analysis for SW2

Maximum shear displacement ( $\Delta s_{max}$ ) for experimental mix SW2 was obtained before maximum lateral load ( $L_{max}$ ) was achieved.

$$\Delta S_{\max} = 0.214 \text{ in}$$

$$L_{\text{shear}_{\max}} = 24,297 \text{ lb}$$

Load–shear displacement curve for SW2 (Figure 3.17) shows wall’s overall response to the lateral loading.

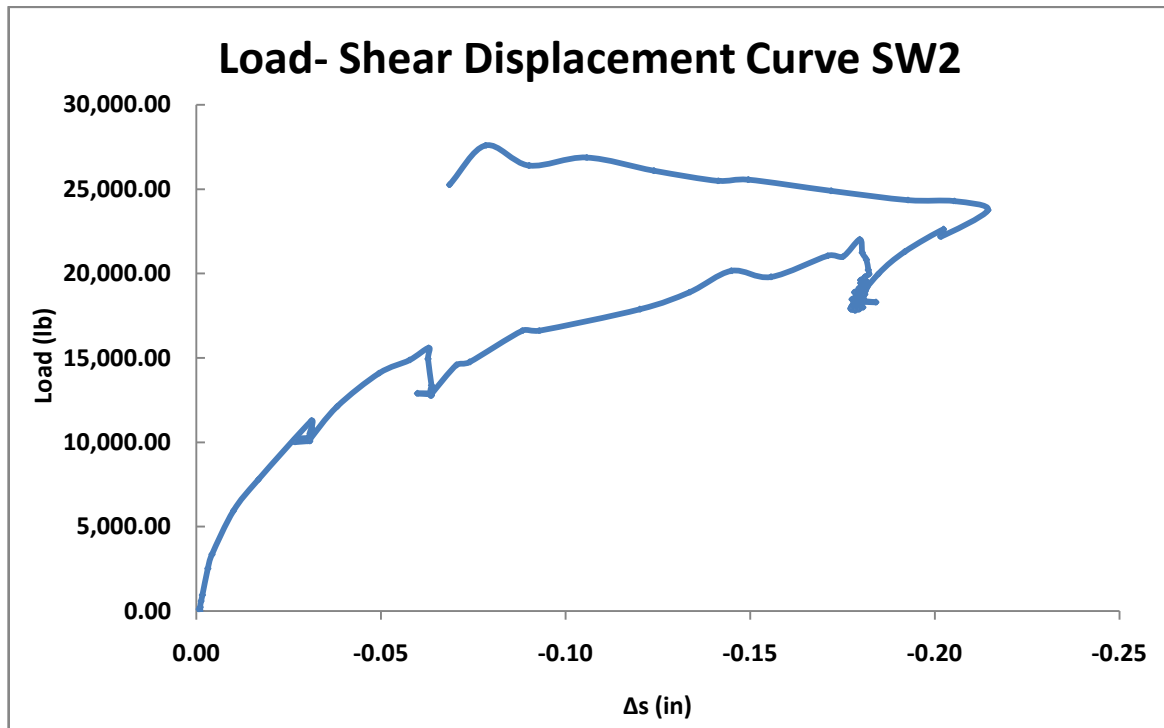


**Figure 3.17. Load Shear Displacement Curve SW2**

Negative values of the shear displacement indicate the wall did not behave in anticipated fashion. It seems that factors such as uplift, slipping and “toe” rotations greatly contributed to the wall’s overall behavior. Additionally, the contribution of the each wall panel to the total shear deflection was analyzed comparing panel’s individual shear deflections (Figure 3.18).

$$\Delta S_{1\max} = -0.235 \text{ in}$$

$$\Delta S_{2\max} = -0.179 \text{ in}$$

Knowing that wall's panel #1 structurally failed in bearing, it was expected that panel #1 has the highest shear deflection. Sudden change in the slope of the shear deflections coincides with start of the bearing failure of the panel #1.

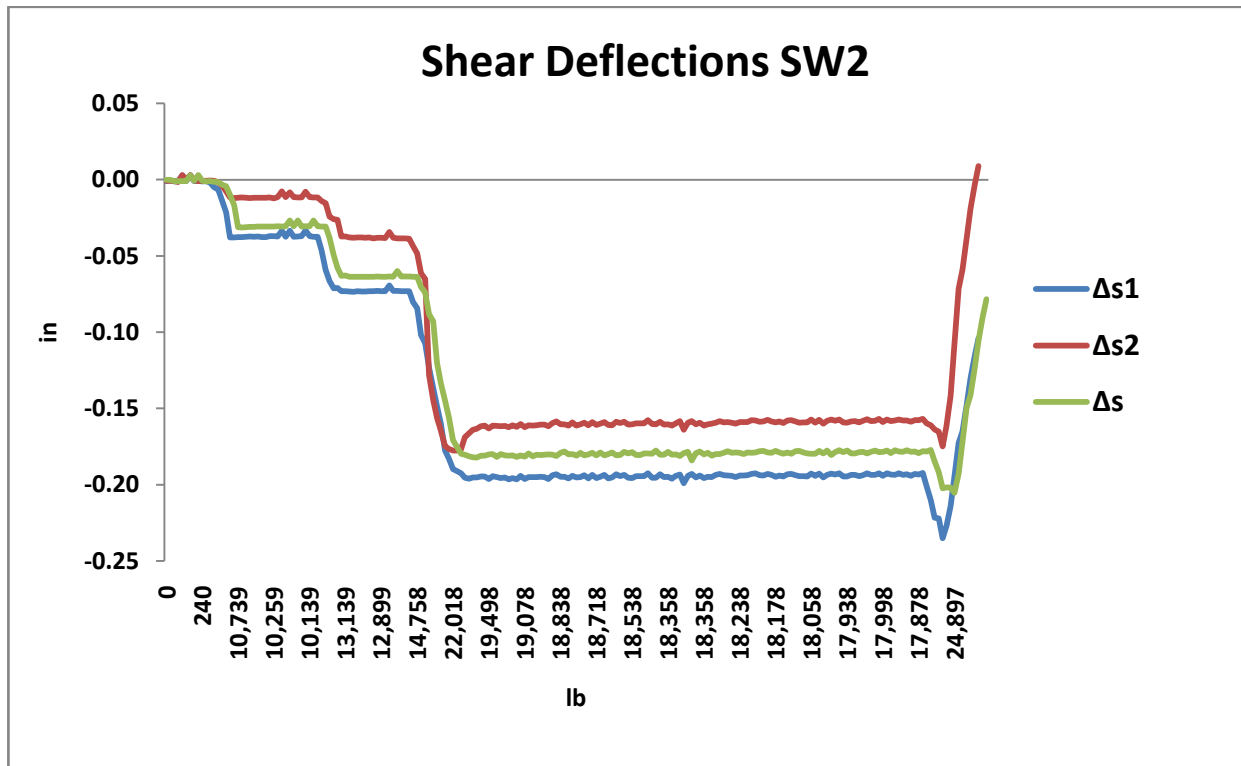


**Figure 3.18. Shear Deflections SW2**

When load-lateral displacement curve was analyzed (Figure 3.19), it revealed that the wall started deflecting in lateral direction only after the bearing failure was already in progress. Rapid progression in a wall's bearing failure coincides with rapid progression in lateral deflection. Maximal lateral deflection ( $\Delta l_{\max} = 0.237$  in), occurred at maximal lateral load ( $L_{\max} = 27,657.18$  lb)

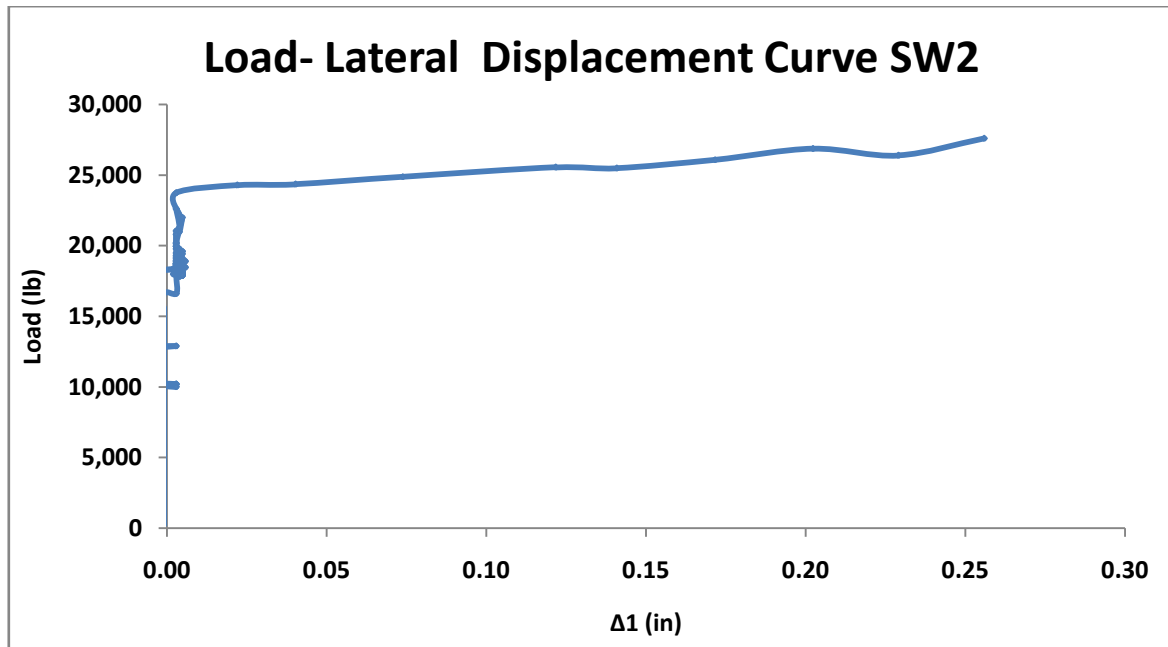


**Figure 3.19. Load-Lateral Displacement Curve SW2**

In order to determine wall's behavior contribution of each LDVT to shear deflection is analyzed (Figure 3.20). Anticipated deflection patterns from LDVT were not confirmed. It seems that upper sections of the shear wall were not deflecting linearly with load increments. Spike in displacement of the wall's upper section was only noticed after bearing failure. Wall's bottom sections remained unaffected by load growth until reached approximately 21,000lb. At that point wall's panels (LVDT3 and LVDT6) were displacing in opposite directions. Significant wall uplift was detected at both panels (LVDT2 and LVDT5).

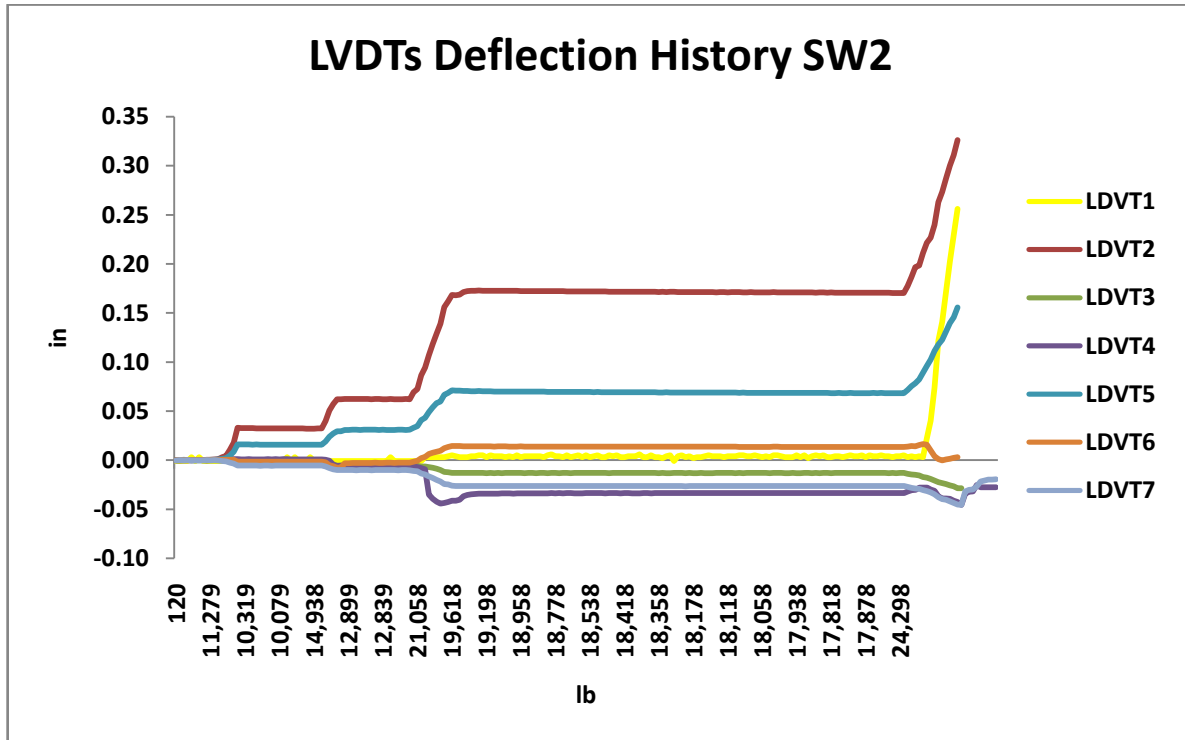


**Figure 3.20. LVDTs Deflection History SW2**

The deflection behavior of the concrete panels was further analyzed comparing matching deflection transducers on the concrete panels:

- a) uplift analysis- LDVT2 vs. LDVT5 (Figure 3.21),
- b) slipping analysis- LDVT3 vs. LDVT6 (Figure 3.23),
- c) rotational analysis (“toe” crushing)- LDVT7 vs. LDVT4 (Figure 3.24).

Both concrete panels showed relatively low resistance to the uplift force when compared to SW1. Maximal uplift deflection for panel #1 was 0.317in, while for panel #2 was 0.150in. Figure 3.21 shows a difference of 0.167in in panels’ uplift deflection. Low uplift resistance affected how wall has behaved when laterally loaded. It seems that wall started deflecting upwards before it started deflecting laterally, giving shear displacement curve negative sign orientation.

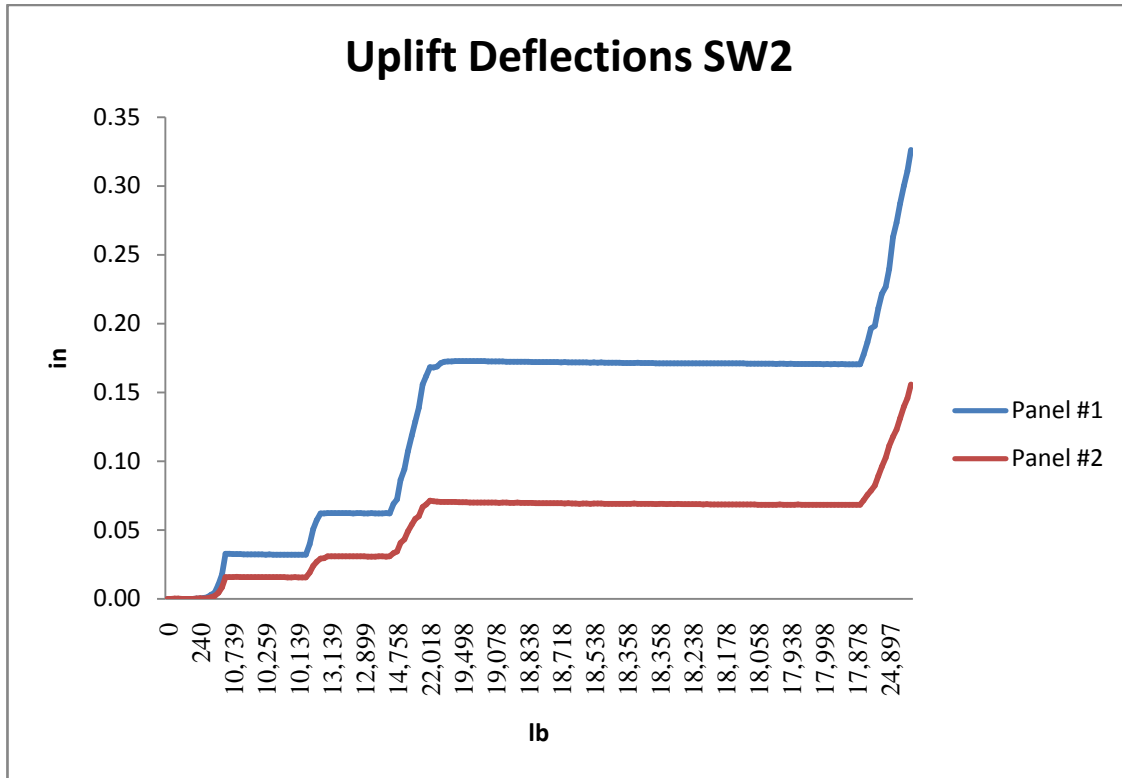


**Figure 3.21. Uplift Deflections SW2**

First major peak in uplift deflection was detected at load of approximately 10,000lb (Figure 3.22). Uplift deflection was linearly increasing with the load, dominating overall wall behavior.



**Figure 3.22. Uplift Deflection at SW2**

Both concrete panels showed low resistance to the slipping force. Maximum slipping deflection for panel #1 was -0.044in while maximum slipping deflection for the panel #2 was 0.016in (Figure 3.23). Negative sign for wall panel#1 means that the wall panel moved in opposite direction than lateral force, while positive sign for panel#2 means that this panel moved in the same direction as lateral force. The panels opposite deflection indicate that the load transfer from panel#1 to panel#2 did not proceed as anticipated.

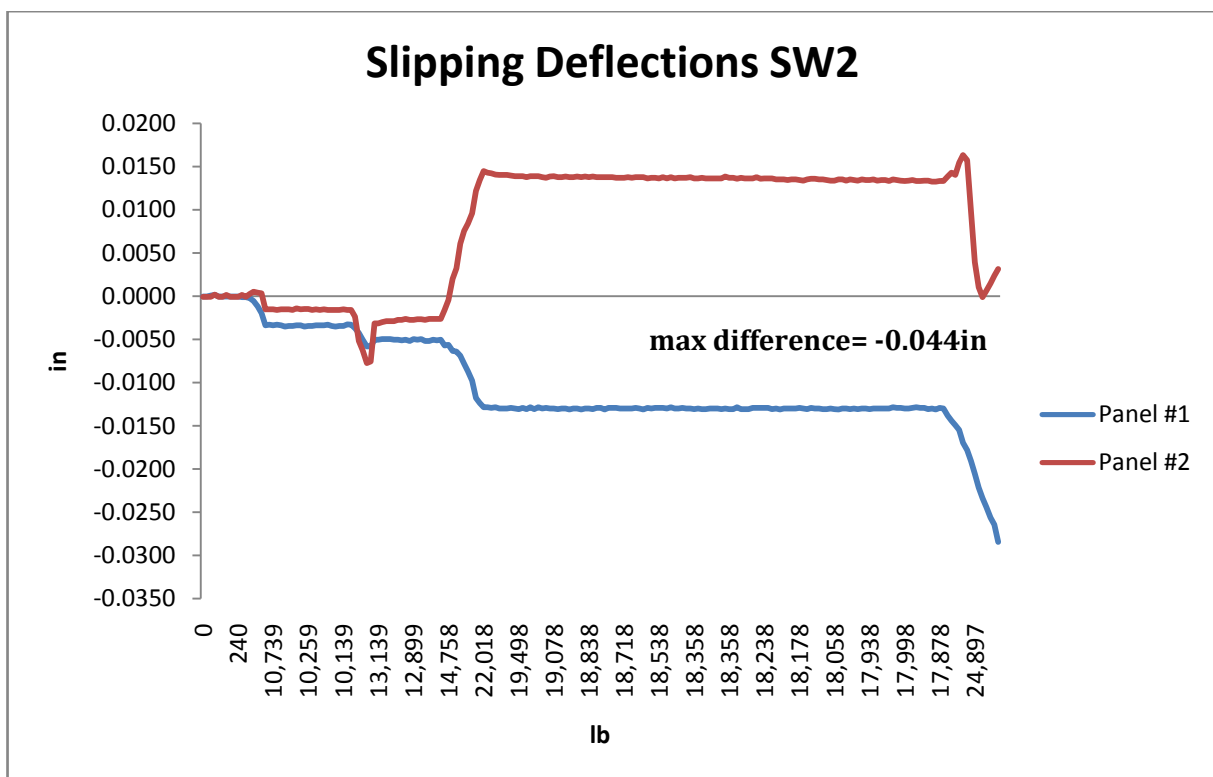


**Figure 3.23. Slipping Deflections SW2**

Rotational analysis showed that both panels deflections have negative sign, indicating that both panels rotated outwards (Figure 3.24). Maximal deflection for panel #1 was -0.0444, while maximal deflection for panel #2 was -0.0443.

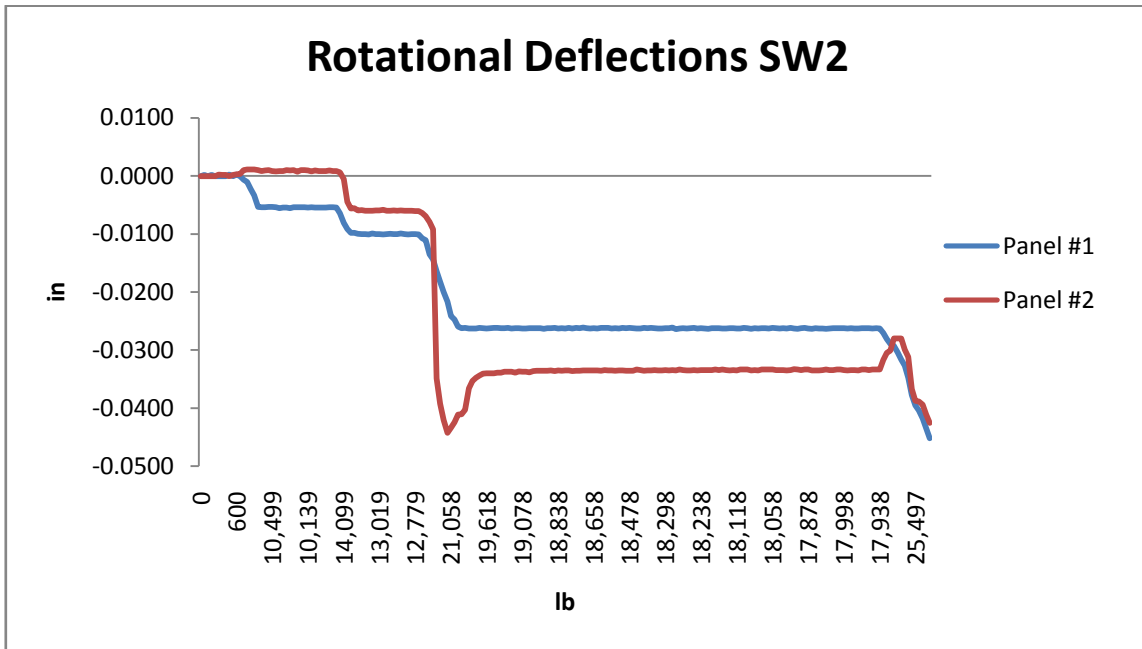


**Figure 3.24. Rotational Deflections SW2**

Load deflection analysis summary is presented in Table 3.5.

**Table 3.5. Load Deflection Analysis Summary SW2**

Load -Shear Deflection		Load-Lateral Deflection		Panel #1 Deflection (in)	Panel #2 Deflection (in)
$\Delta S_{max} =$ -0.214 in	$L_{shear\ max} =$ 27,757lb	$\Delta l_{max} =$ 0.237 in	$L_{max} =$ 27,657lb	uplift max=0.317	uplift <sub>max</sub> =0.15
$\Delta S_{1max} =$ -0.235 in	$L_{S1max} =$ 23,757 lb	$\Delta l_{sap2000} =$ 0.21in	$L_{sap2000} =$ 21,2100lb	slipping <sub>max</sub> = -0.027	slipping <sub>max</sub> = 0.016
$\Delta S_{2max} =$ - 0.179 in	$L_{s2max} =$ 23,337 lb	$\Delta l_{design} =$ 0.003 in	$L_{design} =$ 21,2100lb	rotational <sub>max</sub> = -0.0440	rotational <sub>max</sub> = -0.0443

### 3.2.8. Shear Stiffness (G') for SW2<sup>11</sup>

Shear stiffness was calculated using Equation 3.4 recommended in ASTM E564.

$$G' = \frac{Pl * a}{\Delta l * b} \quad (\text{Equation 3.5})$$

Calculated shear stiffness for SW2 was  $G' = 22,540 \text{ lb/in}$

### 3.2.9. Strain Analysis for SW2

Maximal strain obtained for SW1 was  $-440.32 \mu\text{E}$ . Maximal strain was recorded at the maximal lateral load of 27,597 lb (Figure 3.25).

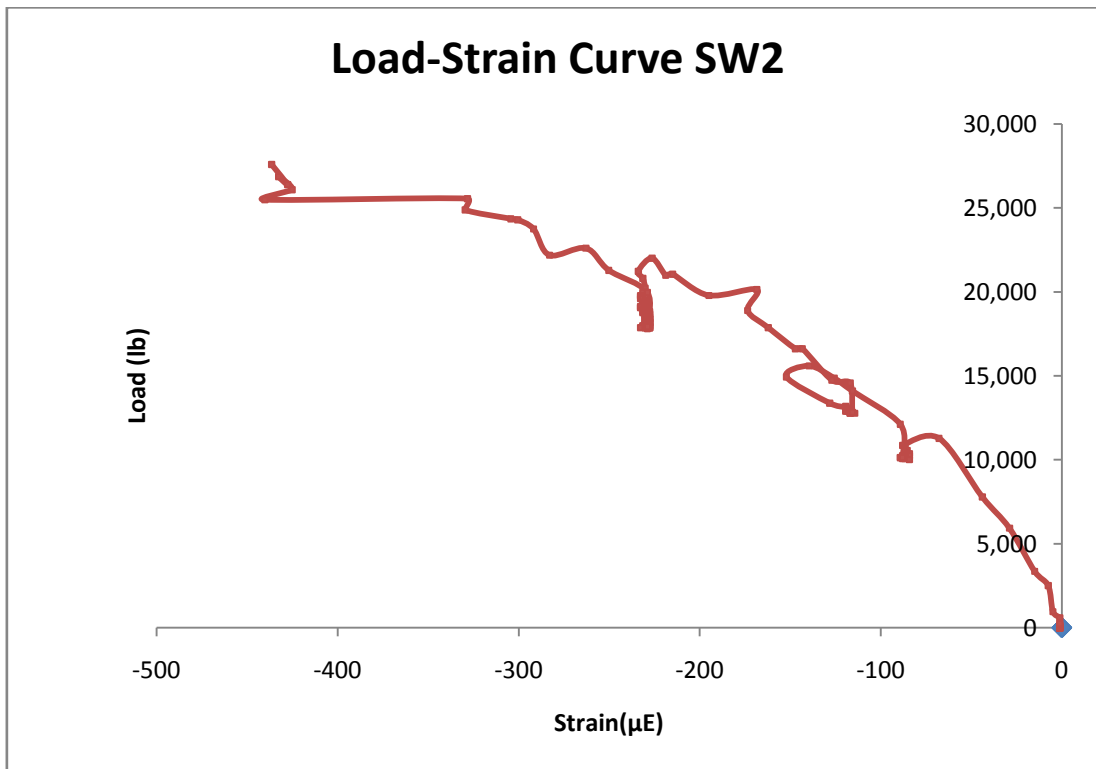


Figure 3.25. Load-Strain Curve SW2

<sup>11</sup> Detailed calculation for shear stiffness is presented in Appendix A-6

Load-Strain curve in Figure 3.25. shows same linear dependency between lateral load and concrete strains as it was shown during testing of SW1. Shape irregularities displayed on the graph are attributed to the gauge's sensitivity to the testing conditions.

### 3.2.10. Concrete Crack Analysis for SW2

Concrete crack development and propagation pattern at SW2 was different than observed at SW1 (Figure 3.26). The cracks were not only detected at the joints between panels and connecting beams but they were grouped at the lower sections of the wall panels as well.

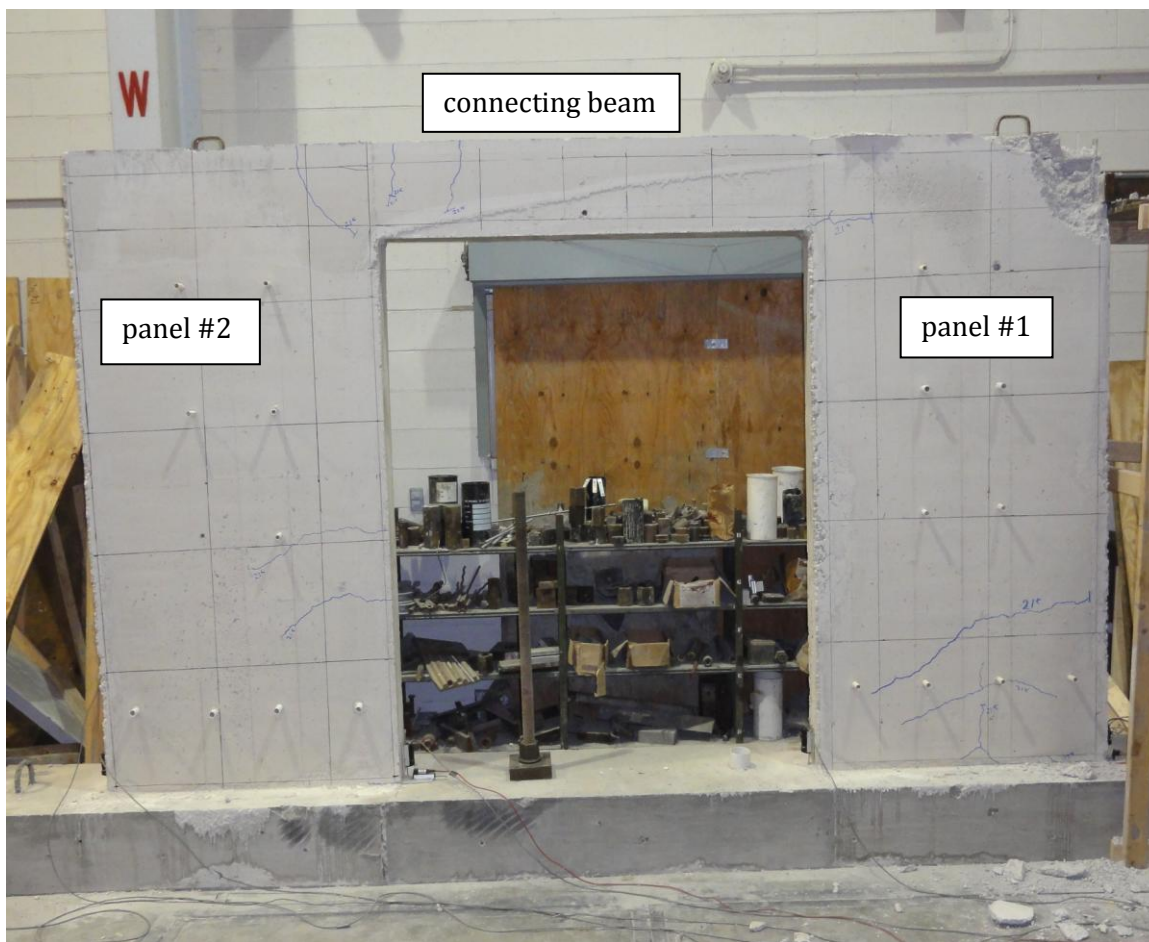


**Figure 3.26. Concrete Crack Development and Propagation SW2**

First cracks were detected at the load of 10,000lb at the joint between footing and bottom section of the panel#1 (Figure 3.27). This finding confirmed assumption that initially the wall was deflecting upwards rather than sideways.

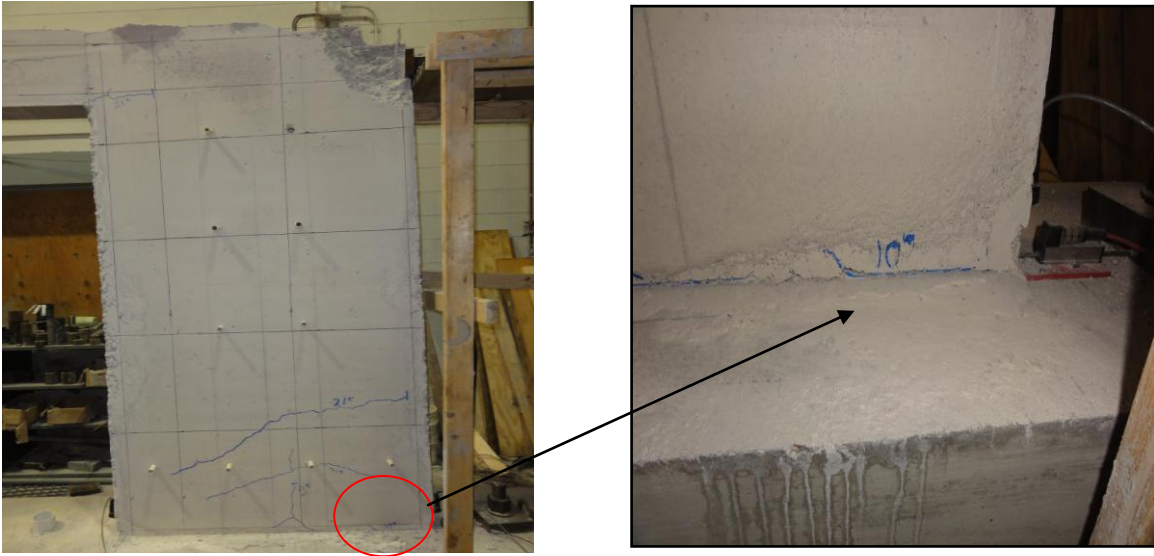


**Figure 3.27. Cracks Generation at Load of 10,000lb (Front Side)**

At design load of 21,000lb additional cracks showed on the joints between connecting beam and both panels (Figure 3.28). At the same load additional cracks were detected at lower sections at both panels (Figure 3.29).



**Figure 3.28. Crack Generation at Load of 21,000lb (Front Side)**

At load of 27,597lb, concrete bearing failure occurred at the upper section of the panel#1 at the point where the load was applied (Figure 3.30). It seems that bearing failure did not affect already formed cracks. No crack propagation was detected on already formed cracks.

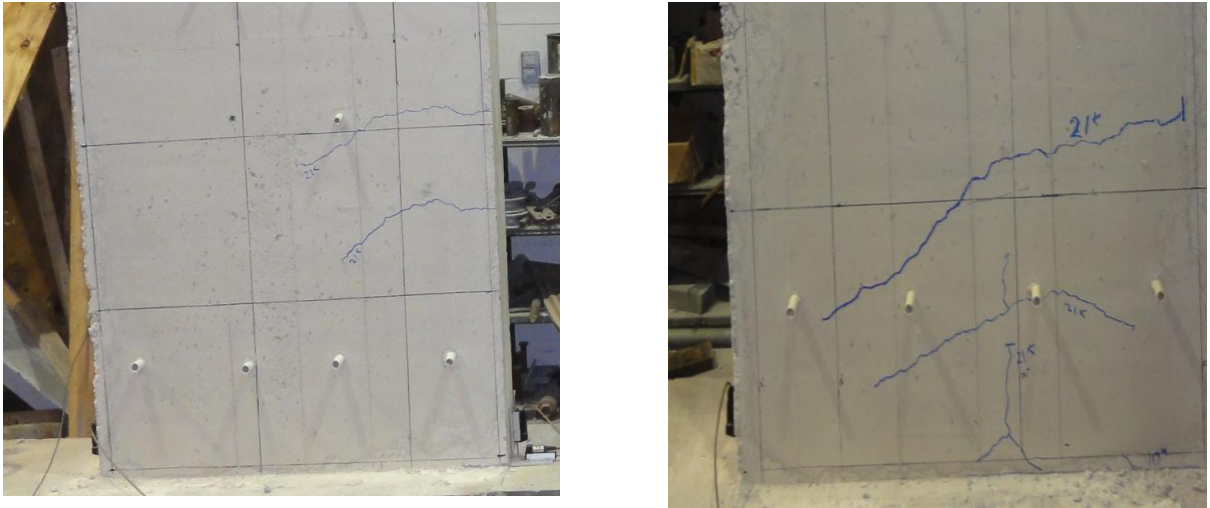


**Figure 3.29. Cracks Development at Load of 21,000 lb ( Lower Front Side)**



**Figure 3.30. Crack Generation at Failure Load (Front Side)**

### 3.3. Cost Analysis

#### 3.3.1. Cost Analysis of Precast (Industry Standard) ICF

The cost estimation of typical precast industry standard ICF walls (Figure 3.31) was obtained from NAHB Research Center and ICF Builder Magazine (2012).

The precast ICF specifications:

- #4 dowels, 48" long, spaced 12" on center
- 6" concrete layer
- #4 bar horizontal at 16" on center and one within 12" of the top of the wall, double at all openings.
- #4 bar vertical at 12" on center, double at all openings.
- 3/8" aggregate 3500 psi concrete.
- \$3.15 per sq. ft. of ICF
- \$3.00 for ICF labor cost

Total cost estimate for precast ICF walls<sup>12</sup> was calculated to be 9.08 \$/ft<sup>2</sup> (Table 3.6).

**Table 3.6. Initial Cost Estimate of Precast ICF Walls**

Item	\$/ft <sup>2</sup>
Dowels	0.55
ICF forms 6"	3.5
Reinforcing steel	0.6
Concrete 6" core at \$80/CY	1.48
Labor	3.25
Waste	0.25
<b>Total</b>	<b>9.08</b>

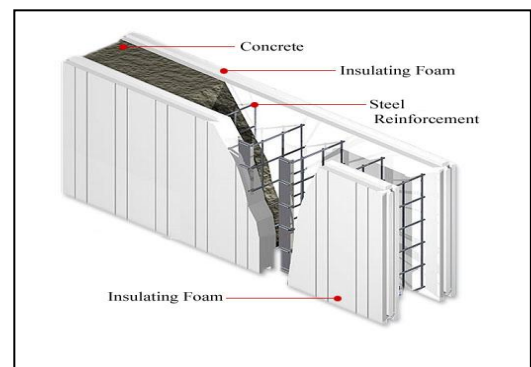


**Figure 3.31. Precast ICF Wall**

<sup>12</sup> Precast ICF Wall Figure is taken from monsterconstructor.com website

### 3.3.2. Cost Analysis of Site-Build ICF Wall System

The cost of material for site build ICF wall was computed from actual material purchases used in project (Table 3.7.)

**Table 3.7. Materials Used in Construction of Site Build ICF Wall System**

Item	Member	Quantity
Sheet	plywood 3/4"	5
Studs	lumber 2x4	20
Wales	lumber 2x4	40
Columns	lumber 2x4	4
Ties	steel rod 72" long	7

The job-build ICF specifications (Figure 3.32):

- #5 dowels, 24" long, spaced 18" on center
- 6" concrete layer
- #4 bar horizontal at 18" on center and one within 12" of the top of the wall
- #4 bar vertical at 18" on center, and one within 6" from the opening.
- 3/4" aggregate 4000 psi concrete.
- EPS Boards 8'x4'x 2"
- Ties- 24" long spaced at 16"
- Plywood 8'x4'x 3/4"
- 2x4 boards 8ft long

Total cost estimate<sup>13</sup> for job build ICF walls was calculated to be 10.86 \$/ft<sup>2</sup> (Table 3.8)

<sup>13</sup> Labor was estimated as exterior wall framing, data was obtained from Home Improvement Resource web site

**Table 3.8. Initial Cost Estimate of Job Build ICF Wall**

Item	\$/ft <sup>2</sup>
Dowels	0.55
EPS Boards 4"	1.53
Reinforcing steel	0.5
Concrete 6" core at \$80/CY	1.48
Plywood 3/4"	1.22
2x4 boards	1.67
Labor <sup>3</sup>	3.00
Ties, Nail	0.66
Waste	0.25
<b>Total</b>	<b>10.86</b>

**Figure 3.32 Formwork Job Build ICF Wall**

### 3.3.3. Cost Analysis of Site-Build Sustainable ICF Wall System

Salvaged plywood and 2x4 boards are used in building of formwork for sustainable job-build ICF system (Figure 3.33). Usually the cost of salvaged lumber is 50-70% of the price of the new lumber.

**Table 3.9. Initial Cost Estimate of Job Build Sustainable ICF Wall**

Item	\$/ft <sup>2</sup>
Dowels	0.55
EPS Boards 4"	1.53
Reinforcing steel	0.5
Concrete 6" core at \$96/CY	1.77
Plywood 3/4"	0.66
2x4 boards	0.8
Labor <sup>2</sup>	3.45
Ties, Nail	0.33
Waste	0.1
<b>Total</b>	<b>9.69</b>

**Figure 3.33. Formwork Job Build Sustainable ICF Wall**

Reusable ties are also used in building of the formwork. Labor cost is increased for 15% compared to job build ICF walls. Labor cost rise was attributed to handling reused lumber materials. Total cost estimate for sustainable job build ICF walls was calculated to be \$9.69 (Table 3.9).

Initial cost of job-build ICF walls is 16.4 % higher than precast ICF walls, while initial cost of job-build sustainable ICF wall is 6.3% higher than precast ICF walls.

## **CHAPTER 4. DISSCUSION AND CONCLUSION**

This chapter summarizes and discusses findings from the Chapter 3. It compares test results with the research hypotheses and makes further research recommendations.

### **4.1. Material Testing Discussion**

Results from material testing showed that experimental mix did not gain designed compression strength. The reason why experimental mix did not gain designed compression strength is either due to chemical or mineral contamination. Chemical contamination of self consolidating agent could cause a very strong retardation. Chemical hydration process and chemical contamination of self consolidating agent could be very difficult to trace. Another source of retardation could be mineral contamination of the aggregate. Recycled aggregate is first on the list of potential contaminated candidates. It could be possible that recycled concrete aggregate in previous utilization cycle was used in mineral contaminated environment (for example environmental conditions were too acidic). Additionally, many minerals could shut down the  $C_3A$ <sup>14</sup> (three calcium aluminate) or  $C_3S$  (three calcium silicate) potential in Portland or IPF cement.

Compression tests results also showed that experimental mix specimen gain strength when exposed to dry conditions. Explanation why the compression cylinders gain strength in dry condition could lie in combination of factors. One of the factors could be that the heat from being out of doors is likely the strength gaining catalyst. Mechanism of this reaction still remains unknown. Results from the Chapter 3 do not support thesis Hypothesis #1 that states that test results for the shear wall made of experimental concrete mix will not be significantly greater than test results for the shear wall of regular concrete.

---

<sup>14</sup>  $C_3A$  and  $C_3S$  control dynamic and heat of hydration of concrete

## 4.2. Shear Wall Testing Discussion

Shear wall testing showed that SW1 has 32 % higher ultimate load capacity, 74.5 % higher lateral deflection and 99.9% higher lateral deflection at design load. SW1 also has 62.6% lower shear stiffness and 73.2% lower strain. Table 4.1 summaries testing results for both walls.

**Table 4.1. Summary of Shear Test Results for Control (SW1) and Experimental (SW2) wall**

Measurement	SW1	SW2
Ultimate lateral load $P_u$ (lb)	40,555	27,597
Max lateral deflection $\Delta_1$ (in)	0.93	0.237
Max shear deflection $\Delta_s$ (in)	0.72	-0.214
Lateral deflection at design load $\Delta_{design}$ (in)	0.41	0.003
Shear stiffness (lb/in)	8,423	22,540
Compression Strain <sup>15</sup> ( $\mu E$ )	118.0	440.32
First crack generation load (lb)	25,000	10,000

The test results showed that walls behaved differently under lateral loading. SW1 mostly deflected laterally with minimal uplift and no slipping, while SW2 first deflected upward before started deflecting laterally. Lateral deflection at SW2 mostly started when concrete bearing failure at load application point occurred. Walls' different load response could be attributed to different concrete mixes used in the study. It seems that concrete to dowel bond in control mix was stronger than concrete to dowel bond in experimental mix. The comparative evaluation of shear deflection and shear stiffness between SW1 and SW2 should be taken with lot of reserves. It seems that both suggested algorithms (Equations 3.1 and 3.4) are heavily influenced by walls

---

<sup>15</sup> Strain on the wall's compression side

uplift deflections. Calculated max shear deflection for SW2 has negative sign which imply that wall just partially deflected as designed (as rhomboid). Additionally, just looking at shear stiffness value we could wrongly conclude that SW2 has higher capacity to resist shear forces compared to SW1. Very interesting finding is that SW2 has higher compression strain capacity than SW1. Results obtained from the Chapter 3 do not support thesis hypothesis #2 that states that test results gotten from the testing a residential shear wall with control mix (SW1) will not be significantly greater than results gotten from the testing a residential shear wall with experimental mix (SW2)

### **4.3. Cost Analysis Discussion**

Cost analysis showed that when precast ICF walls are less costly than job build ICF walls. However this holds true just for initial material and labor costs analysis. In order to compare overall cost of pre cast ICF vs. job build walls we needed more profound cost analysis. The value of job built ICF walls is its ability to withstand high gravity construction loads. Job built ICF formwork's high structural rigidity allows cast in-place of both, floor's slab and accompanying walls. Precast ICF walls do not have high compressive strength (60 psi) and therefore combined slab-walls cast in-place is not possible.

There are two other potential benefits from combined cast in place concrete placement. First potential benefit is that construction cost is lower. Generally, on small projects such as concrete walls, 20-30 % of concrete casting cost is going towards transportation costs and handling fees for concrete mixing trucks. Concrete slabs in general take more concrete volume than concrete walls. If fewer times concrete mixing trucks are needed on the site project, lower are overall construction costs.

Second potential benefit is a higher construction pace. Precast ICF systems are generally constrained by lower concrete placement rate. A concrete placement rate for precast ICF systems is about 3 ft/hr. A concrete placement rate for job build ICF systems is between 10 ft/hr and 15 ft/hr depending of the formwork design. High concrete placement rate allows lower labor cost and accelerated construction process. Accelerated construction could be very important issues in uncharacteristic construction circumstances such as relief efforts after earthquakes, tornados, hurricanes or wars. In these circumstances reliable, safe, cost effective and quick construction systems could vital for the public safety and benefit.

If we assumed that job build ICF formwork is going to be reused at least 5 times before discarded and that concrete cost for job build ICF wall per project is going to be 20% lower than it would be for pre cast ICF wall than we get a better approximation of real overall cost of ICF wall systems. Figure 4.1 shows comparison between initial and overall cost of ICF wall systems.

Overall cost of job build ICF wall remain almost unchanged (\$ 10.56) but overall cost of sustainable job build ICF wall dropped significantly ( \$ 7.84). When comparing overall cost of sustainable job build ICF wall to precast ICF wall we can see that cost of building sustainable ICF wall is 13.6% is less expensive than building precast ICF wall.

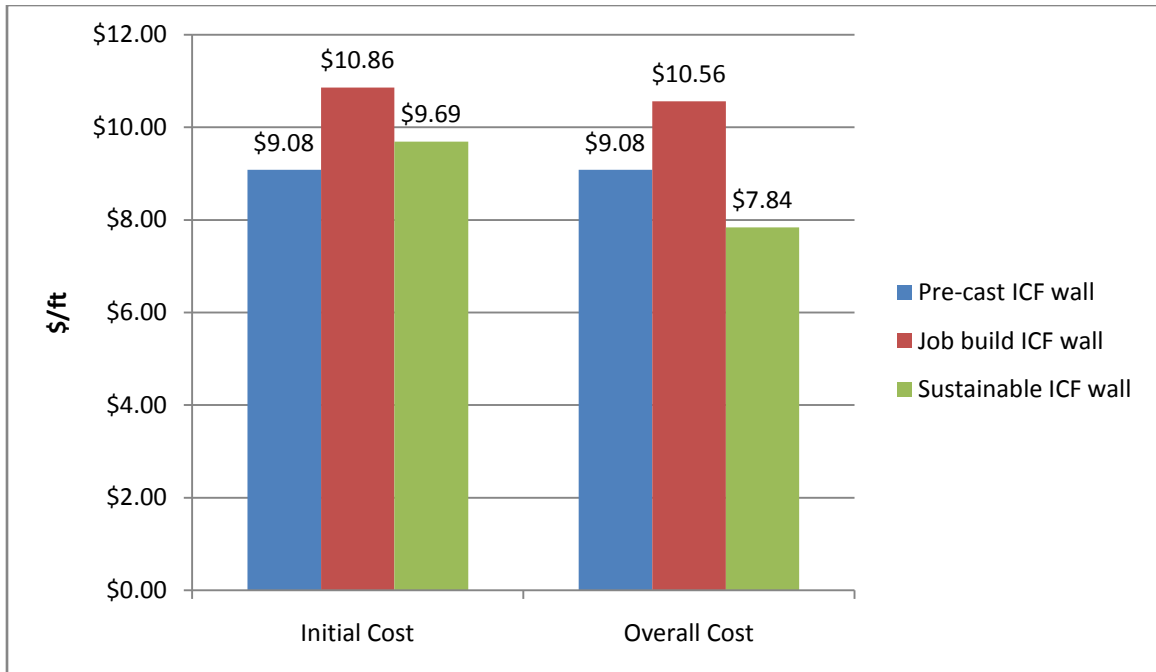


**Figure 4.1. Initial to Overall Cost Analysis Comparison among ICF Wall Systems**

Results of overall cost analysis of ICF wall systems support thesis hypothesis #3 that stated that the cost of the construction of the job build insulated concrete form walls is not going to be significantly more expensive than the cost of construction of a precast insulated concrete form walls.

#### 4.4. Conclusion

The results showed that compressive strength of the experimental mix (1,164 psi) is below safe minimum limits required for residential structural concrete (2,500 psi). However, flexural strength of experimental mix (2,399 psi) showed no signs of flexural strength retardation. The cause and mechanism of compressive strength retardation remains unclear and unknown.

The results showed that shear wall with experimental mix (SW2) showed significantly lower shear capacity (27.7 kips) compared to the shear capacity (40.5 kips) of the wall with control mix (SW1). However obtained shear capacity for both walls was greater than shear demand (21.1kips).

The results also showed that implementing sustainability concept in residential construction process did not affect its cost competitiveness. Overall cost of construction of job-build sustainable ICF shear wall is 13.6% less expensive than conventional pre-cast ICF wall.

The proposed system was shown to be cost competitive, environmentally friendly and structurally safe, despite excessive compressive strength retardation of experimental concrete mix caused by mineral or chemical contamination.

#### **4.5. Recommendations for Future Work**

For the future work I recommend replicating the experimental concrete mix and testing its compression strength. The literature review does not provide any evidence that using RCA, fly ash and self consolidating admixture would decrease its compressive strength that dramatically, but contrary all evidence point that using self consolidating admixture should increase concrete's mix compressive strength. In order to rule out any ambiguities experimental mix should use more than one source of RCA and self consolidating agent.

Additional work should be done in testing different type of connections between footing and the wall. As seen from the shear wall testing bonding between concrete and dowel at the shear wall with experimental mix, played major role how wall deflected under lateral load. Since

the bond wasn't strong enough, the wall started deflecting upwards before started deflecting laterally. For the future studies I recommend testing different types footing to wall connection by varying shape of dowel design, length and spacing.

Finally the second look should be given to the equation that calculates wall's shear stiffness. Using this equation blindly we could erroneously conclude that the wall with experimental mix had larger shear stiffness, which was obviously not the case. This equation is heavily influenced by lateral deflection of the upper leading corner. As seen from the results of this study, the wall necessary does not deflect purely laterally, but it can deflect differently than predicted. This especially holds true for the walls with openings.

## **References:**

1. Acker, V. A. (1997). Recycling of concrete at a precast concrete plant. *Sustainable Construction Part*, 321-332
2. Ali, A., & Wight, J. K. (1990). Reinforced structural walls with staggered opening configurations under reversed cyclic loading. *No. UMCE 90-05.*, Ann Arbor, MI: Department of Civil Engineering, University of Michigan.
3. Ali, E. E., & Al-Tersawy, S. (2010). Self-compacting concrete using coarse recycled concrete aggregates. *HBRC Journal*, 6, 3.
4. Angulo, S. C. (2002). Construction and demolition waste its variability and recycling in Brazil. *Proceedings of Sustainable Building 2002 Conference*,
5. ASTM. C39 Compressive strength of cylindrical concrete specimens.
6. ASTM. C192 Making and curing concrete test specimens in the laboratory.
7. ASTM. C617 Capping cylindrical concrete specimens.
8. ASTM E 564 - 2000 Standard Practice for Static Load Test for Shear Resistance of Framed Walls for Buildings.
9. Berndt, M. L. (2009). Properties of sustainable concrete containing fly ash slag and recycled concrete aggregate. *Construction and Building Materials*, 23, 2606–2613.
10. Bruening, S. F., & Chini, A. (2003). Deconstruction and material reuse in the united states. *The Future of Sustainable Construction*,
11. Buck, A. D. (1977). Recycled concrete as a source of aggregate. *ACI Journal*, 74(22), 212-219.
12. Cardenas, A. E., Russel, H. G., & Corley, W. G. (1980). Strength of low rise structural walls. *American Concrete Institute*, SP-63
13. Corinaldesi, V., & Moriconi, G. (2004). The role of recycled aggregates in self-compacting concrete. *Proc., 8th CANMET/ACI Int. Conf. on Fly Ash, Silica Fume, Slag and Natural Pozzolans in Concrete*, 941–955.
14. Doebber, I., & Ellis, M. (2005). Thermal performance benefits of precast concrete panel and integrated concrete form technologies for residential construction. *ASHRAE Transactions*, 1112(240-252).

15. Dolan, J. and Johnson, A., *Cyclic and Monotonic Tests of Long Shear Walls with Openings*, Prepared for the American Forest & Paper Association by Virginia Polytechnic Institute (1996)
16. Dosho, Y. (2007). Development of a sustainable concrete waste recycling system - application of recycled aggregate concrete produced by aggregate replacing method. *Journal of Advanced Concrete Technology*, 5(1), 27-42.
17. Dyer, T., Paine, K., Dhir, R., & Ravindra. (2000). Sustainable construction: Use of incinerator ash. *Thomas Telford Publishing*.
18. FEMA Report 342. (1999). "Mitigation Assessment Team Report for May 3, 1999" . *Federal Emergency Management Agency Report NO 342*.
19. FHWA. (2004). Transportation applications of recycled concrete aggregate. *State of the Practice National Review*.,
20. Franklin Associates. (1998). Characterization of building-related construction and demolition debris in the U.S. , *A Report to the US Environmental Protection Agency Office of Solid Waste and Energy Response*. Washington, D.C.
21. Frondistou-Yannas, S. (1977). Waste concrete as aggregate for new concrete. *ACI J .Proc*, 74(8), 373-376.
22. Gao, J. M., Qian, C. X., Liu, H. F., Wang, B., & Li, L. (2005). ITZ microstructure of concrete containing GGBS. *Cem. Concr. Res.*, 35(7), 1299–304.
23. Hansen, T. (1992). Recycling of demolished concrete and masonry. ( No. 6).*RILEM*.
24. Hansen, T. C., & Narud, H. (1983). Strength of recycled concrete made from crushed concrete coarse aggregate. *Concrete International*, 5(1), 79-83.
25. Harrington, J. (2005). Recycled roadways. *Federal Highway Administration, Publications , Public Roads*, 68(4)
26. International Building Code (2006).
27. Hendriks, C. F., & Janssen, G. M. T. (2001). Reuse of construction and demolition waste in the Netherlands for road construction. *Heron*, 46, 109-117.
28. Kim, J., Sun, Y., & Falkner, V. (2006). Seismic performance of frame structures with recycled aggregate concrete. *Engineering Structures*, 28, 1-8.
29. Limbachiya, M. (2000). Use of recycled Concrete Aggregate in high strength concrete. *Materials and Structures*, 33, 574-580.

30. Limbachiya, M. C. (2004). Performance of recycled aggregate concrete. *RILEM International Symposium on Environment-Conscious Materials and Systems for Sustainable Development*.
31. Malhotra, V. M. (2000). Role of supplementary cementing materials in reducing greenhouse gas emissions. *Concrete Technology for a Sustainable Development in the 21st Century*.
32. Mehrabi, A. (1999). In-plane lateral load resistance of wall panels in residential buildings. *Prepared for the Portland Cement Association by Construction Technology Laboratories, Inc.. Skokie, IL*.
33. Mehta P., K. (2001). Reducing the environmental impact of concrete. *Concrete International*, 23, 61-66.
34. Mehta, P. K. (2002). Greening of the concrete industry for sustainable development. *Concrete International*, 23-29.
35. Molin, C., Larsson, K., & Arvidsson, H. (2004). Quality of reused crushed concrete strength, contamination and crushing technique. *Proceedings of International RILEM Conference on the use of the Recycled Materials in Buildings and Structures*. 150 -155.
36. Nagaraj, T. S., Shashiprakash, S. G., & Raghuprasad, B. K. (1993). Re-proportioning concrete mixes. *ACI Mater*, 90(1), 50-58.
37. NAHB Research Center. (1997). Insulating concrete forms for residential construction - demonstration homes. *Report for US Urban and Housing Development Agency*. NAHB Research Center.
38. NAHB Research Center. (2001). Costs and benefits of insulating concrete forms for residential construction. . *Report for the U.S. Department of Housing and Urban Development Office of Policy Development and Research*.
39. NAHB Research Center. (2002). In-plane shear resistance of insulating concrete form walls. . *Report for US Urban and Housing Development Agency*.
40. Naik, T. (2008). Sustainability of concrete construction *Pract.Period.Struct.Des. Constr.*, 13, 98-104.
41. Otsuki, N., Miyazato, S., & Yodsudjai, W. (2003). Influence of recycled aggregate on interfacial transition zone, strength, chloride penetration and carbonation of concrete. *J Mater Civ Eng.*, 15, 443–51.
42. NAHB Research Center. (1998). Prescriptive method for insulating concrete forms in residential construction. *Report for US Urban and Housing Development Agency*.

43. Richardson, A., Allain, P., & Veuille, M. (2010). Concrete with crushed, graded and washed recycled construction demolition waste as a coarse aggregate replacement. *Structural Survey*, 28(2), 142 – 148.
44. Russell. (2002). *Evaluation of hurricane-resistant single-family residential structures*. (Master Thesis, University of Florida.).
45. Sagoe, K., & Brown, T. (2002). Durability and performance characteristics of recycled aggregate concrete. ( No. 090). UK: CSIRO Publishing.
46. Sogo. (2007). Shear behavior of recycled concrete beams. *Proceedings from International RILEM Conference on the use of Recycled Materials in Buildings and Structures, Vol .2* 610-619.
47. Tam, V. (2007). Economic comparison of concrete recycling: A case study approach. *Resources, Conservation and Recycling*, 52, 821-828.
48. Tavakoli, M., & Soroushian, P. (1996). Strengths of recycled aggregate concrete made using field-demolished concrete as aggregate. *ACI Mater.*, 93(2), 182–90.
49. Taylor, C. P., Cote, P. A., & Wallace, J. W. (1998). Design of slender reinforced concrete walls with openings *ACI Structural Journal*, 95(4), 420-433.
50. The Concrete Centre. (2011). *Specifying sustainable concrete*. Mineral Products Association.
51. Topçu, B., & Sengel, S. (2004). Properties of concretes produced with waste concrete aggregate. *Cem.Concr. Res.*, 38(4), 1307-1312.
52. TopçuBa. (1997). Physical and mechanical properties of concretes produced with waste concrete. *Cem.Concr. Res.*, 27(12), 817-823.
53. Tovey, A. (2007). Design and construction using insulating concrete formwork. *Published for The Concrete Centre by The Concrete Society*.
54. Tsung- Yueh, T. (2006). Properties of HPC with recycled aggregates. *Cement and concrete research* (pp. 943-950.)
55. Tu, T. (2005). The application of recycled aggregates in self-consolidating concrete. *SCC'2005-China: 1st International Symposium on Design, Performance and use of Self-Consolidating Concrete*, 145-146-152.
56. Uniform Building Code, (1997) Vol. 2, International Council of Building Officials, Whittier, CA,

57. Weber, e. a. (2009). *Market analysis of construction and demolition material reuse in the chicago region.* (). University of Illinois at Chicago:
58. Wen-Chen Jau, e. a. (2004). Study of feasibility and mechanical properties for producing high flowing concrete with recycled coarse aggregates. *Proceedings of the International Workshop on Sustainable Development & Concrete Technology*, , 89-102.
59. Yang, C. (2009). Composition of demolition wastes from Chi-Chi earthquake-damaged structures and the properties of their inert materials. *Canadian Geotechnical Journal*, 46, 470-481.
60. Yaprak, H., Aruntas Yılmaz, H., Demir, I., Simsek, O., & Durmus, G. (2011). Effects of the fine recycled concrete aggregates on the concrete properties. *International Journal of the Physical Sciences*, 6(10), 2455–2461.

**APPENDIX A**

## **A-1. Wind Load Calculations**

### **Step 1.** Calculate Velocity Pressure Coefficient

$$q_z = 0.00256 K_z K_{zt} K_d V^2 I$$

where:  $K_z$  is velocity exposure coefficient evaluated at height  $z$ (ft),  $K_{zt}$  is topographical factor (flat surface assumed),  $K_d$  is wind directional factor and  $I$  is building importance factor.

$$K_z = 0.85$$

$$K_{zt} = 1.00$$

$$K_d = 0.85$$

$$V = 170 \text{ mph}$$

$$I = 1.00 \text{ (Category II building, Table 1-1. ASCE 7)}$$

$$q_z = 0.00256 * 0.85 * 1.00 * 0.85 * 170^2 * 1.00$$

$$q_z = 53.45 \text{ psf}$$

$$q_z = q_h$$

$$q_h = 53.45 \text{ psf}$$

### **Step 2.** Calculate External Pressure Coefficients ( $GC_p$ )

External Pressure Coefficients are calculated using appropriate coefficients from Appendix A-1 Table 1. and 2.

#### **Appendix A-1 Table 1. Wall External Pressure Coefficient from the ASCE 07-10 Table 27.4-1**

<b>Wall Pressure Coefficients, <math>C_p</math></b>			
<b>Surface</b>	<b>L/B</b>	<b><math>C_p</math></b>	<b>Use With</b>
Windward Wall	All values	0.8	$q_z$
Leeward Wall	0-1	-0.5	$q_h$
	2	-0.3	
	$\geq 4$	-0.2	
Side Wall	All values	-0.7	$q_h$

$h$  = mean roof height (ft)

$L$  = horizontal dimension of the building (ft) measured parallel to the wind

$B$  = horizontal dimension of the building (ft) measured normal to the wind

$G=0.85$  –gust factor for rigid building

Windward wall - All values

$$C_p=0.8$$

$$GC_p=0.85*0.8$$

$$GC_p=0.68$$

Leeward wall -  $L/B=48/50=0.96$ ;

$$C_p=-0.5$$

$$GC_p=0.85*0.5$$

$$GC_p=0.425$$

Roof Windward-  $h/L=15/48=0.312$ ; Angle  $\theta=15^\circ$

$$C_p=-0.7$$

$$GC_p=0.85*-0.7$$

$$GC_p=-0.595$$

Roof Leeward - Angle  $\theta=15^\circ$

$$C_p=-0.5$$

$$GC_p=0.85*-0.5$$

$$GC_p=-0.425$$

**Appendix A-1 Table 2. Roof External Pressure Coefficients from the ASCE 07-10 27.4-1.**

Roof Pressure Coefficients, $C_p$ , for use with $q_h$													
Wind Direction	Windward									Leeward			
	Angle, $\theta$ (degrees)									Angle, $\theta$ (degrees)			
	$h/L$	10	15	20	25	30	35	45	$\geq 60^\circ$	10	15	$\geq 20$	
Normal to ridge for $\theta \geq 10^\circ$	$\leq 0.25$	-0.7	-0.5	-0.3	-0.2	-0.2	0.0*	0.4	0.4	0.01 $\theta$	-0.3	-0.5	-0.6
	0.5	-0.9	-0.7	-0.4	-0.3	-0.2	-0.2	0.0*	0.4	0.01 $\theta$	-0.5	-0.5	-0.6
	$\geq 1.0$	-1.3**	-1.0	-0.7	-0.5	-0.3	-0.2	0.0*	0.3	0.01 $\theta$	-0.7	-0.6	-0.6

**Step 2.** Calculate Design Pressure ( $p$ )

Wind Pressure Equation used (Equation 2.2) for calculating the pressure design ( $p$ ) combines internal and external design pressures ASCE 07-10, Section 27.4-1.

$$p = qG C_p - q_i(G C_{pi})$$

Since only external pressure equation is used for the design of shear walls we can simplify this equation to:

$$p = qG C_p$$

Windward wall pressure

$$p = q_z * G * C_p$$

$$p = 53.45 * 0.68$$

$$p = \mathbf{36.34 \text{ lb/ft}^2}$$

Leeward wall pressure

$$p = q_h * G * C_p$$

$$p = 53.45 * 0.425$$

$$p = \mathbf{22.71 \text{ lb/ft}^2}$$

Total wind load wall pressure:  $p_w =$  Windward wall pressure + Leeward wall pressure

Total wind load wall pressure:  $p_w = 36.34 + 22.71$

**Total wind load wall pressure:  $p_w = 59.05 \text{ lb/ft}^2$**

Roof windward pressure

$$p = q_h * G * C_p$$

$$p = 53.45 * -0.595$$

$$p = \mathbf{- 31.80 \text{ lb/ft}^2}$$

Roof leeward pressure

$$p = q_h * G * C_p$$

$$p = 53.45 * -0.425$$

$$p = \mathbf{- 22.71 \text{ lb/ft}^2}$$

Total wind load roof pressure:  $p_r =$  Windward roof pressure + Leeward roof pressure

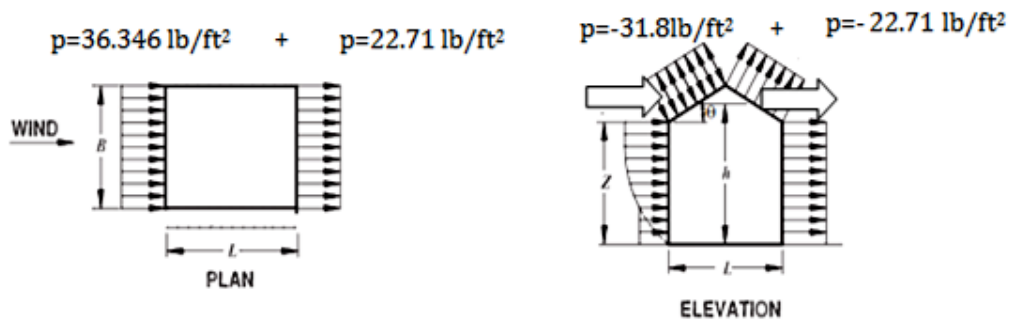
Total wind load roof pressure:  $p_r = 31.80 + 22.71$

**Total wind load roof pressure:  $p_r = 53.79 \text{ lb/ft}^2$**

Both roof wind pressures contribute to shear demand of the walls, and they are included in the computation of the total wind load on the structure (Appendix A-1 Figure 1.). Since the

slope of the roof is relatively small it is conservatively assumed that total roof load is acting horizontally (parallel to the shear wall).

It is assumed that there is no roof overhang on the structure and that is the reason why overhang wind load are not included in the calculations.



**Appendix A-1 Figure 1. Wind Load Wall ( $p_w$ ) and Roof Pressures ( $p_r$ )**

**Step 3.** Calculate Total Wind Load ( $W$ )

Total wind loads acting on the structure come from the wind wall pressure and from the roof's wind pressures.

Total wind loads acting on structure:

$$W = p_w * h_w + p_r * h_{rh},$$

where  $h_w$  is height of the wall in ft, and  $h_{rh}$  median roof height in ft.

$$W = 59.05 \text{ lb/ft}^2 * 8 \text{ ft} + 53.79 \text{ lb/ft}^2 * 7 \text{ ft}$$

<b>W = 848.93 lb/ft</b>
-------------------------

**Step 4.** Calculate Lateral Wind Force ( $P_w$ )

Lateral wind force ( $P_w$ ) is wall is calculated from the total wind load ( $W$ ) acting parallel to the shear wall

$$P_w = W * B / 2,$$

where  $W$  is wind load ( $\text{lb}/\text{ft}^2$ ) and  $B$  is length of the wind wall base (ft)

$$P_w = \frac{848.93 \frac{\text{lb}}{\text{ft}} * 50 \text{ ft}}{2}$$

$$P_w = 21223.25 \text{ lb}$$

$P_w = 21.22 \text{ kips}$
----------------------------

## **A-2. Sizing the Shear Wall Calculations**

ACI 318-08 code requires that all shear walls have to have minimum shear reinforcement no-matter how small shear demand is. The code stipulates that where  $V_u$  is less than  $0.5\phi V_c$  only minimum shear reinforcement is needed (ACI 318-08, Sections 11.9.8 and 14.3.1.).

$$V_u \leq 0.5\phi V_c$$

For the calculation of the nominal shear strength ( $V_c$ ) of the concrete section equations ACI 318-08 11.9.5 was used:

$$V_c = 2\lambda\sqrt{f'_c} hd$$

Where,

$V_c$  is nominal shear strength provided by concrete (ACI 318-08, Section 11-2),

$\lambda$  is concrete modification factor (ACI 318-08, Section 8.6.1). It is 1.00 for normal weight concrete,

$f'_c$  is concrete strength in psi,

$h$  is thickness of the wall in inches (ACI 318-08, Section 11.9.3),

$d = 0.8l_w$  (ACI 318-08, Section 11.9.4),

where  $l_w$  is overall length of the wall in inches,

$\phi$  is strength reduction factor for shear;  $\phi = 0.75$  (ACI 318-08, Section 9.3.2.3).

In order to get preliminary length of the shear wall Equations 5. and 6.were combined to get:

$$V_u = 0.5 * \phi * 2\lambda \sqrt{f'c} h d$$

According to International Residential Code for One and Two Story Family Dwelling (2012) minimum flat wall thickness is 4", therefore 4" wall thickness was used in preliminary calculations.

$$V_u = 0.5 * \phi * 2\lambda \sqrt{f'c} h d$$

$$21220 = 0.5 * 0.75 * 2 * \sqrt{4000} * 4 * d$$

$$d = 111.83 \text{ in}$$

Since  $d = 0.8l_w$ , therefore total length of the wall

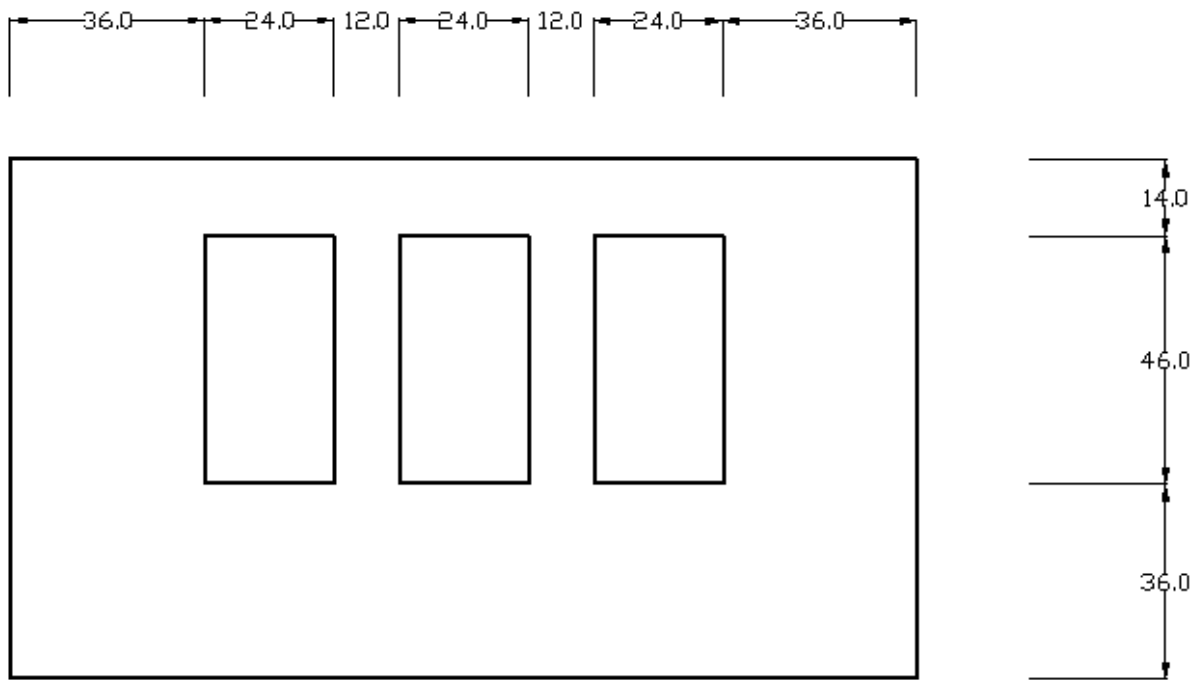
$$l_w = 111.83 / 0.8$$

$$l_w = 139.79 \text{ in} = \underline{11.65 \text{ ft}}$$

It was proposed that openings occupies 30 % of the total area of the wall, therefore it was decided to add approximately 30% extra length to the preliminary size of the wall. Therefore, the final longitudinal dimensions of the shear wall, used for numerical analysis, was determined to be 14 ft.

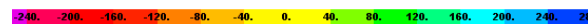
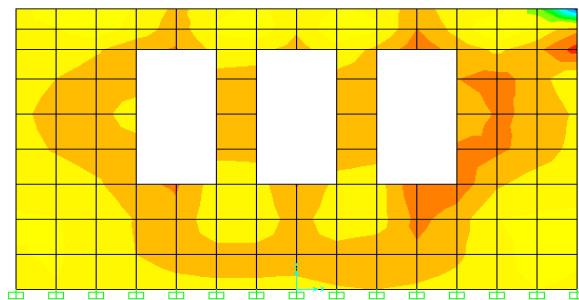
### **A-3. F.E. Models of Shear Walls With Openings**

a) Group 1. Walls With Three Single Window Openings (2ft x 4ft)

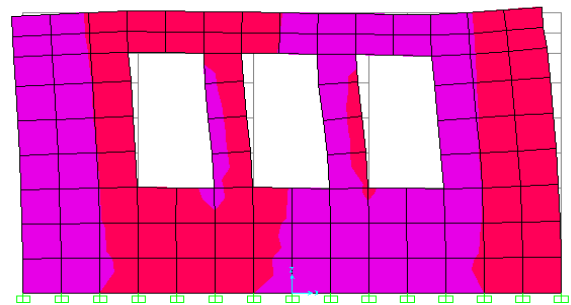


Appendix A-3. Figure 1. Group 1. Model Dimensions

1. F.E. model with three single window opening and wall thickness of 4”.

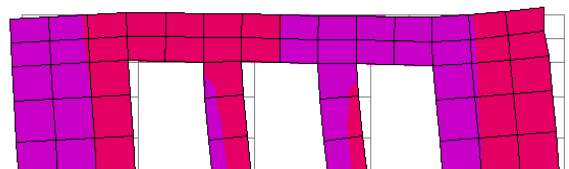
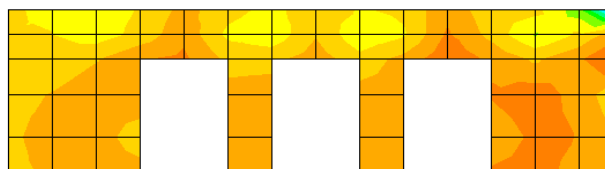


Max shear stress = -141.1 psi

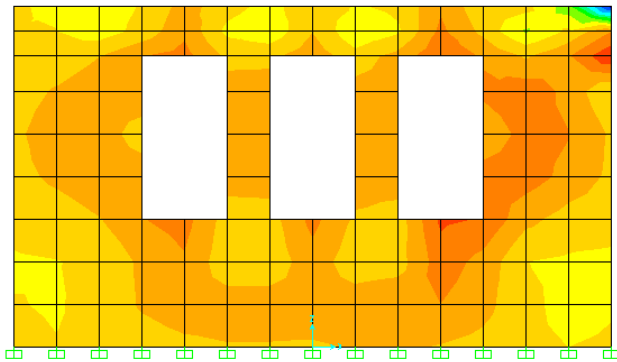


Max deflection horizontal=-0.0194 in

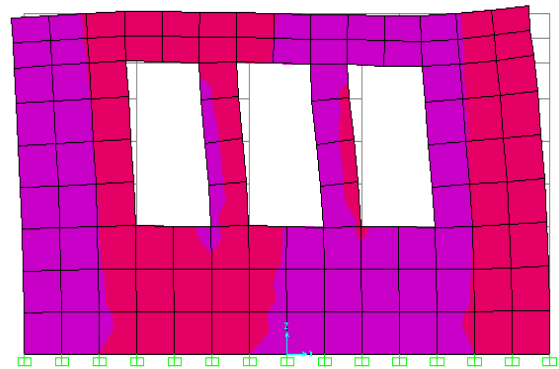
2. F.E. model with three single window opening and wall thickness of 5”



3. F.E. model with three single window opening and wall thickness of 6''

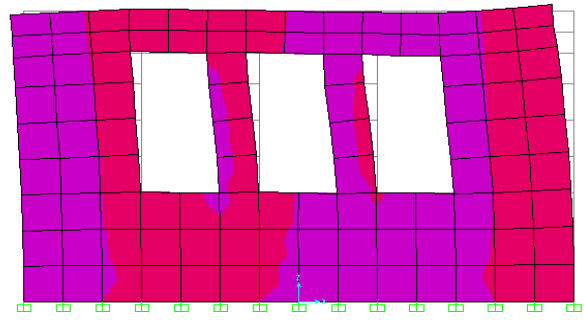
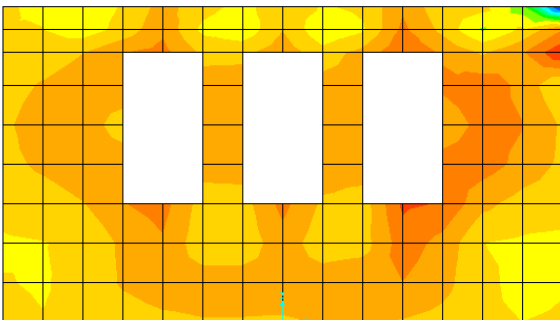


**Max shear stress = -94.22 psi**

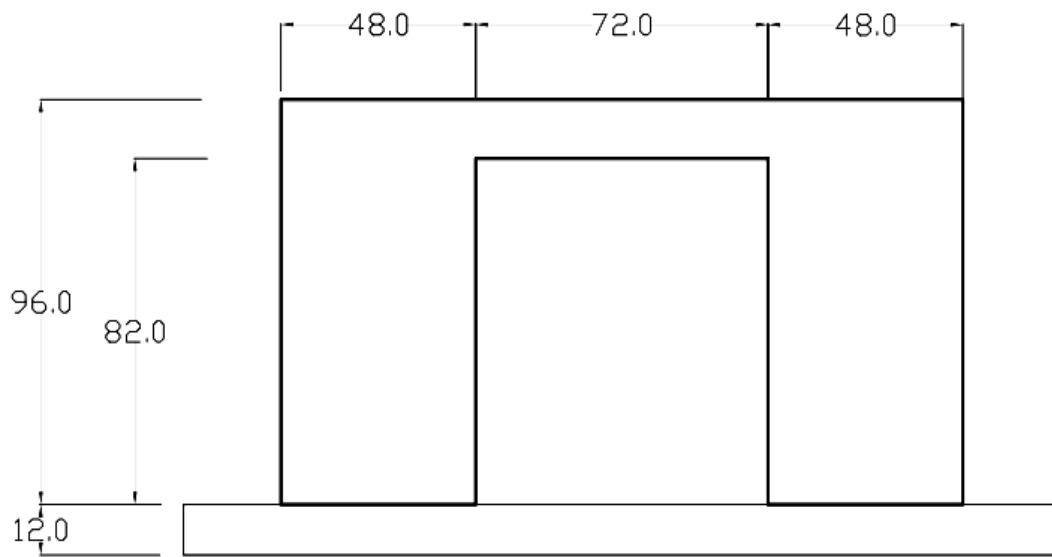


**Max deflection horizontal=- 0.013in**

4. F.E. model with three single window opening and wall thickness of 8''

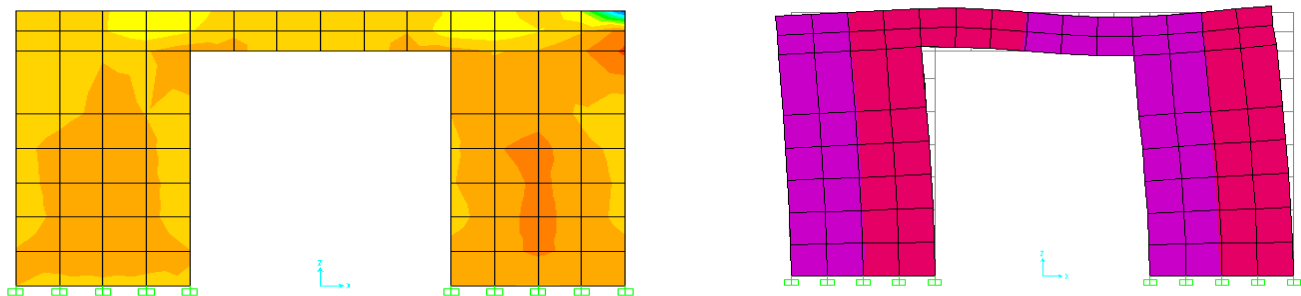


b) Group 2. Walls With Double Door Opening (6ft x 6.83ft)

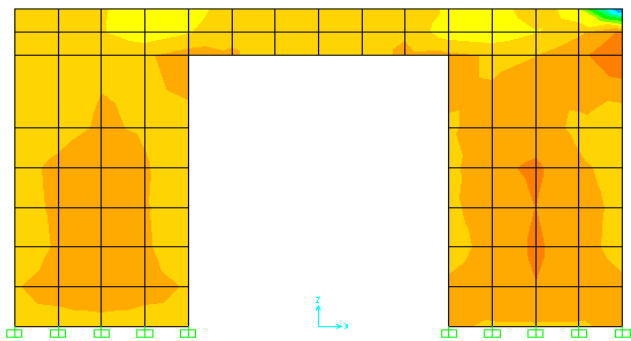


Appendix A-3. Figure 2. Wall With Double Door Opening Dimensions

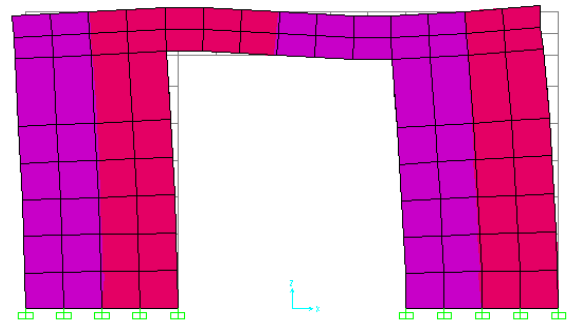
1. F.E. model with double door opening and wall thickness of 4"



2. F.E. model with double door opening and wall thickness of 5''

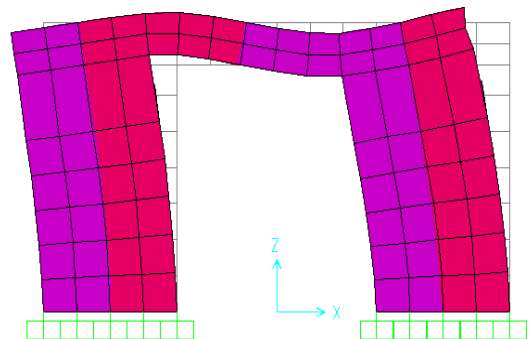
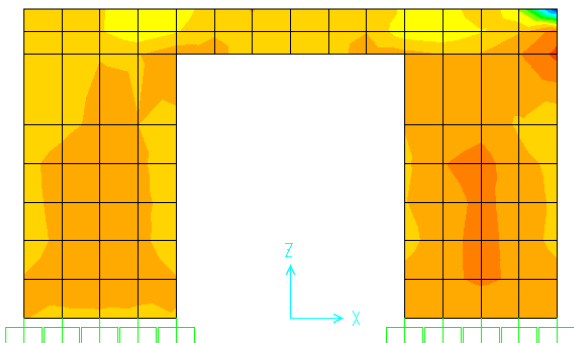


Max shear stress = -103.55 psi

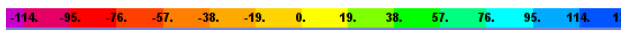
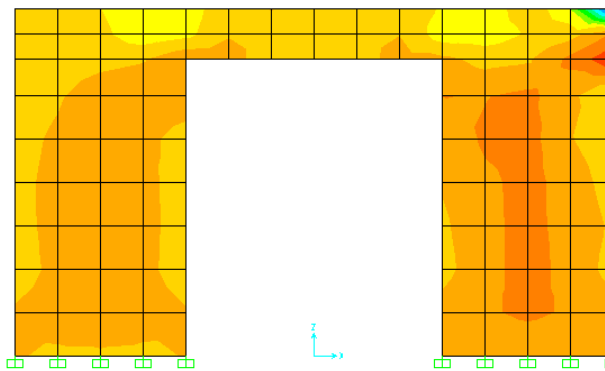


Max deflection horizontal=-0.02 in

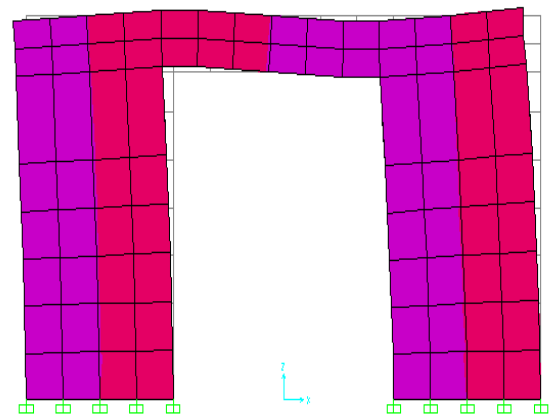
3. F.E. model with double door opening and wall thickness 6''



4. F.E. model with double door opening and wall thickness 8"



**Max Shear stress = -74.19 psi**



**Max deflection horizontal=-0.0121**

The wall with thickness of 4" had the stress demand of 149.5 psi, which is higher than the maximum concrete shear stress capacity. The maximum shear stress that concrete can resist is given by equation ACI 318-07, Section 11.9.5

$$v_c = 2\lambda\sqrt{f'_c}(\text{psi}),$$

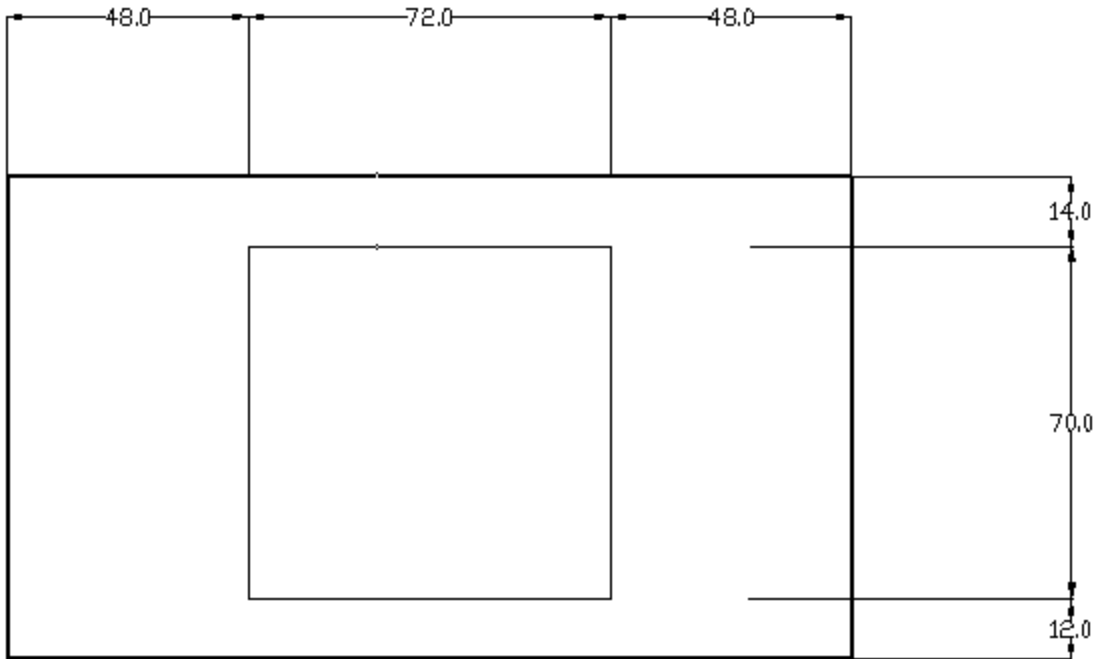
$\nu_c = 109.5$  psi.

Acknowledging that complete shear failure is unlikely event, due to presence of minimum reinforcement requirement, we still wanted to stay away from concrete cracking.

Once the concrete section is cracked it starts to behave in fairly nonlinear fashion which hard to model and test. All three of remaining candidates (5", 6" and 8" thickness) satisfied stress condition requirement. Although, Prescriptive Methods stipulated minimum 8" wall thickness around opening, structural analysis showed that this stipulation is highly over conservative from structural design standpoint and more expensive form construction stand point. Additional reason why we decided not to include 8" wall thickness into further consideration comes from architectural reasons as well. Considering that we have to add 4" of additional foam boards plus 1" of final wall's covering we end up with 13" deep walls. The wall that deep would require custom made windows and doors which would add to extra construction cost of the structure.

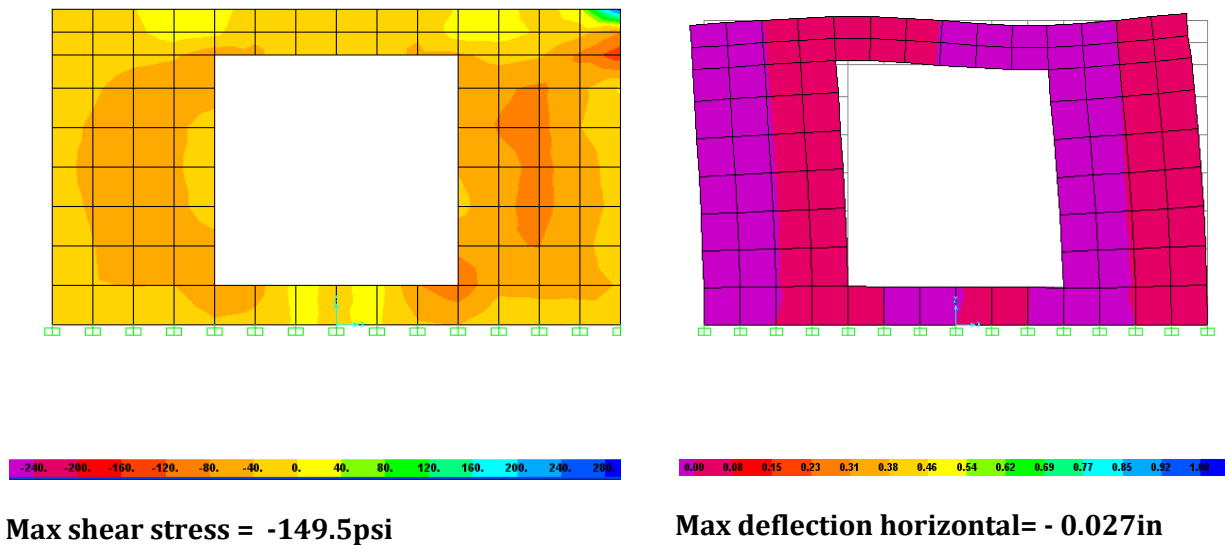
Finally it was decided that 6" thick wall is better testing candidate than 5" thick wall for mostly construction reasons. Knowing that reinforcement has to be put in place inside the wall, and knowing that minimum of 1.5" clear cover is needed for exterior walls (ACI 318-07, Section 7.7.1) it was decided that 6" thick wall would give us more room to operate if any correction is needed in placing reinforcement mesh.

c) Group3. Walls with Large Double Window Opening (6ft x 5.8ft)

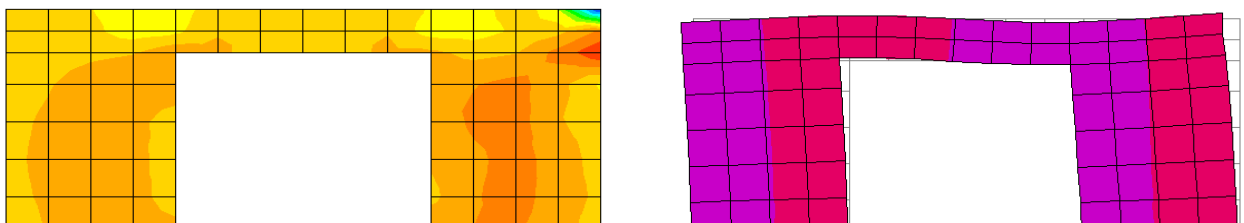


**Appendix A-3. Figure 3. Walls with Large Double Window Opening Dimensions**

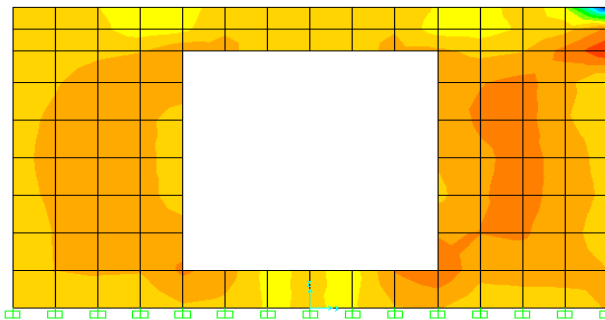
1. F.E. model with large double window opening and wall thickness 4''



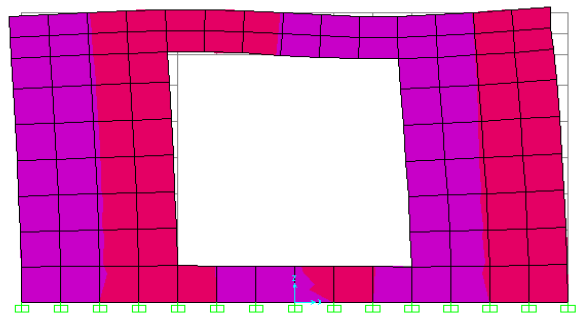
2. F.E. model with large double window opening and wall thickness 5''



3. F.E. model with large double window opening and wall thickness 6''

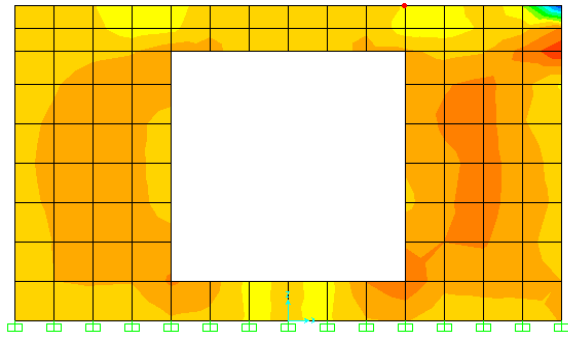


**Max Shear stress = -119.2psi**

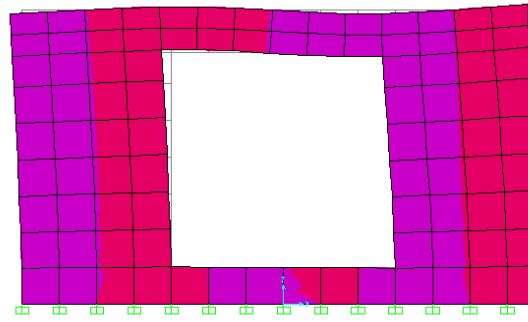


**Max deflection horizontal=-0.0185in in**

4. F.E. model with large double window opening and wall thickness 8''



**Max Shear stress = -74.66 psi**



**Max deflection horizontal=- 0.0114in**

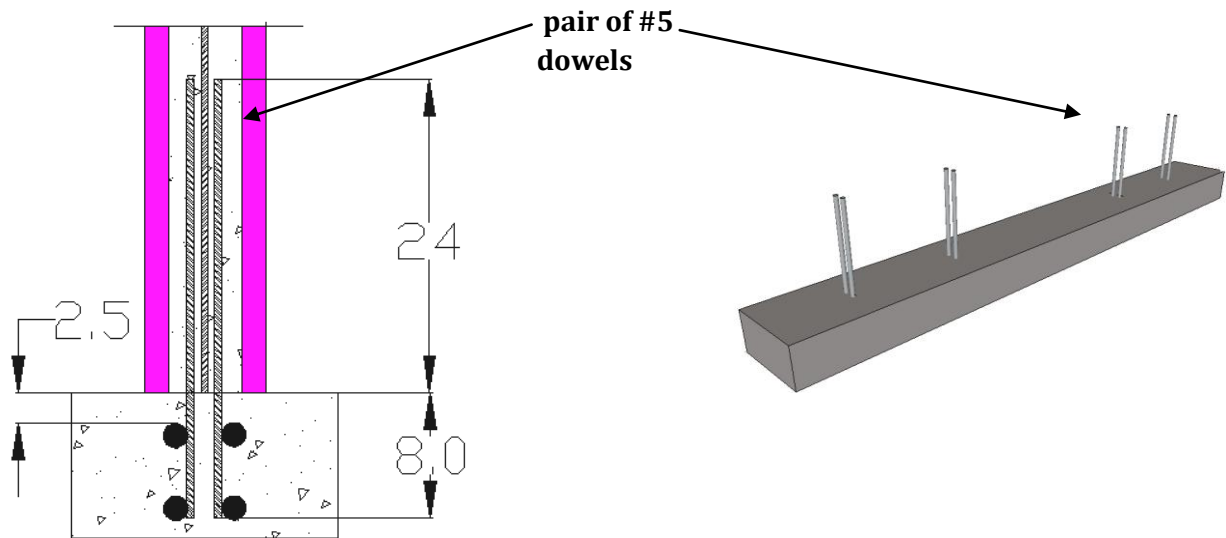
**A-4. Dowel Design Calculations**

Minimum splice length  $l = 40 d_b$ ,

where,  $d_b$  is diameter of the vertical reinforcement.

$$l = 40 * 0.5 = 20 \text{ in} \leq 24 \text{ in}$$

The dowel ends with 90° twelve inch long hook parallel to the length to the end of footing



### A-5. Formwork Design Calculations

Concrete lateral pressure was calculated using ACI equations:

$$p_{\max} = C_w * C_c [ 150 + 43,400/T + 2800 R/T ]$$

$$p_{\max} \geq 600 C_w$$

$$p_{\text{fluid}} \leq \gamma h$$

$C_c = 1.4$ - Chemistry Coefficient; for other types of blend with admixtures containing less than 70% slag or less than 40% fly ash. Once lateral pressure is determined it is used for calculating stud spacing.

$$C_w = 1.00 ; \quad R = 10 ; \quad T = 60 \text{ F};$$

$$P_{\text{fluid}} = 1200.00 \text{ lb/ft}^2$$

$$P_{\text{max}} = 1340.00 \text{ lb/ft}^2$$

$$P_{\text{design}} = \mathbf{1200.00 \text{ lb/ft}^2}$$

### Stud spacing

There are 3 limit states that governed studs spacing:

1. Bending limit  $l = 10.95 \sqrt{\frac{F_b S}{w}}$ ;

where :

$F_b$  plywood's maximum bending strength = 1545 psi

$S = \frac{bh^2}{6}$  is elastic section modulus, = 0.412 in<sup>3</sup>.

$w$  is calculated lateral pressure per unit width = 1200 lb/ft

$$l = \mathbf{8.92 \text{ in}}$$

2. Deflection limit governed by span length  $L/360$  and  $1/16$

$$l_{(L/360)} = 1.69 \sqrt[3]{\frac{EI}{w}}$$

where:

$E$  is Modulus of elasticity of plywood = 1,500,000 psi,

$$I = \frac{bh^3}{12} \text{ is moment of inertia} = 0.197 \text{ in}^4;$$

$$w = 1200 \text{ lb/ft}$$

$$l_{(L/360)} = \mathbf{10.59 \text{ in}}$$

$$l_{(1/16)} = \mathbf{12.08 \text{ in}}$$

3. Shear limit state is governed by

$$l_{(\text{shear})} = \frac{20 F_v * I * b}{w * Q};$$

where:

$F_v$  is shear strength of plywood = 57 psi

$b$  is section unit width = 12 in

$h$  is plywood thickness = 3/4"

$Q = \frac{bh^2}{8}$  is first moment of area = 0.843

$$l_{(\text{shear})} = \mathbf{8.03 \text{ in governs}}$$

Wales spacing

Wales spacing is governed by bending limit state (shear).

$$l = 10.95 \sqrt{\frac{F'_b S}{w}},$$

where:

$F'_b$  is adjusted bending strength of studs = 1940 psi

$S = \frac{bh^2}{6}$  is elastic section modulus, = 1.31 in<sup>3</sup>.

$$w = 1200 * 8.03 / 12 = 803 \text{ lb/ft}$$

$$l_{\text{bending}} = \mathbf{19.5 \text{ in}}$$

Tie spacing

Tie spacing is governed by the same limit state (shear) as studs spacing except the shear is governed by equation

$$l_{\text{shear}} = 13.33 * F'v \frac{bd}{w} + 2d$$

where:

$d$  is section depth = 7 in

$b$  is section thickness = 1.5 in

$F'v$  is adjusted shear strength = 225 psi

$w = 1200 \text{ lb/ft}^2 * 19.05/12 = 1905 \text{ lb/ft}$

$$l_{\text{shear}} = \underline{\underline{15.11 \text{ in}}}$$

Ties were also checked for strength capacity

Tie capacity = 3500 lb

$T = 1200 * 15.11 * 19.5/144 = 2437 \text{ lb}$  -tension force in tie

Tie capacity > T safe

### A-6. Shear Stiffness Calculations

To calculate shear stiffness we used equation

$$G' = \frac{Pl * a}{\Delta 1 * b}$$

where:

$G'$  is the global shear stiffness ( $G'$ ),

$Pl$  is 1/3 of the maximal resistance load obtained from the load displacement curve,

$a$  is height of the wall =96 in,

$b$  is length of the wall =164 in.

$\Delta 1$  is lateral displacement at maximal lateral resistance

### SW1

$$Pl = 0.33 * 40,555 = 13,383 \text{ lb}$$

$$\Delta 1 = 0.93 \text{ in}$$

$$G' = \frac{Pl * a}{\Delta 1 * b} = \frac{13,383 * 96}{0.93 * 164}$$

$$G' = 8,423.60 \text{ lb/in}$$

### SW2

$$Pl = 0.33 * 27,657.18 = 9,126 \text{ lb}$$

$$\Delta 1 = 0.237 \text{ in.}$$

$$G' = \frac{Pl * a}{\Delta 1 * b} = \frac{9,126 * 96}{0.237 * 164}$$

$$G' = 22,540 \text{ lb/in}$$